NATIONAL ADVISORY COMMITTEE

NATIONAL ADVISORY COMMITTEE FOR AERONAUTICS

TECHNICAL NOTE 2507

EXPERIMENTAL INVESTIGATION OF OIL FILM PRESSURE DISTRIBUTION FOR MISALINED PLAIN BEARINGS

By G. B. DuBois, H. H. Mabie, and F. W. Ocvirk

SUMMARY

The effect of axial and twisting misalining couples on the oil film pressure distribution of a loaded bearing is shown by photographs of a number of three-dimensional plaster models representing averaged oil film pressure distribution under representative conditions. The experimental data from which the models were made are shown on profile curves included in this report. The oil film pressure data were obtained from seven small pressure sampling holes in a line connected to high pressure gages. The bearing shell containing the sampling holes could be rotated 130° while the shaft was rotating.

Five models were made from test data on a 1.62- by 1.62-inch bearing at a shaft speed of 5000 rpm, carrying a centrally applied load giving 833 pounds per square inch on projected area, and misalining couples as follows:

Model	Condition
1	Axial misalining couple equivalent to moving load 16 percent of bearing length from center line of bearing
2	Zero misalining couple
3	Twisting misalining couple about load line equivalent to central load times 17 percent of bearing length
4	Twisting couple equivalent to central load times 8 percent of bearing length
5	Zero misalining load after bearing had been bellmouthed by misalining tests

Perhaps the most enlightening effect of axial misalinement on oil film pressure distribution is the relatively small displacement of the load from the center of the bearing, represented here as 16 percent of the bearing length, to produce the disturbance of the oil film pressure illustrated.

For each of the five models, curves showing the distribution of bearing temperature are also included. The temperature data were taken simultaneously with the pressure data, using thermocouples embedded in the bearing shell, 1/16 inch from the oil film. The average temperature rise of the oil above the inlet temperature of 140° F is approximately 50° to 60° F. The variation of temperatures in the heavily loaded region of the bearing shown by the models is approximately 15° to 20° F.

INTRODUCTION

A series of tests were conducted from October 1949 through February 1950 on a special bearing test machine at Cornell University, Ithaca, New York, with central loading on the bearing and with or without either axial or twisting misalining couples applied. The purpose of the tests was to study the effect of misalining couples upon oil film pressure distribution.

These tests were conducted by applying known misalining couples in addition to the main load, because it is easier to apply and to measure these couples than it is to measure the related angular displacement. The angular misalinement resulting from these couples is small and remains to be determined.

Axial misalinement is defined herein as the condition where a couple is applied to the bearing in a plane containing the line of action of the central load and the axis of the shaft journal. Twisting misalinement is defined as the condition where a couple is applied to the bearing in a plane perpendicular to the line of action of the main load.

It should be noted that planes of these two couples are at right angles, the third-direction plane being that containing the friction couple. Thus any couple may be resolved into component couples in these three planes. The component couple in the friction plane theoretically should have no effect on the oil film. To simplify the study of the effects of the misalining and twisting couples, they have been tested separately.

An axial misalining couple has the same effect as a displacement of the line of action of the load a certain distance from the center line of the bearing. In order to relate the axial misalining couple to the load and to the length of the bearing, it is convenient to measure the couple by the amount of displacement of the main load required to produce an equivalent couple. This can be stated as a percent of bearing length. Thus zero-percent misalinement places the main load at the center of the bearing, and 50-percent axial misalinement places the main load at the edge of the bearing.

A twisting misalining couple can be expressed in percent by comparing it with an axial misalining couple of the same size or by the following formula which applies for either type:

$$\text{Percent misalinement} = \frac{\text{Couple}}{\text{Main load} \times \text{Bearing length}} \times 100$$

The action of an axial misalining couple on a plain journal bearing may be classified in the following manner:

(1) When the line of action of the main load lies between 0 and 50 percent of this bearing length, the pressure distribution theoretically will be along the entire length of the bearing on the loaded side, as shown in the curves of this report.

(2) If the line of action of the main load lies beyond the confines of the bearing, or is at a point greater than 50 percent of the bearing length, one end of the journal tends to move to the opposite side of the clearance and builds up pressure on this unloaded side of the bearing. This pressure on the unloaded side of the bearing is in addition to the high pressure on the loaded side of the bearing which exists only over part of the length of the bearing.

(3) If the central load is removed from the bearing, and only the couple remains, there will be equal pressure distribution on each side of the bearing. In this condition with zero load, there is no distinction between axial and twisting misalining couples.

In this report the area of study has been confined to the class of misalinement in which a main load is applied, and the line of action of the load lies within the confines of the length of the bearing. Numerically this limit can be described as 50-percent axial misalinement. Cases of twisting misalinement within these limits are also investigated.

This work was conducted at Cornell University under the sponsorship and with the financial assistance of the National Advisory Committee for Aeronautics.

DESCRIPTION OF APPARATUS

Figures 1 to 3 show diagrams of the element containing the test bearing. These figures show the means for applying the central load, the means for applying couples inducing an axial or twisting misalinement, and the methods for measuring the oil film pressure and bearing temperature.

Figures 4 to 6 show the test bearings and journals used in these experiments. The bearings were approximately $1\frac{5}{8}$ inches long by $1\frac{5}{8}$ inches in diameter. Bearing and journal 2 were used for models 1 and 2. Bearing and journal 3 were used for models 3, 4, and 5.

An 1120 Aviation oil was supplied to the center of the bearing at 140° F and 40 pounds per square inch through two 1/8-inch oil ports 45° apart on the unloaded side of the bearing. This can be seen in figure 3.

The oil film pressure was measured by seven 0.031-inch sampling holes in a line 1/4 inch apart along the length of the bearing surface. The gages used for measuring the oil film pressure were graduated in 100-pound-per-square-inch increments reading from 0 to 10,000 pounds per square inch. Calibration curves were made from 0 to 5000 pounds per square inch before the tests for use in correcting the readings. All pressure readings given on the curves in this report are corrected readings.

As a means of control of test conditions, bearing temperatures were indicated by iron-constantan themocouples inserted in 0.094-inch-diameter holes to within 0.060 inch of the bearing surface. Spaced 1/4 inch apart along the length of the bearing, the thermocouples are located 15° from the pressure sampling holes as shown in figures 1 and 3. A Leeds & Northrup potentiometer, with automatic cold junction compensation and Fahrenheit temperature scale, was used to measure bearing temperatures.

TEST PROCEDURE

Five three-dimensional plaster models were made to represent the effect of axial and twisting misalining couples on the oil film pressure distribution of a loaded bearing under representative conditions. Photographs of these models are shown in figures 7 to 11 and the experimental data from which each model was made were obtained as follows:

Model 1.- After a warm-up period of approximately 1 hour, the data for model 1 (fig. 7) were obtained by running the journal at 5000 rpm and applying a central load of 2200 pounds (833 lb/ sq in. on projected bearing area) on the test bearing and an axial misalining load of 28 pounds parallel to the central load at a moment arm of $20\frac{3}{32}$ inches. The test bearing was rotated through 130° to give the pressure distribution in the oil film for 65° each side of the center line of the bearing.

The shaft was run at the above speed in a clockwise and in a counterclockwise direction. The 28-pound misalining load was applied in first an "up" direction and then in a "down" direction for each angle setting. The 2200-pound load was corrected for a tare weight, but the 1-percent effect of the 28 pounds was neglected to permit averaging.

If the bearing is loaded with a force and a couple in the same plane, another force offset a distance h from the center line of the bearing can be considered to replace the original force and couple. With the data given above, the distance h is 0.256 inch which is approximately 16 percent of the bearing length. These calculations are shown in figure 12.

Some of the data at halfway points between the sampling holes were obtained by displacing the load about one-half of the h distance mentioned above and applying the remainder as a couple. Since the data obtained in this way fitted the curves, it has been demonstrated that the two methods are interchangeable.

Model 2.- Tests for model 2 (fig. 8) were made under the same conditions as for model 1 except with no misalining load.

Model 3.- The data for model 3 (fig. 9) were obtained at a journal speed of 5000 rpm and a central load of 2200 pounds on the test bearing. A twisting misalining load of 43 pounds perpendicular to the central load was applied at the moment arm of 14.34 inches. The test bearing was rotated through 130° to give the pressure distribution in the oil film for 65° from each side of the center line of the bearing. The journal was rotated in a clockwise and in a counterclockwise direction.

Since it is useful for comparative purposes to measure the twisting couples as a percent the same mathematical process was used for the twisting couples as for the axial misalining couples.

It is not possible to replace the load and the twisting couple acting upon the test bearing by a single force because the load and the couple are not in the same plane. However, the twisting couple acts in the horizontal plane and, to visualize the effect, the forces of the couple may be considered to be equivalent to the central load in magnitude and separated by a distance of 0.280 inch. This distance is approximately 17 percent of the bearing length. (See fig. 13.)

Model 4.- Tests for model 4 (fig. 10) were made under the same conditions as for model 3 with the exception that the twisting misalining load was 20 pounds at a moment arm of 14.34 inches. The distance between the forces of the equivalent horizontal couple is 0.130 inch. This distance is approximately 8 percent of the bearing length. (See fig. 14.)

Model 5.- Tests for model 5 (fig. 11) were made under the same conditions as for model 3 except with no misalining load. By the time that this run was made the bearing had become bellmouthed from the trial misalinement runs.

The log sheets for these tests are on file in the Department of Machine Design, Cornell University.

CHRONOLOGY OF TESTS

Preliminary:

(1) Bearing 2 and journal 2 were new in June 1949.

(2) June to August 15, 1949 - Friction and temperature tests - central loading.

Model 2:

(1) Pressure traverse with no misalinement - September 7, 1949.

(2) Trial runs for pressure traverse with axial misalinement - October 4, 5, and 6, 1949.

Model 1:

(1) Pressure traverse with 16-percent axial misalinement - October 11, 12, 13, 14, and 18, 1949.

(2) Bearing 2 seized at end of run with axial misalinement - October 18, 1949.

(3) Oil pressure holes cleared of smeared babbit caused by seizure. Trial runs with axial misalinement to repeat October 25 and 26 previous data. Bearing size changed because of seizing.

(4) Trial runs for pressure traverse with twisting misalinement - October 27 and 28, and November 1, 1949.

(5) November 3 through November 22, 1949 was used for trial friction tests under misalinement.

(6) Install bearing 3 - December 12, 1949.

(7) Run-in new bearing. Pressure gages would not give symmetrical readings along length of bearing nor would clockwise and counterclockwise rotation give the same pressure readings - December 14, 1949 through January 7, 1950. More run-in or wear needed.

(8) January 11 through January 13, 1950. Calibration of friction manometer. This also served to run-in the new bearing.

(9) January 17 through February 8, 1950. The effect of axial and twisting misalinement upon friction. This also served to run-in and/or bellmouth the new bearing.

(10) February 8 through February 10, 1950. The effect of twisting misalinement upon bearing temperature. This also served to run-in and/or bellmouth the new bearing.

(11) Trial runs to check pressure distribution - February 13, 1950. Pressure readings reasonably symmetrical.

Model 5:

Pressure traverse with no misalinement - February 15, 1950. Bearing apparently bellmouthed as compared with model 2.

Model 3:

Pressure traverse with 17-percent twisting misalinement - February 20, 1950.

Model 4:

Pressure traverse with 8-percent twisting misalinement - February 27, 1950.

PRECISION

The oil film pressure was measured by seven 0.031-inch sampling holes in a line 1/4 inch apart along the length of the bearing. The gages used for measuring the oil film pressure were graduated in 100-pound-per-square-inch increments from 0 to 10,000 pounds per square inch. These gages were calibrated over a range of 0 to 5000 pounds per square inch to an accuracy of ±1 percent. Calibration curves were plotted and all pressure readings in this report have been corrected.

The other variables in this test were the central load and the misalining couples. The central load was applied by a hydraulic pressure capsule, the pressure being read on a calibrated test gage accurate to within 1 percent. The load is probably accurate to within 2 percent and is substantiated by the numerical integration of model 2. (See table I.)

The misalining couples were applied by calibrated weights acting over ball-bearing pulleys with moment arms measured to a fraction of 1 percent.

The Leeds & Northrup temperature potentiometer used to measure bearing temperature could be read to an accuracy of about 2° F. A thermocouple, attached to the bulb of a laboratory thermometer giving room temperature near the machine, checked the thermometer temperature to within 1° F. No calibration of the potentiometer was made.

RESULTS

Oil Film Pressure Distribution

Model 1.- Figures 15(a) and 15(b) show the test data for model 1 plotted for a clockwise direction of rotation and the misalining load applied up and down. On these figures is also shown an average of the pressure for up and down loads. Figures 15(c) and 15(d) show similar plots for counterclockwise rotation and in figures 15(e) and 15(f) the pressures are averaged for clockwise and counterclockwise rotation. In figure 15(g) is shown all of the curves for the various pressure sampling points which were obtained by averaging the up and down loads and the clockwise and counterclockwise rotations. These curves are similar to those used to mold the longitudinal section of model 1. The solid lines represent actual test data and the dotted lines represent extrapolated points.

Figure 15(h) is a cross plot of figure 15(g) and shows curves for transverse sections of the model. If a misalining load had not been applied, the curves in figure 15(h) would have been approximately symmetrical about the line of point 4.

Model 2.- Data for model 2 were obtained with no misalining load and, therefore, it was necessary only to plot pressures for clockwise and counterclockwise rotation and the average of the two directions as shown in figures 16(a) to 16(d). Figure 16(e) shows the curves plotted for all of the pressure sampling points; these curves are the ones obtained by averaging the data for clockwise and counterclockwise rotation. On this curve sheet the curves representing points 1 and 7, 2 and 6, and 3 and 5 were averaged together in groups of two and their result shown. Theoretically the above curves (for points 1 and 7, 2 and 6, and 3 and 5) should be identical because they are symmetrical about the midpoint (position 4) of the bearing. However, with actual equipment there are some differences which were averaged out.

Figure 16(f) shows the actual transverse pressure plot for the sampling points cross-plotted from figure 16(e) for two given angle settings of the bearing, namely 90° and $112\frac{1}{2}^{\circ}$. Also shown are the average curves which were taken from figure 16(e).

Figure 16(g) shows the curves of the averages of points 1 and 7, 2 and 6, 3 and 5, and 4 drawn with the original data as solid lines and the curves through extrapolated points as dotted lines. These curves represent a longitudinal section of model 2.

Figure 16(h) is a cross plot of figure 17(g) and shows curves for transverse sections of the model. Because there was no misalining load and because minor irregularities due to the apparatus were removed by averaging the pressure at corresponding sampling points, the curves are symmetrical about the point 4.

Model 3.- Data for model 3 were obtained with 17-percent twisting misalinement together with a central load. Figure 17(a) shows data for clockwise and counterclockwise rotation for sampling points 1 and 7. The data of point 1 counterclockwise and that of point 7 clockwise were averaged together as were 7 counterclockwise and 1 clockwise. These were corresponding pressure sampling points which should give the same readings when the direction of rotation was reversed; that is, 1 counterclockwise is equivalent to 7 clockwise if the bearing is an ideal cylinder.

Figures 17(b) and (c) show the plot of points 2 and 6 and 3 and 5 and their averages. Figure 17(d) shows the plot of point 4 for clockwise and counterclockwise rotation. Figure 17(e) shows the average curves taken from figures 17(a) to 17(d). All of the curves except 4 have a double number which means that it is the result of averaging the first number in a clockwise direction with the second number in a counter-clockwise direction. These curves give a longitudinal section of the model.

Figure 17(f) shows the data from figure 17(e) cross-plotted to give the transverse section of the model. The effect of applying twisting misalinement together with a central load can be seen in the formation of two distinct peaks in the data. By comparing these curves with those of models 1 and 2, it is seen that with only a central load the distribution is symmetrical about the center line of the bearing. An axial misalining load throws the peak to one side and a twisting couple causes two peaks to occur.

Model 4.- The curves for model 4 (8-percent twisting misalinement), as shown in figure 18, were plotted in the same way as for model 3. In figure 18(f) it can be observed that the peaks of the model are not separated so distinctly as in model 3 which is due to the lower twisting misalinement being applied.

Model 5.- The data for model 5 were obtained with a central load and no misalining load. The bearing was bellmouthed because of the misalining tests previously conducted on it. The curves (fig. 19) were plotted the same as were those for model 2.

Figure 19(e) which is a cross plot from figure 19(d) shows the effect of bellmouthing. The pressure at sampling points at the ends of the bearing are much lower than they would have been if the bearing had not been bellmouthed. This gives a more pronounced peak to the curves as compared with that of model 2 (fig. 16(f)). Figure 19(g) which was cross-plotted from figure 19(f) to give the transverse section of the model also shows the effect of bellmouthing.

Bearing Temperature Distribution

For each of the five models of pressure distribution, curves are presented of the circumferential bearing temperature distribution. The amount of temperature data taken varies as follows: In model 1 (fig. 20), temperatures at all seven points were taken; in model 2 (fig. 21), at point 4 only (midpoint); and in models 3, 4, and 5 (figs. 22 to 24), at points 2, 4, and 6.

The bearing temperature data were averaged in a manner similar to that employed in determining average film pressure distribution. From the curves it may be seen that the temperature data follow a wavy pattern around the average lines. This may be partially attributed to a lack of allowing sufficient time to reach the last few degrees of equilibrium temperature after each angular setting of the test bearing. The curves representing averages are shown as smooth curves without local variations.

Figures 1 and 3 show that the line of seven thermocouples is offset circumferentially at an angle of 15° from the pressure sampling holes. As a result, for a given angle setting on the test machine, the recorded bearing temperature data were taken for locations 15° removed from the location of film pressure measurement. In the plotting of temperatures of the bearing, however, the temperature data were shifted 15° in order that the abscissas of the temperature distributions would appear in correct relation to the load line.

For each model, the average curves of bearing temperature are shown on one chart (see figs. 20(h), 21, 22(d), 23(d), and 24(d)). These curves represent three-dimensional models of bearing temperature distribution for comparison with the models of pressure distribution. In order to aid in this comparison, angular locations of peak film pressure are indicated on the temperature-distribution curves.

Friction

Friction data for the bearing and shaft used for model 2 under central load are given in figure 25 which shows the relation of bearing friction coefficient to Sommerfeld number. In computing data for this curve the clearance for each point was obtained from a straight-line plot of experimental data showing variation of clearance with temperature.

The Sommerfeld number for model 2 is 0.16 as calculated from the following conditions: Speed, 5,000 rpm; bearing pressure on projected area, 833 pounds per square inch; operating film temperature, 197° F; viscosity, 2.42×10^{-6} reyn; clearance, 0.00123 inch per inch.

ANALYSIS AND DISCUSSION

Effect of Run-In

As was apparent in the section "Chronology of Tests," considerable difficulty was experienced in obtaining reliable pressure readings on new bearing 3. When bearing 3 was installed, it was first carefully bored and lapped with optical rouge, and then had to be run-in for a considerable period before the pressure gages would give symmetrical readings along the length of the bearing. Also, it was found that a bearing would not give the same pressure readings in both a clockwise and counterclockwise rotation of the shaft unless it had a long run-in. From the indications mentioned above it was possible to tell when a bearing had been run-in sufficiently.

If the journal rotation is started before the load is applied, run-in seems to be very slow. The bearing was started and stopped repeatedly under moderate load in order to shorten the run-in periods. This procedure has the disadvantage, however, that it will sometimes smear the oil pressure sampling holes.

It is very interesting to note that after the bearing had been carefully bored and lapped unevenness in the bearing surface could only be detected by a difference in pressure readings and could not be seen or measured with an ordinary inside micrometer.

Numerical Integrations from Plaster Models

The plaster models shown in figures 7 through 11 describe the pressure distribution in the oil film under cases of normal loading with or without loads producing misalinement. In order to evaluate quantitatively the accuracy of these distributions, numerical integrations were made of the pressures and the moments of the pressures as given by the models for comparison with the loads and moments which were applied during the tests. Table I shows the comparison of these values.

As shown in the sketches accompanying table I, coordinate axes at the center of the journal were chosen such that the y-axis is parallel to the applied central load P and the z-axis is coincident with the axis of the journal. The summation of the model pressure components in the y-direction were compared with the applied load P of 2200 pounds and the summation of the components in the x-direction were compared with the side load of 0 pounds. These summations are given by the following expressions:

$$F_y' = \sum\sum p(\Delta z)(r\Delta\theta) \cos\theta$$

$$F_x = \sum\sum p(\Delta z)(r\Delta\theta) \sin\theta$$

For models 1, 3, and 4 summations were made of the moments of the model pressures with respect to the x- and y-axes for comparison with the applied axial misalining moment M_a and with the applied twisting misalining moment M_t. These summations are given as follows:

$$F_y\bar{z} = \sum\sum p(z\Delta z)(r\Delta\theta) \cos\theta \text{ for axial misalinement}$$
$$F_x\bar{z} = \sum\sum p(z\Delta z)(r\Delta\theta) \sin\theta \text{ for twisting misalinement}$$

In the above expressions p is oil film pressure and r is the radius of the journal. The summation $\Sigma p(\Delta z)$ was made by taking the planimeter value of the area of the templet giving the longitudinal pressure distribution of the model. The summation $\Sigma p(z\Delta z)$ was made from the product of the templet area and the distance z from the center of the journal to the centroid of the templet. From plots of $\Sigma p(\Delta z)$ against θ and $\Sigma p(z\Delta z)$ against θ summations with respect to θ were made for $\Delta\theta = 5^{\circ}$.

As shown in table I, the most reasonable agreement between integrated values and applied values of load is for the case of model 2 which was without misalinement. For model 5, also without misalinement, the agreement is quite close. However, for the cases representing conditions under misalinement the agreement is less satisfactory. This may be partially explained by the fact that it was necessary to estimate the magnitudes and locations of peak pressures between data points obtained from the seven pressure sampling holes. In the case of models 2 and 5, from symmetry, the peak pressure positions are known to be at the center of the bearing.

For the axial misalinement case an attempt was made to secure pressure data at intermediate positions between the seven pressure sampling locations by shifting the shaft axially and adjusting the applied misalining couple. The data obtained in this manner correlated well with previously obtained data for only a portion of the bearing length and showed deviations in a region of the bearing which had been accidentally damaged by the cutting of a deep groove in the journal. For this reason only the previously obtained data were used for the ordinates of model 1. It is important to point out that intermediate data may be obtained in this manner provided the journal is shouldered as shown for bearing 2 in figure 4(a). With a shouldered bearing as in bearing 3 this cannot be done.

Critical Pressure Region of an Axially Misalined Bearing

In the case of model 1, 16-percent axial misalinement represents a displacement of the normal load a distance of one-sixth the length of the bearing. The peak pressure induced in the oil film is seen to be at approximately one-third the distance from the center or one-sixth the distance from the end of the bearing. The critical portion of a misalined bearing is probably at the end where the extremely steep pressure gradient may cause failure of the bearing material.

It may be visualized that the load capacity of a misalined bearing is dependent upon the load-carrying capacity of a much shorter portion of the bearing near one end. Model 1, for example, may be considered to have a critical length of 1/3 L. The peak pressure of the model is at the midpoint of that portion.

This critical portion may be compared with a hypothetical centrally loaded short bearing of this length carrying more than its fair share of the load. In model 1, for example, one-half of the load is carried on one-third of the length giving values of peak pressure and pressure on projected area that are 150 percent of the values without misalinement, as illustrated in figure 26.

Integration of the pressures of model 1 acting on the critical length resulted in an average pressure of 987 pounds or 51 percent of the total integrated load of 1940 pounds. Since the actual load applied was 2200 pounds the 51 percent carried by the critical portion of the bearing was approximately 1120 pounds. As a second method of checking for this critical length, the average pressure on the projected area was 1225 pounds per square inch which is 47 percent greater than the average pressure of 833 pounds per square inch for the entire bearing.

A considerable increase in magnitude of peak pressure is caused by 16-percent misalinement; model 1 gives a peak pressure of approximately 3100 pounds per square inch, an increase of 48 percent over the peak pressure of 2100 pounds per square inch of model 2 without misalinement.

The pressure and temperature data of model 1 for 16-percent axial misalinement and model 2 for central load show that the peak pressure rose from 2100 pounds per square inch at the midpoint 4, to 3100 pounds per square inch at point 6. The bearing temperature at the midpoint 4 is the same for both within 1° F, the peak temperature rising 3° at point 7, and falling 5° at point 1. Apparently 16-percent axial misalinement is within the range a bearing may tolerate, at least for the period of these tests.

The steep axial pressure gradient from 3000 to 0 pounds per square inch in 0.31 inch apparently is a critical condition. This pressure gradient may be determined for model 1 (fig. 15(h)) as 15,600 pounds per square inch per inch of bearing length and for model 2 (fig. 16(h)) as about 5100 pounds per square inch per inch.

Perhaps the most enlightening point is the relatively small displacement of the load from the center of the bearing, represented here as 16 percent of bearing length, to produce the disturbance of the oil film pressure illustrated.

It is interesting to note that the critical portion can be likened to a hypothetical short bearing with central loading which coincides, in the case of model 1, with that portion of the length between the load and the near end. (See fig. 26.) In other words, for 16-percent misalinement the equivalent critical length in this case was (50 - 16 percent) or 34 percent of the length. Theoretically this portion should carry a little more than 50 percent of the load because of the shorter lever arm in comparison with the more lightly loaded wide portion.

Value of Models

In summary, the results presented in this report are of qualitative value and describe graphically the effect of misalinement on oil film pressure distribution. The peak pressure increases greatly because of misalinement and is situated approximately halfway between the load line and the near edge of the bearing. The region of the bearing near the end is made to carry a larger portion of the load. The value of the peak pressure and its position along the bearing will vary with bellmouthing, clearance, L/D ratio, and so forth, of the bearing.

While bellmouthing has an appreciable effect on pressure distribution, failure in the sense of scoring the bearing surfaces did not occur in the babbitt-lined bearing because of the plastic flow of the material.

Quantitatively, the accuracy of the results of this report is adequate for cases of normal central loading and somewhat less accurate for the cases of misalinement. In all cases the quantitative values giving the characteristics of bearing pressure distribution are sensitive to small variations in the manufacture of the bearings. These models represent conditions for an L/D ratio of 1. It is hoped that similiar data can be obtained later at other L/D ratios for comparison.

Bearing Temperature Distribution

The temperature of the bearing shell $2\frac{1}{8}$ inches from the oil film is approximately 30° F lower than the temperature at the thermocouple at the center of the bearing located 1/16 inch from the bearing surface. Assuming a linear temperature gradient in the bearing wall, the temperature at the bearing surface should be approximately 1° F greater than that measured by the thermocouple near the surface.

As shown in the temperature curves, it may be seen that the location of maximum bearing temperature is beyond the location of maximum film pressure in the direction of fluid flow. The maximum bearing temperature appears to be near the location of minimum film thickness where the shearing rate on the stationary side of the film is greatest.

A comparison of models 1 and 2 shows that axial misalinement results in a large increase in peak pressure and a comparatively small increase in peak temperature. As shown in temperature curves for models 3, 4, and 5, twisting misalinement also gives small increases in peak temperature.

The curves show that the average temperature rise from an inlet temperature of 140° F is approximately 50° F for bearing 2 and 60° F for bearing 3. The maximum variation in temperature in any given model is shown to be 15° to 20° F.

CONCLUSIONS

From an investigation of the effect of axial and twisting misalining couples on oil film pressure distribution of a loaded bearing, the following conclusions may be drawn:

1. A displacement of the line of action of the load toward the end of a bearing results in a pressure peak between the load line and the end of the bearing.

2. For a bearing 1.62 by 1.62 inches, displacing the load line one-sixth of the bearing length from the center raised the peak pressure 50 percent.

3. A twisting couple in a plane perpendicular to the line of action of the main load tends to form two peaks in the oil film pressure distribution.

4. Any particular bearing has minor variations from a smooth pressure distribution due to unavoidable inaccuracy in finishing.

5. A babbitt-lined bearing is able to accommodate itself somewhat to misalinement by bellmouthing.

6. Although the effect of misalinement on the oil film pressure distribution of a bearing under central normal loading is great, the effect on temperature is comparatively slight.

Cornell University
Ithaca, N. Y., May 29, 1950

TABLE I - COMPARISON OF APPLIED LOADS AND MOMENTS WITH THOSE OBTAINED BY NUMERICAL INTEGRATIONS OF PRESSURES AND MOMENTS OF PRESSURES FROM MODELS OF PRESSURE DISTRIBUTION IN OIL FILM

Model	Case	Central load			Side load			Axial misalining couple			Twisting misalining couple		
		Applied load, P (lb)	From model, F_y (lb)	Difference (percent)	Applied load (lb)	From model, F_x (lb)	Percent of load, P	Applied moment, M_a (in-lb)	From model, $F_y\bar{z}$ (in-lb)	Difference (percent)	Applied moment, M_t (in-lb)	From model, $F_x\bar{z}$ (in-lb)	Difference (percent)
1	Central load, 16-percent axial misalinement	2200	1940	-11.8	0	60	2.7	560	390	30.4	0	23	----
2	Central load	2200	2245	2.0	0	80	3.6	0	0	----	0	0	----
3	Central load, 17-percent twisting misalinement	2200	1870	-15.0	0	30	1.4	0	60	----	615	412	33.0
4	Central load, 8-percent twisting misalinement	2200	2430	10.5	0	40	1.8	0	7	----	285	245	14.0
5	Central load, bellmouthed	2200	2050	-6.8	0	20	0.9	0	0	----	0	0	----

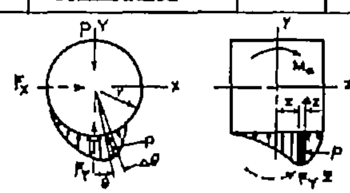

$$F_y = \sum\sum p(\Delta x)(r\Delta\theta)\cos\theta$$
$$F_x = \sum\sum p(\Delta x)(r\Delta\theta)\sin\theta$$
$$F_y\bar{z} = \sum\sum p(z\Delta z)(r\Delta\theta)\cos\theta$$
$$F_x\bar{z} = \sum\sum p(z\Delta z)(r\Delta\theta)\sin\theta$$

p, bearing pressure
r, radius of journal

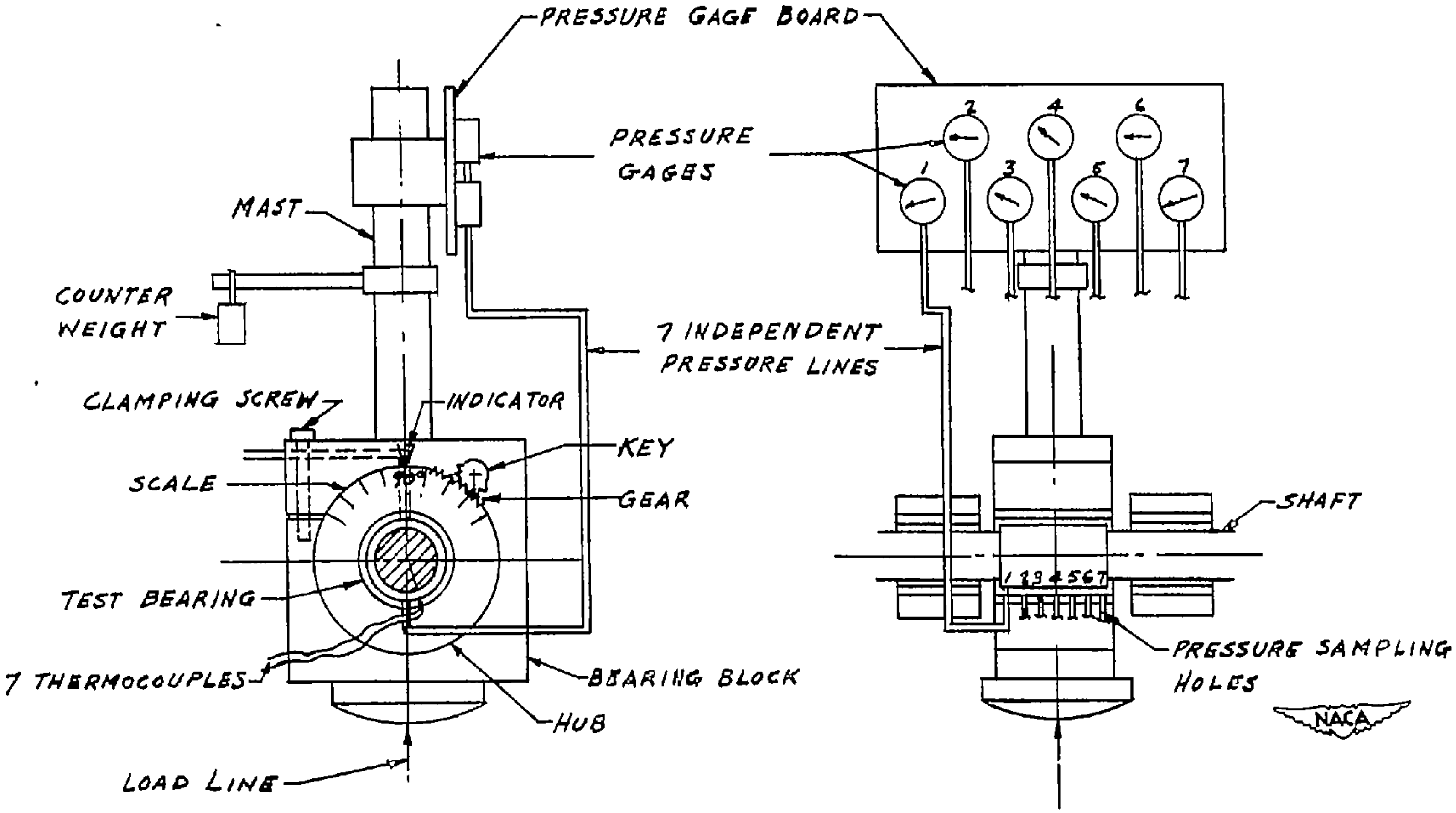

Figure 1.- Diagram of test element.

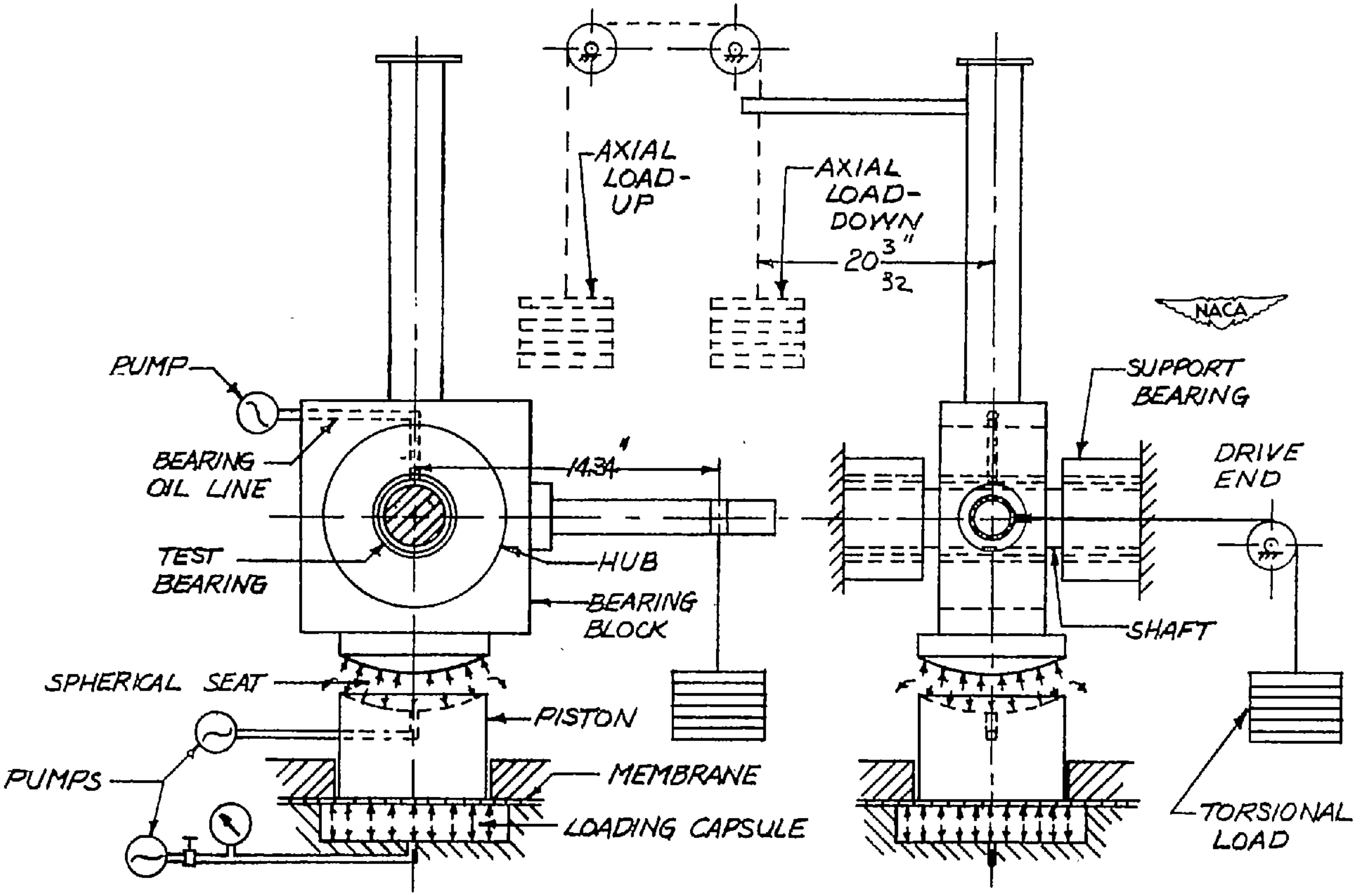

Figure 2.- Diagram of test element showing weights for applying axial and torsional misalinement.

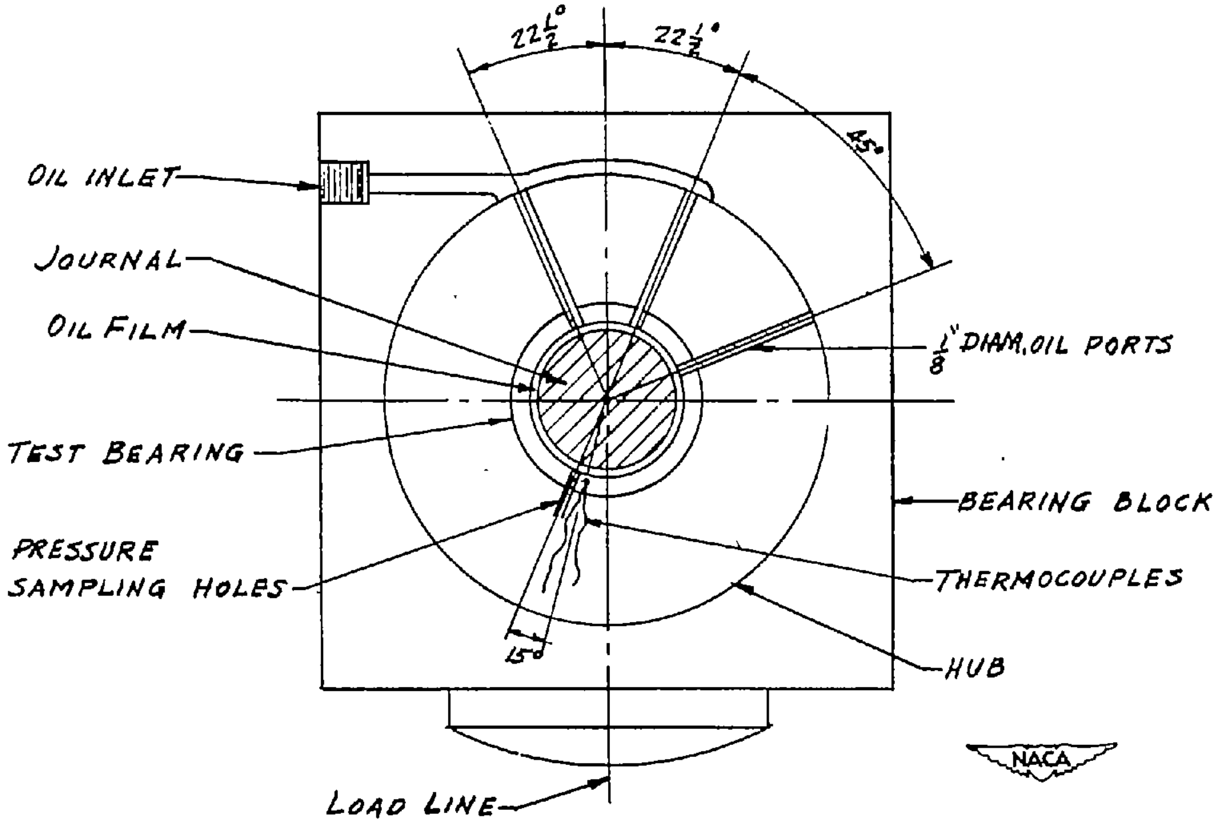

Figure 3.- Location of oil inlet holes, pressure sampling holes, and thermocouples.

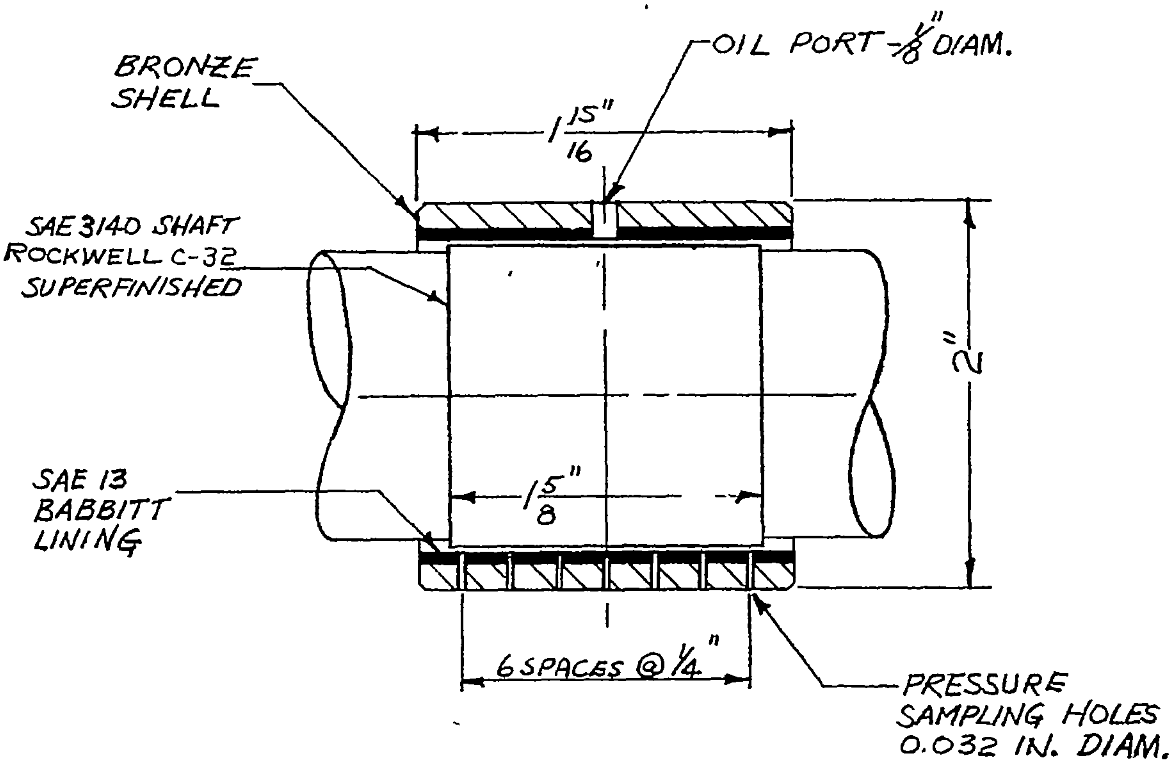

(a) Bearing 2. (See fig. 5 for dimensions of bearing and journal 2.)

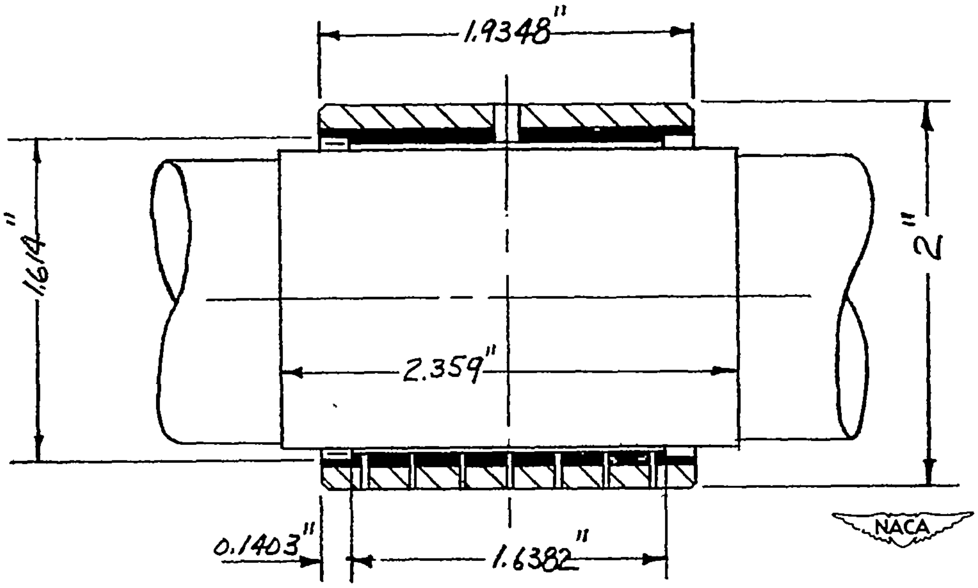

(b) Bearing 3. (See fig. 6 for dimensions of bearing and journal 3.)

Figure 4.- Test bearings and journals.

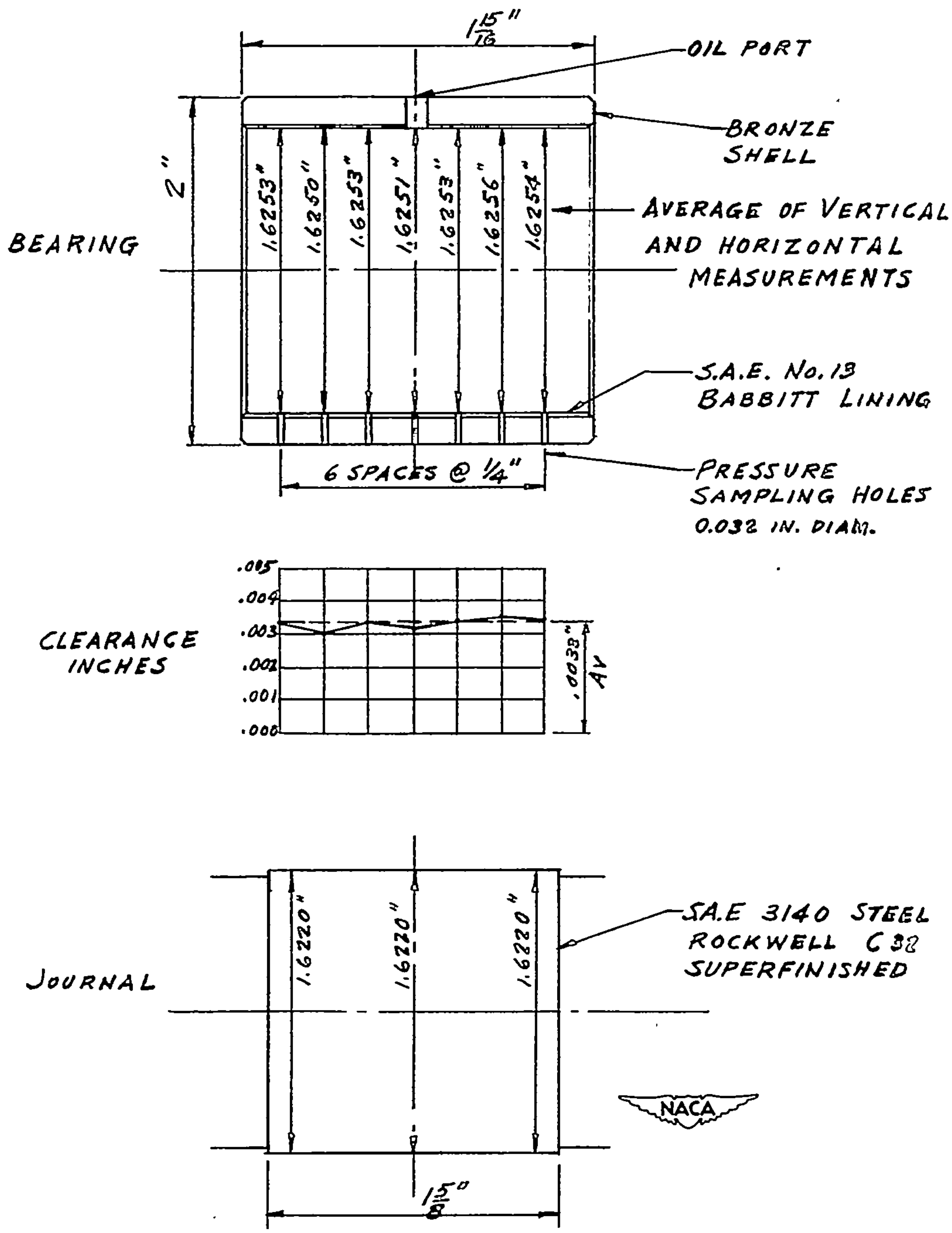

Figure 5.- Dimensions and clearance of test bearing 2 and test journal 2.

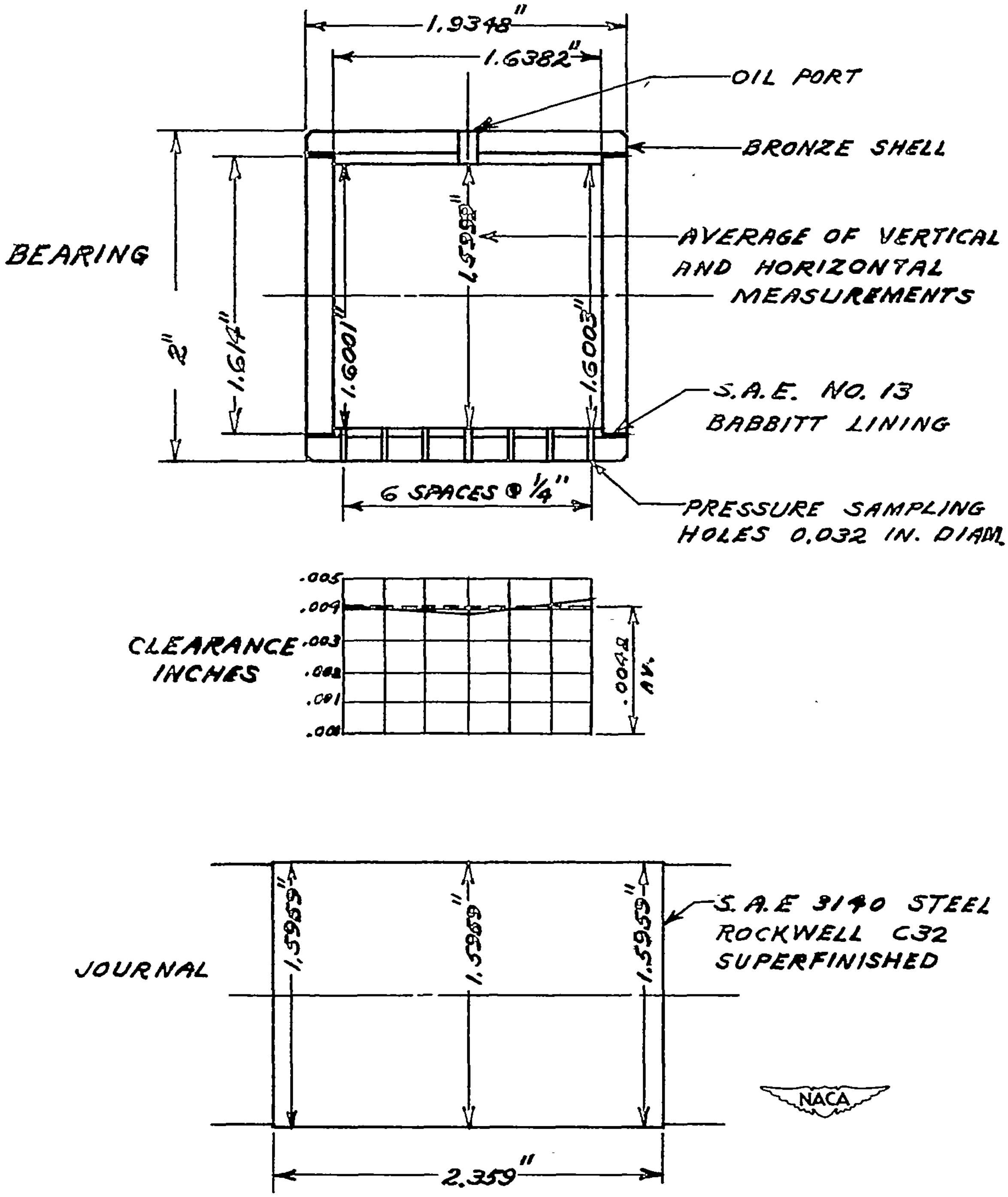

Figure 6.- Dimensions and clearance of test bearing 3 and test journal 3.

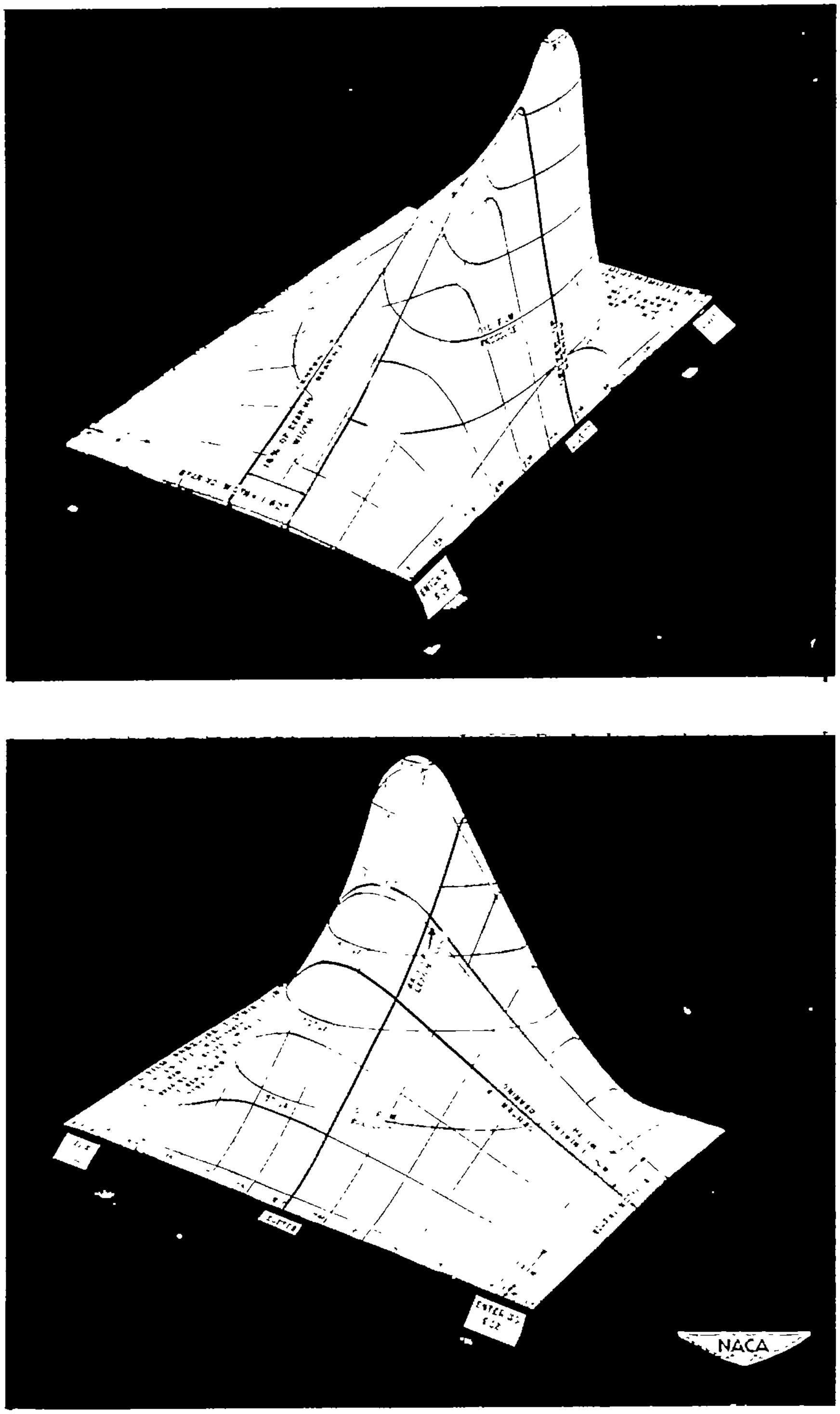

Figure 7.- Oil film pressure distribution with load displaced from center by 16 percent of bearing width (model 1). Load on projected area, 850 pounds per square inch; shaft speed, 5000 rpm; bearing diameter, 1.62 inches; bearing length, 1.62 inches; clearance, 0.002 inch per inch.

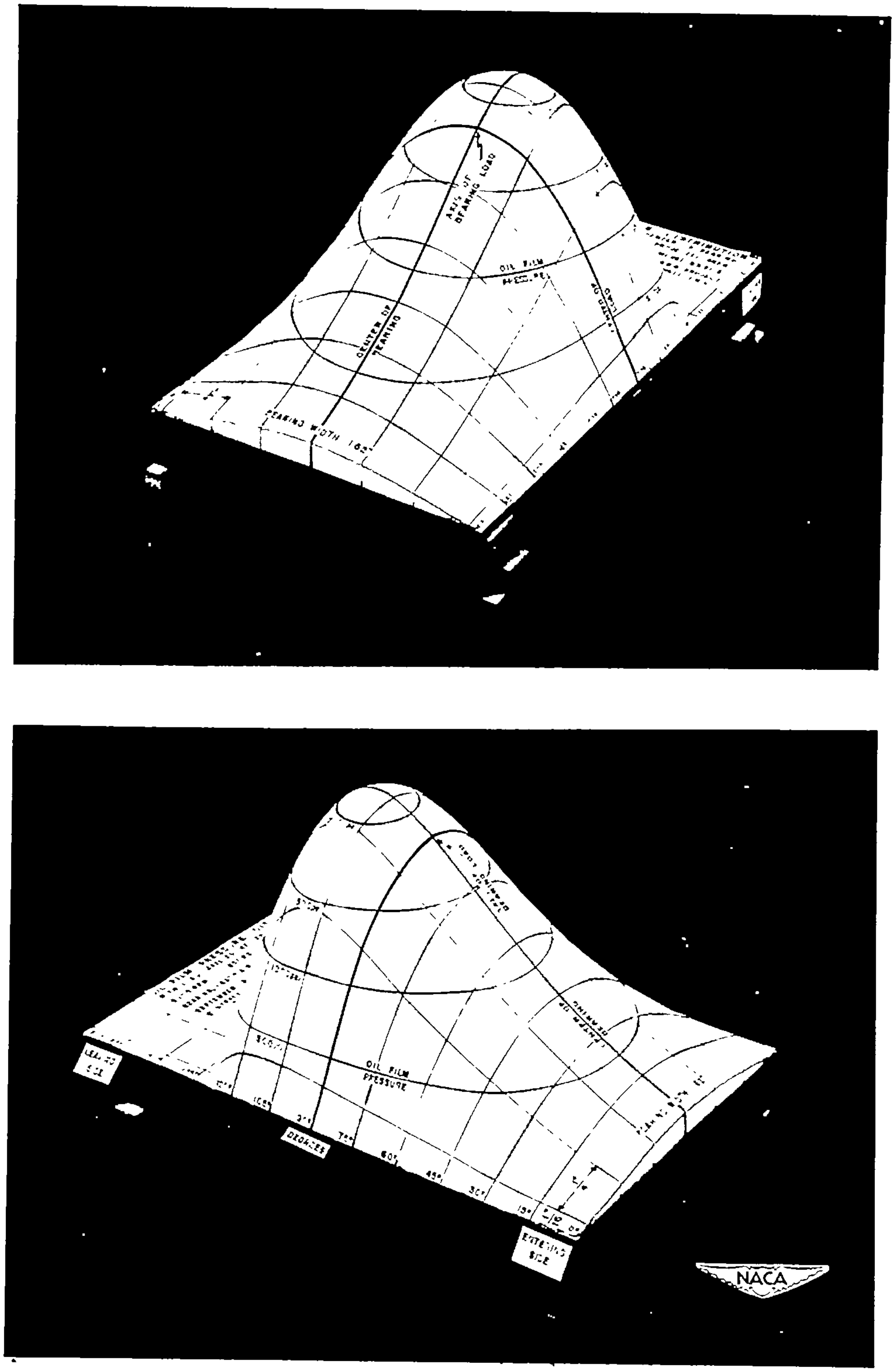

Figure 8.- Oil film pressure distribution with central load and zero misalinement (model 2). Load on projected area, 850 pounds per square inch; shaft speed, 5000 rpm; bearing diameter, 1.62 inches; bearing length, 1.62 inches; clearance, 0.002 inch per inch.

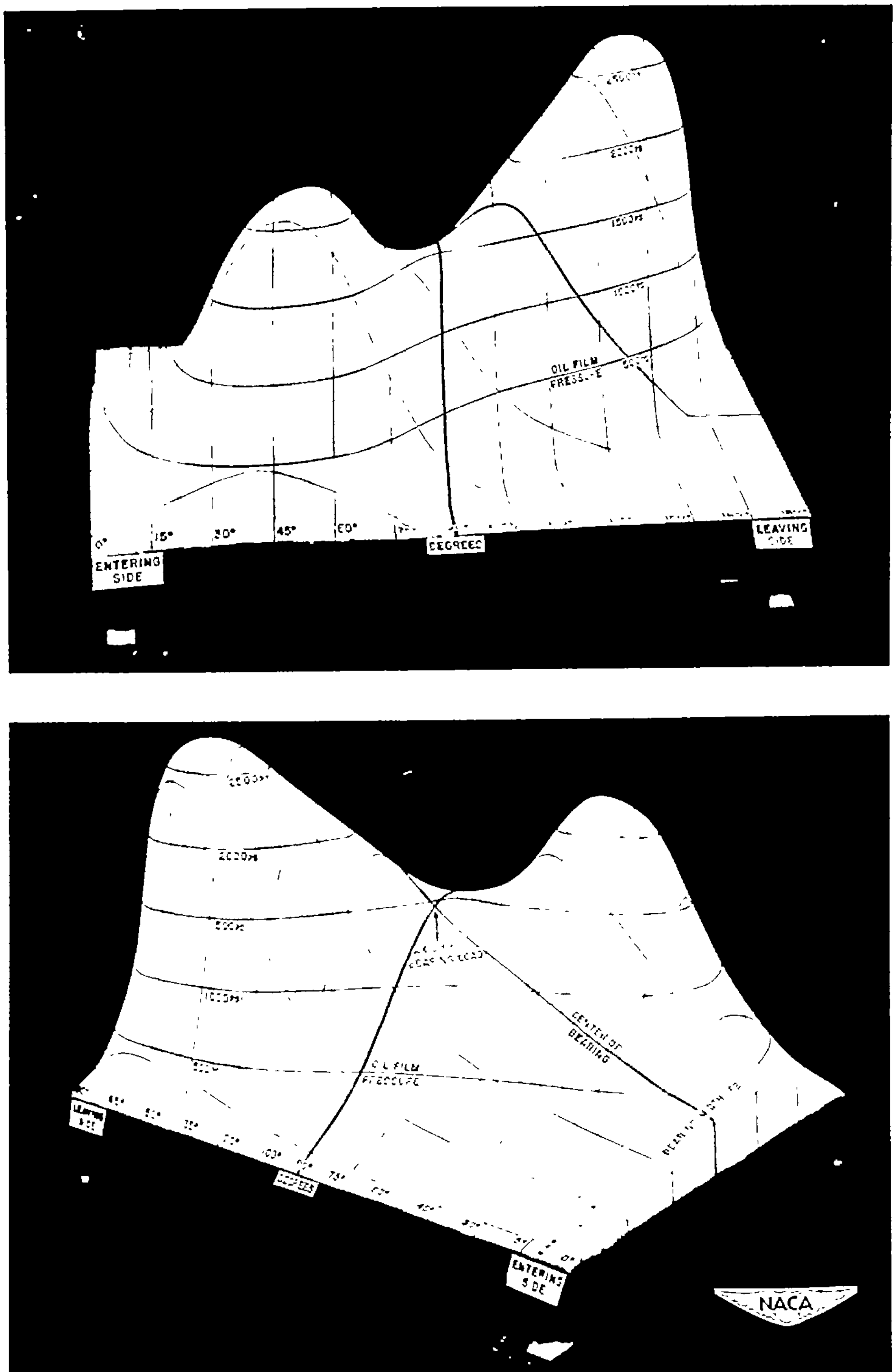

Figure 9.- Oil film pressure distribution with central load and 17-percent twist (model 3). Twisting couple about load line equal to 17 percent of load times bearing length. Load on projected area, 850 pounds per square inch; shaft speed, 5000 rpm; bearing diameter, 1.62 inches; bearing length, 1.62 inches; clearance, 0.0026 inch per inch.

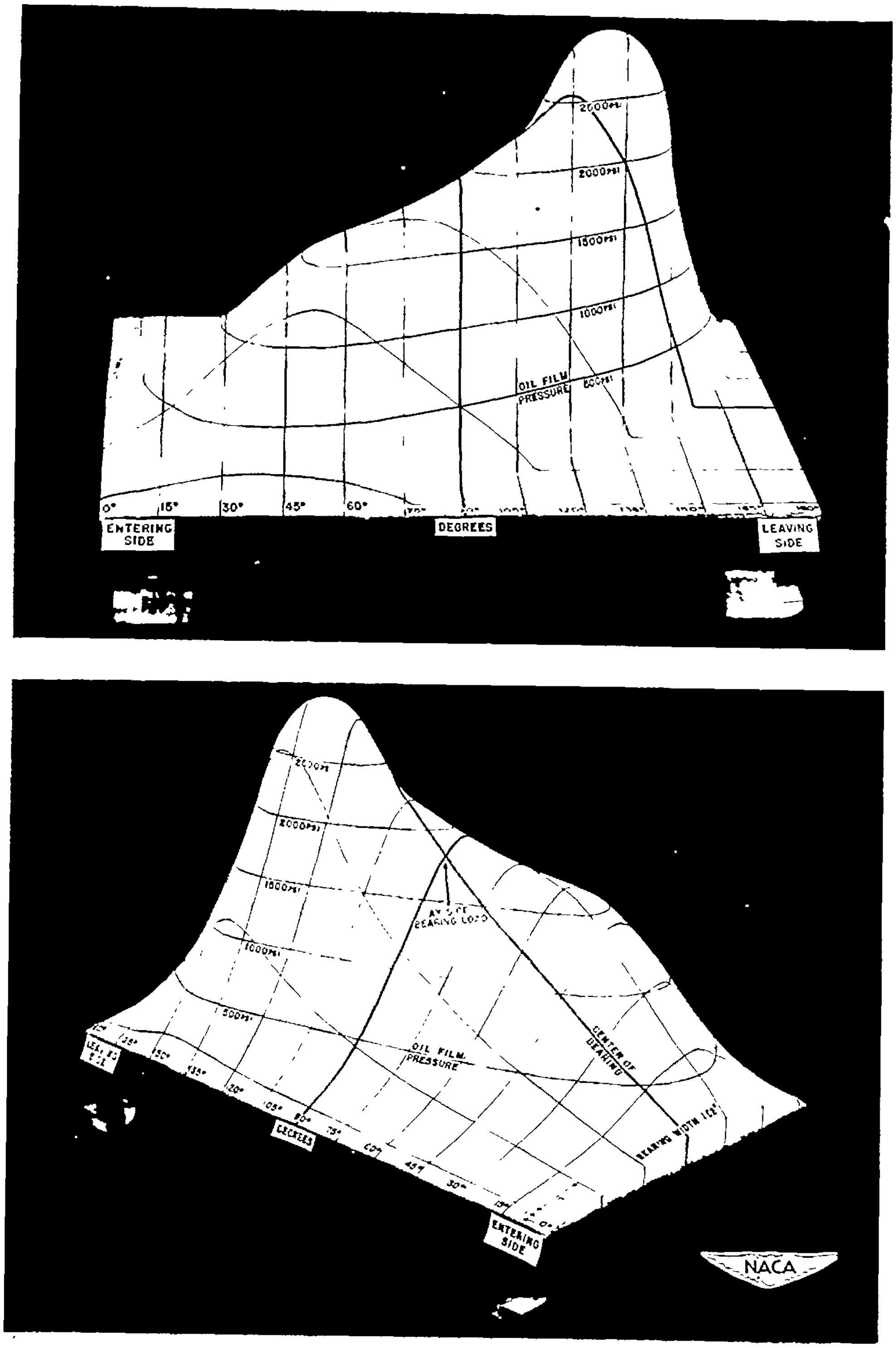

Figure 10.- Oil film pressure distribution with central load and 8-percent twist (model 4). Twisting couple about load line equal to 8 percent of load times bearing length. Load on projected area, 850 pounds per square inch; shaft speed, 5000 rpm; bearing diameter, 1.62 inches; bearing length, 1.62 inches; clearance, 0.0026 inch per inch.

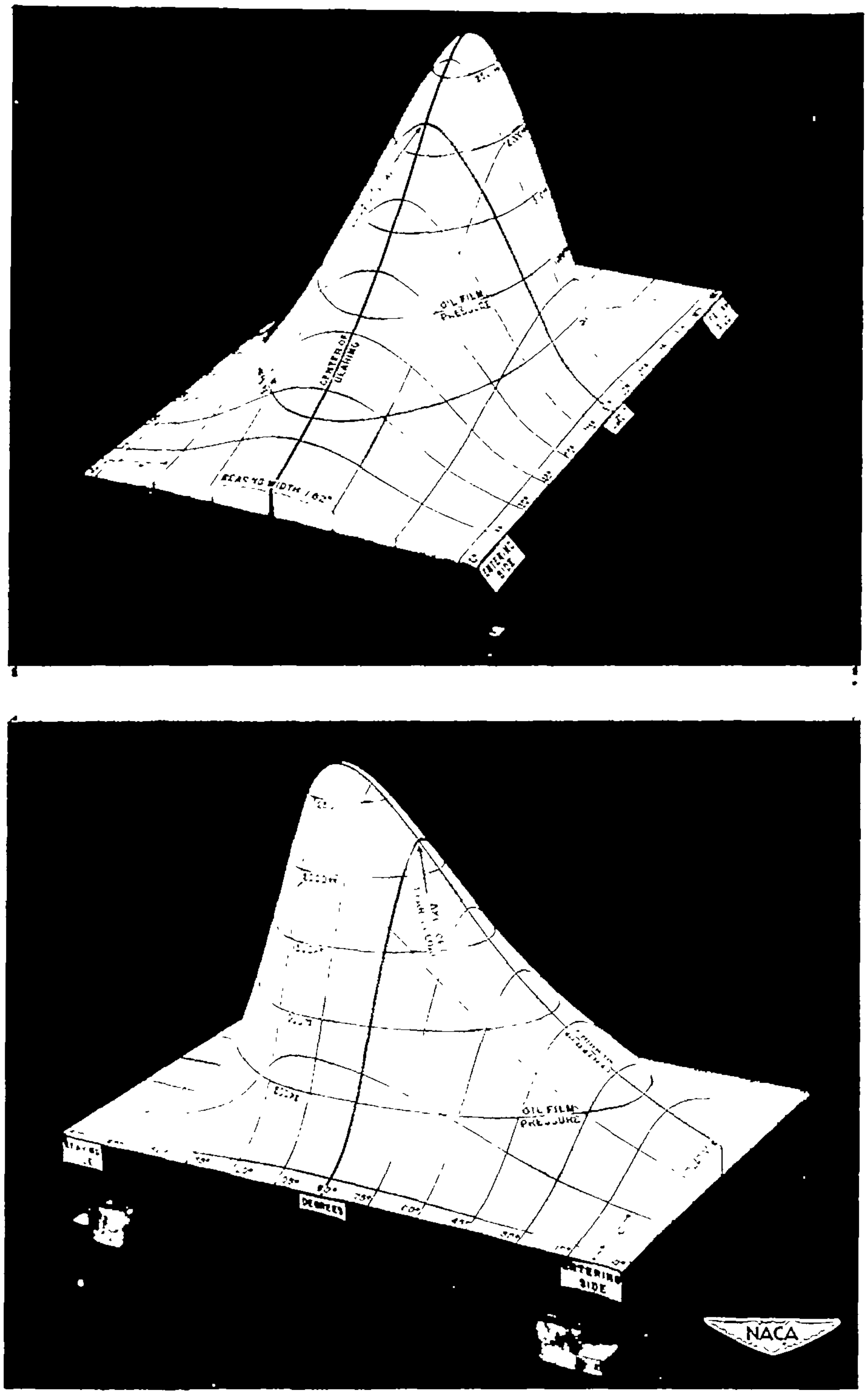

Figure 11.- Oil film pressure distribution with central load and zero misalinement after bellmouthing by misalinement tests (model 5). Load on projected area, 850 pounds per square inch; shaft speed, 5000 rpm; bearing diameter, 1.62 inches; bearing length, 1.62 inches; clearance, 0.0026 inch per inch.

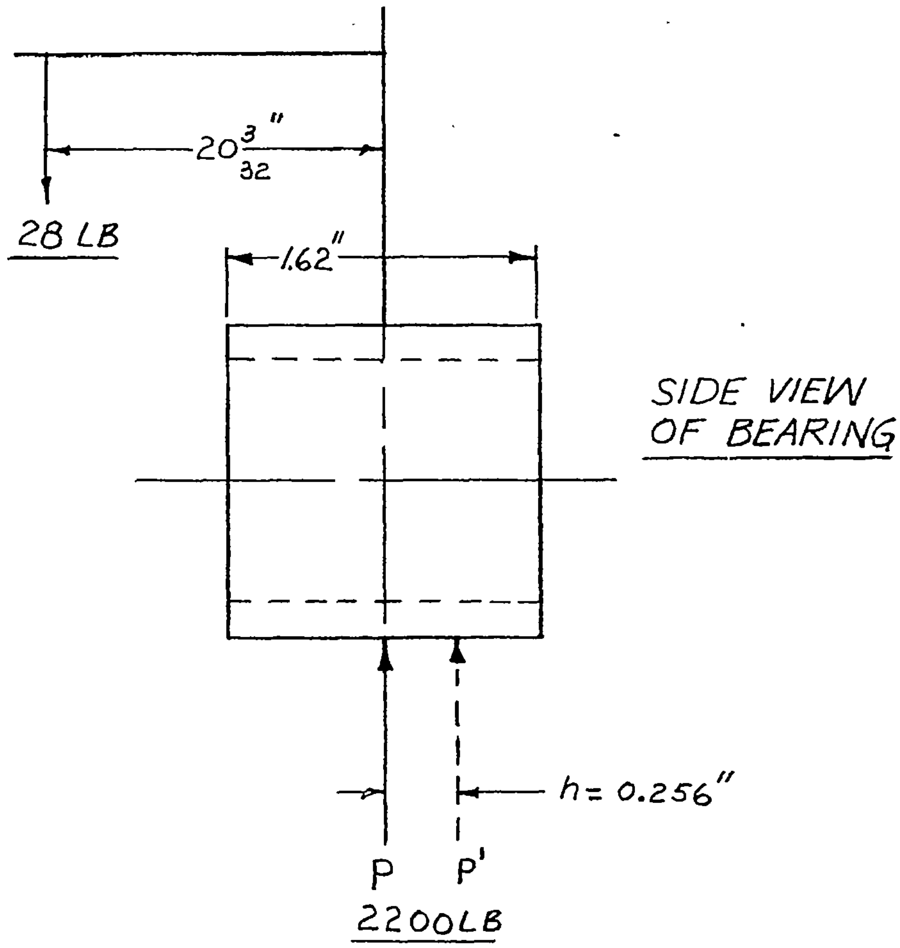

$$h = \frac{\text{Couple}}{\text{Force}} = \frac{28 \times 20\text{-}3/32}{2200} = 0.256 \text{ in.}$$

$$\% \text{ bearing length} = \frac{0.256 \times 100}{1.622} = 15.8\% \text{ or } 16\%$$

Figure 12.- Application of force and couple for case of 16-percent axial misalinement.

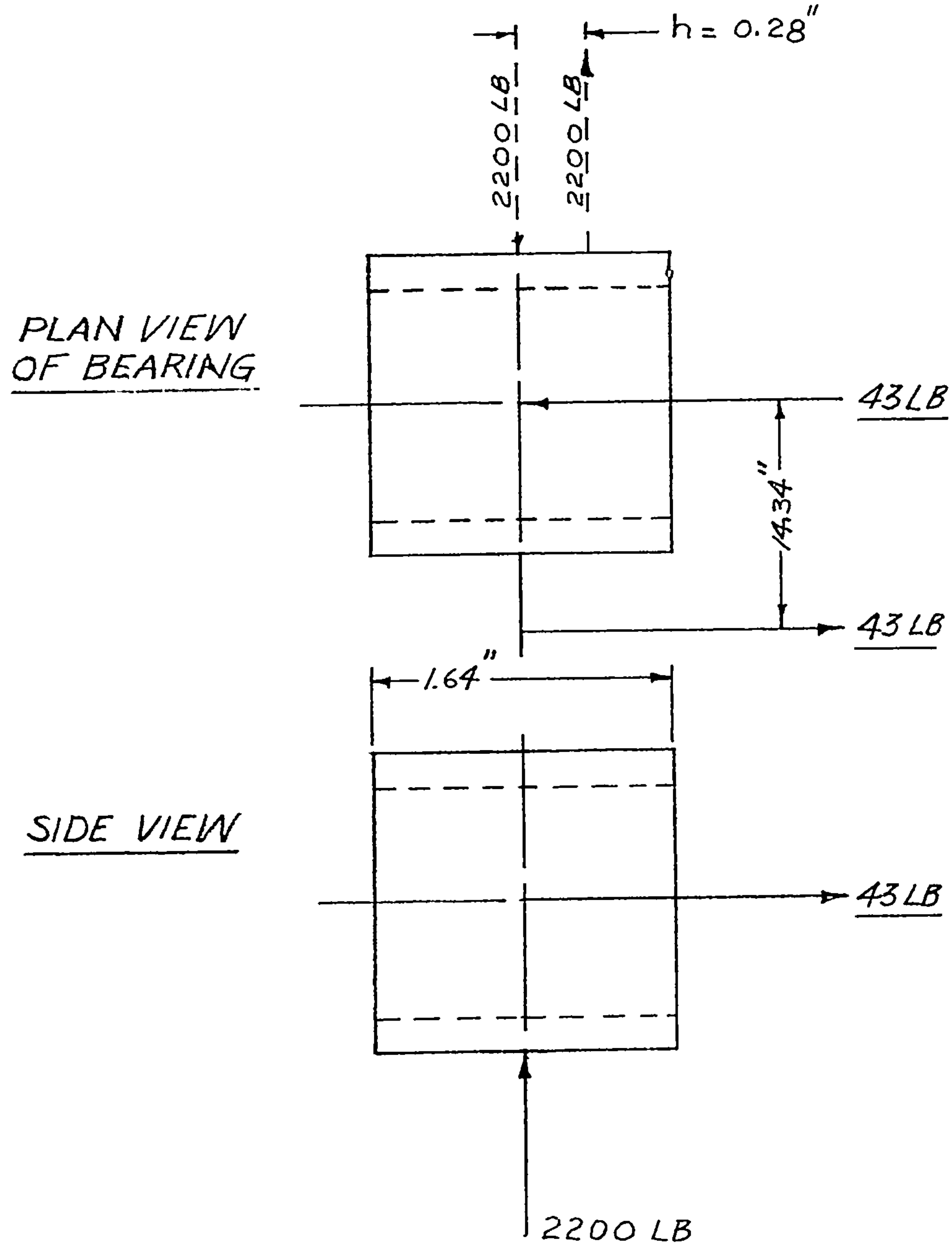

$$h = \frac{\text{Couple}}{\text{Force}} = \frac{43 \times 14.34}{2200} = 0.28 \text{ in.}$$

$$\% \text{ bearing length} = \frac{0.28 \times 100}{1.64} = 17.1\% \text{ or } 17\%$$

Figure 13.- Application of force and couple for case of 17-percent twisting misalinement.

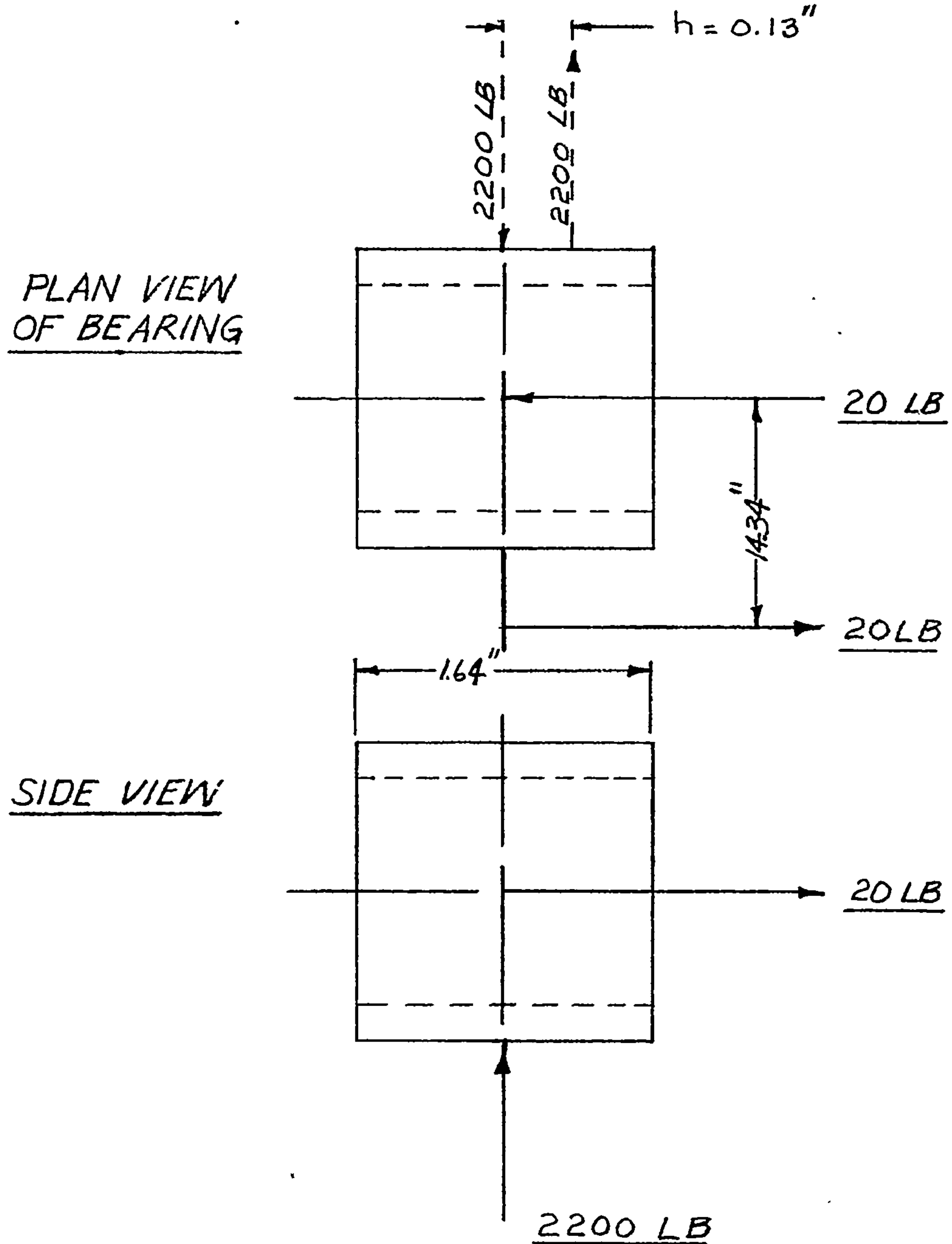

$$h = \frac{\text{Couple}}{\text{Force}} = \frac{20 \times 14.34}{2200} = 0.130 \text{ in.}$$

$$\% \text{ bearing length} = \frac{0.130 \times 100}{1.64} = 7.95\% \text{ or } 8\%$$

Figure 14.- Application of force and couple for case of 8-percent twisting misalinement.

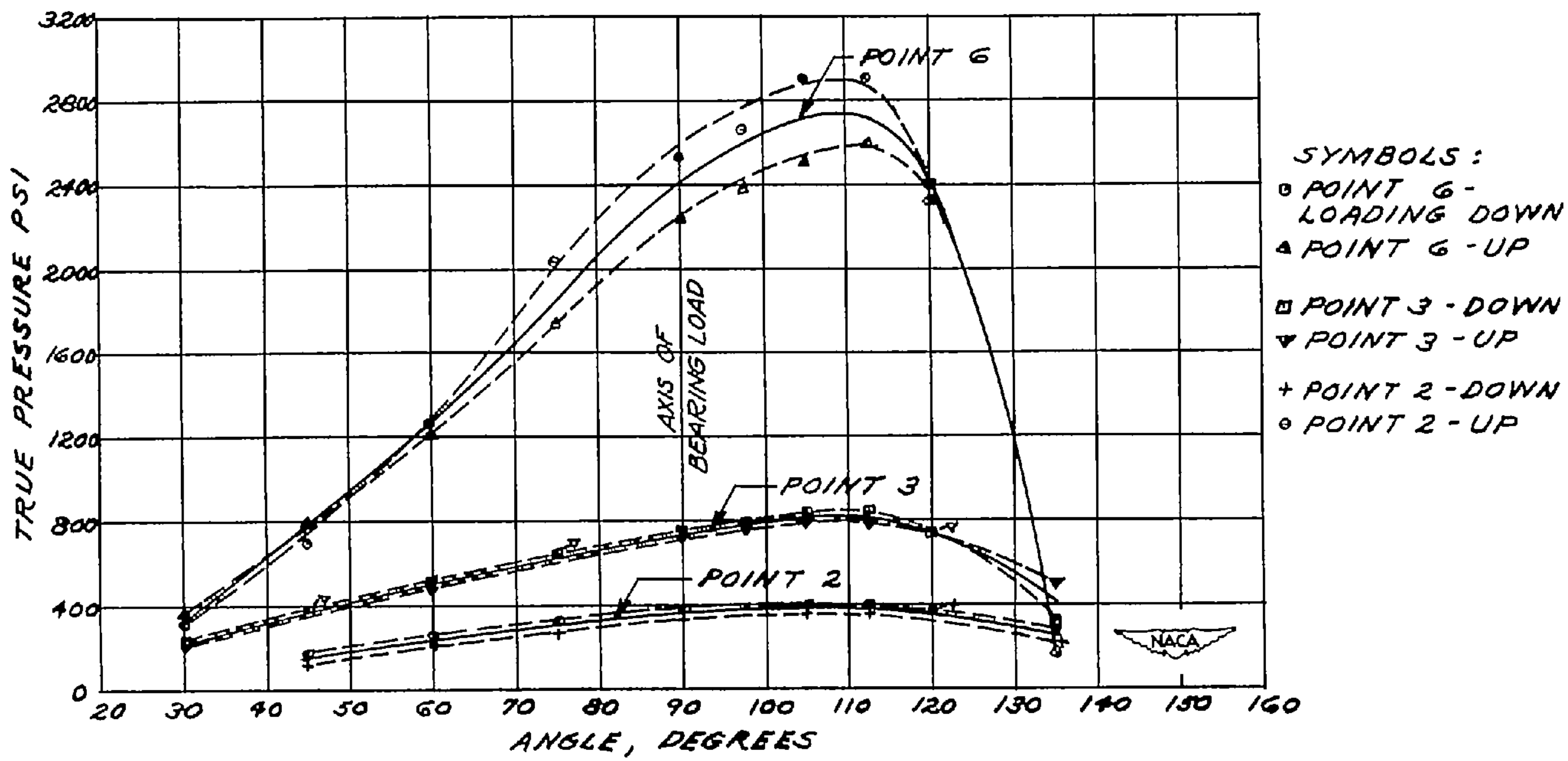

(a) Circumferential pressure distribution at points 2, 3, and 6 for clockwise rotation, average of up and down axial misalinement.

Figure 15.- Oil film pressure distribution with central load and 16-percent axial misalinement (data for model 1). Shaft speed, 5000 rpm; load on projected area, 850 pounds per square inch; bearing diameter, 1.62 inches; bearing length, 1.62 inches; bearing clearance, 0.002 inch per inch of diameter.

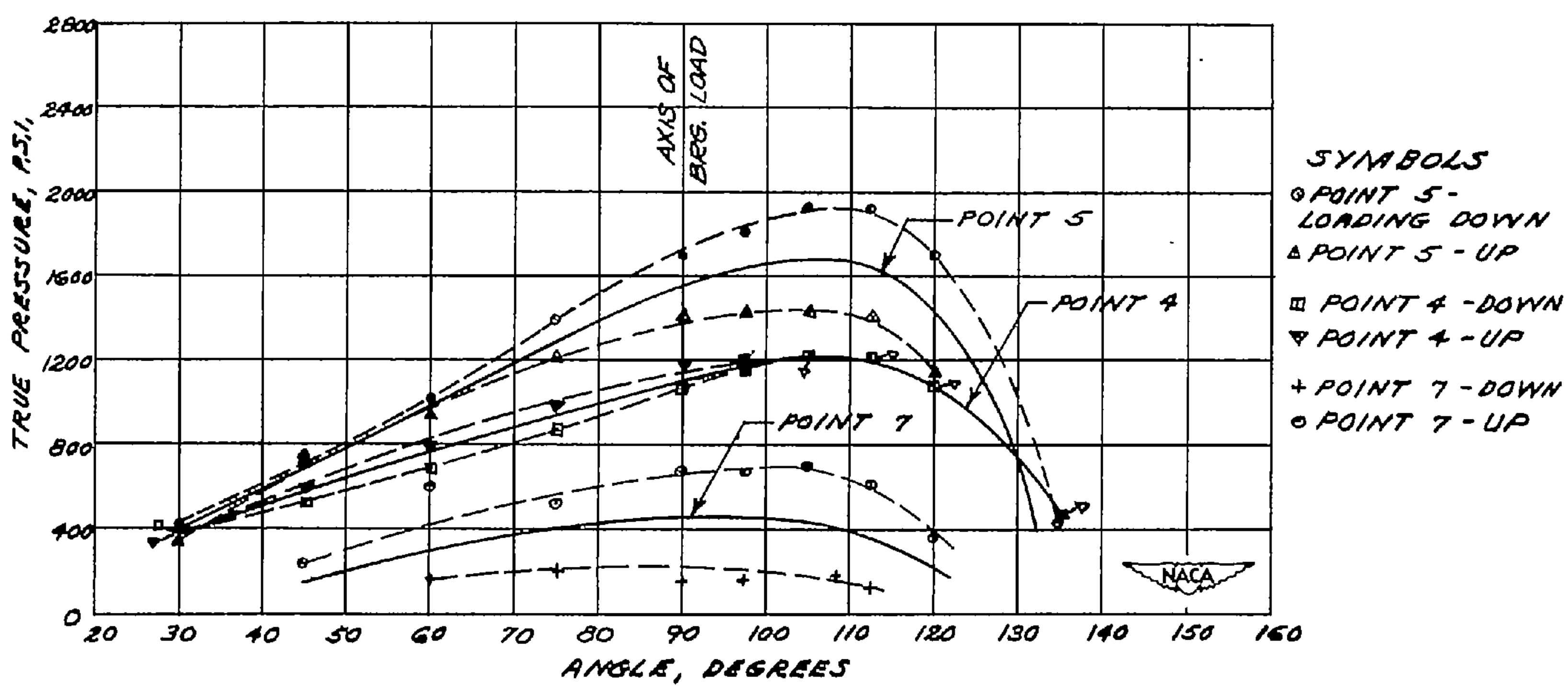

(b) Circumferential pressure distribution at points 4, 5, and 7 for clockwise rotation, average of up and down axial misalinement.

Figure 15.- Continued.

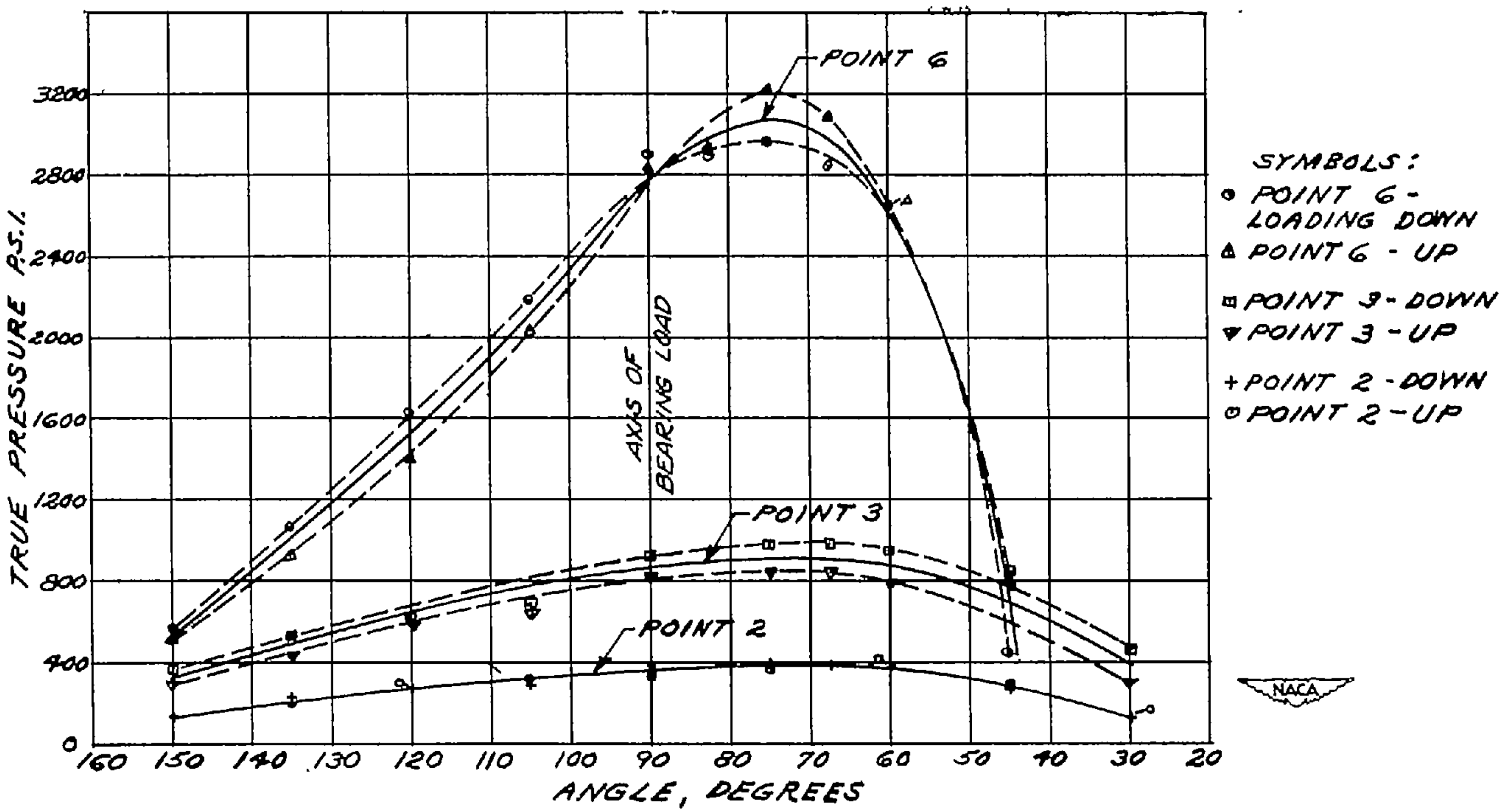

(c) Circumferential pressure distribution at points 2, 3, and 6 for counterclockwise rotation, average of up and down axial misalinement.

Figure 15.- Continued.

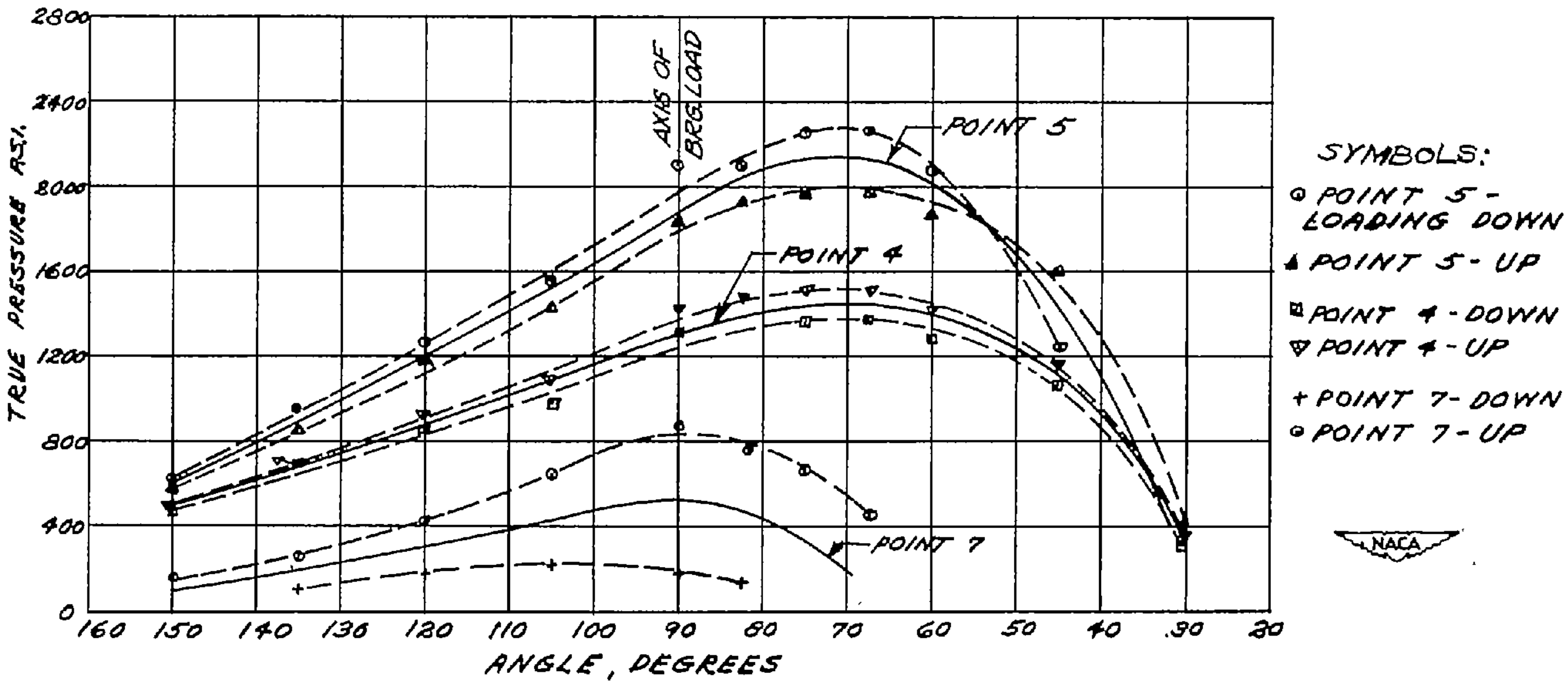

(d) Circumferential pressure distribution at points 4, 5, and 7 for counterclockwise rotation, average of up and down axial misalinement.

Figure 15.- Continued.

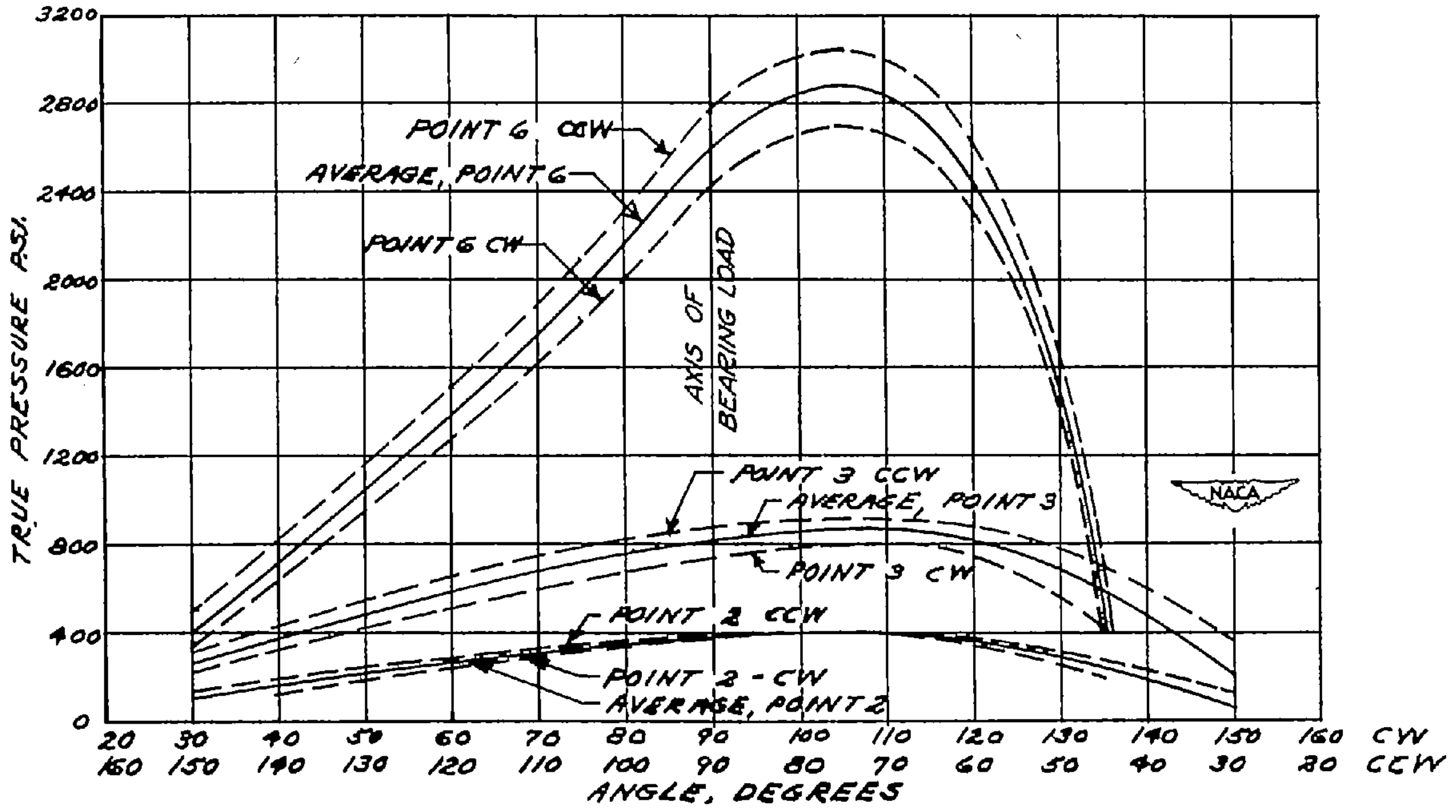

(e) Circumferential pressure distribution at points 2, 3, and 6, average of clockwise and counterclockwise rotation.

Figure 15.- Continued.

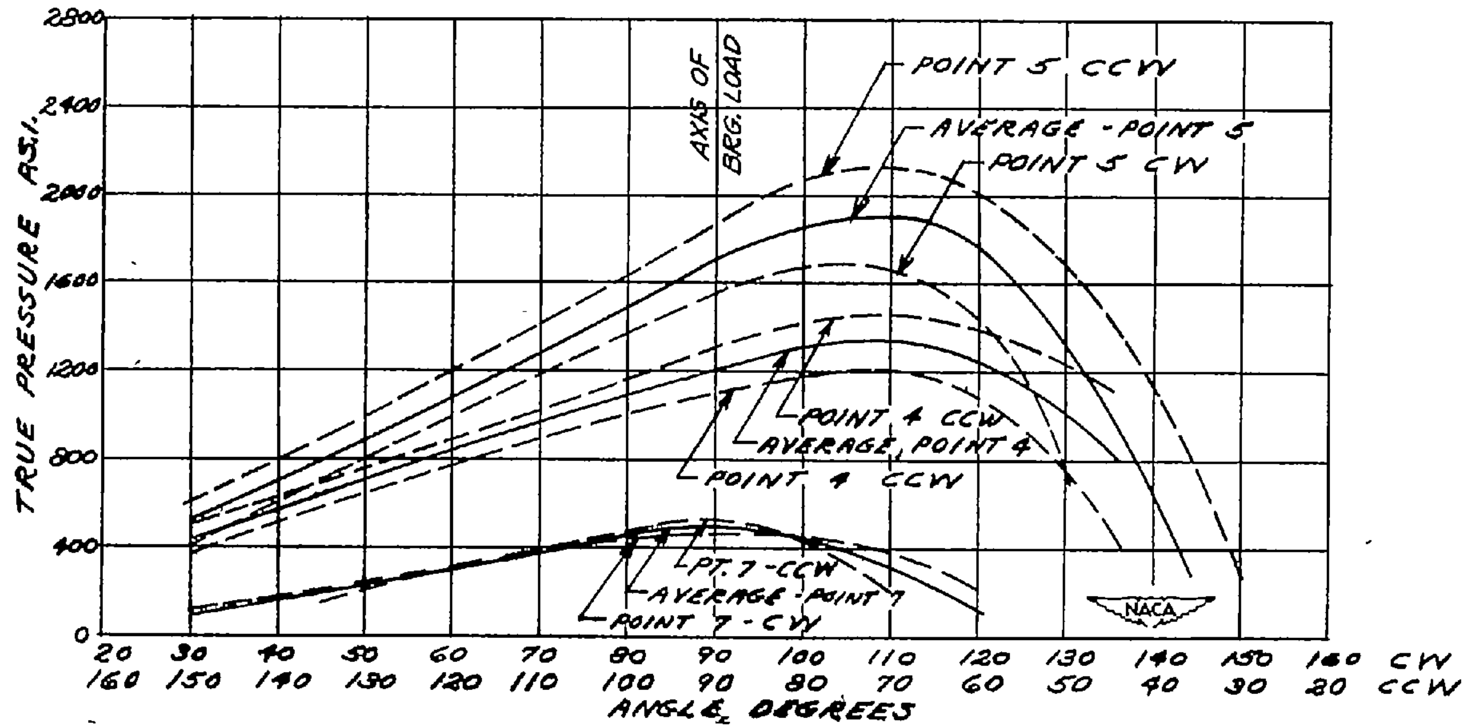

(f) Circumferential pressure distribution at points 4, 5, and 7, average of clockwise and counterclockwise rotation.

Figure 15.- Continued.

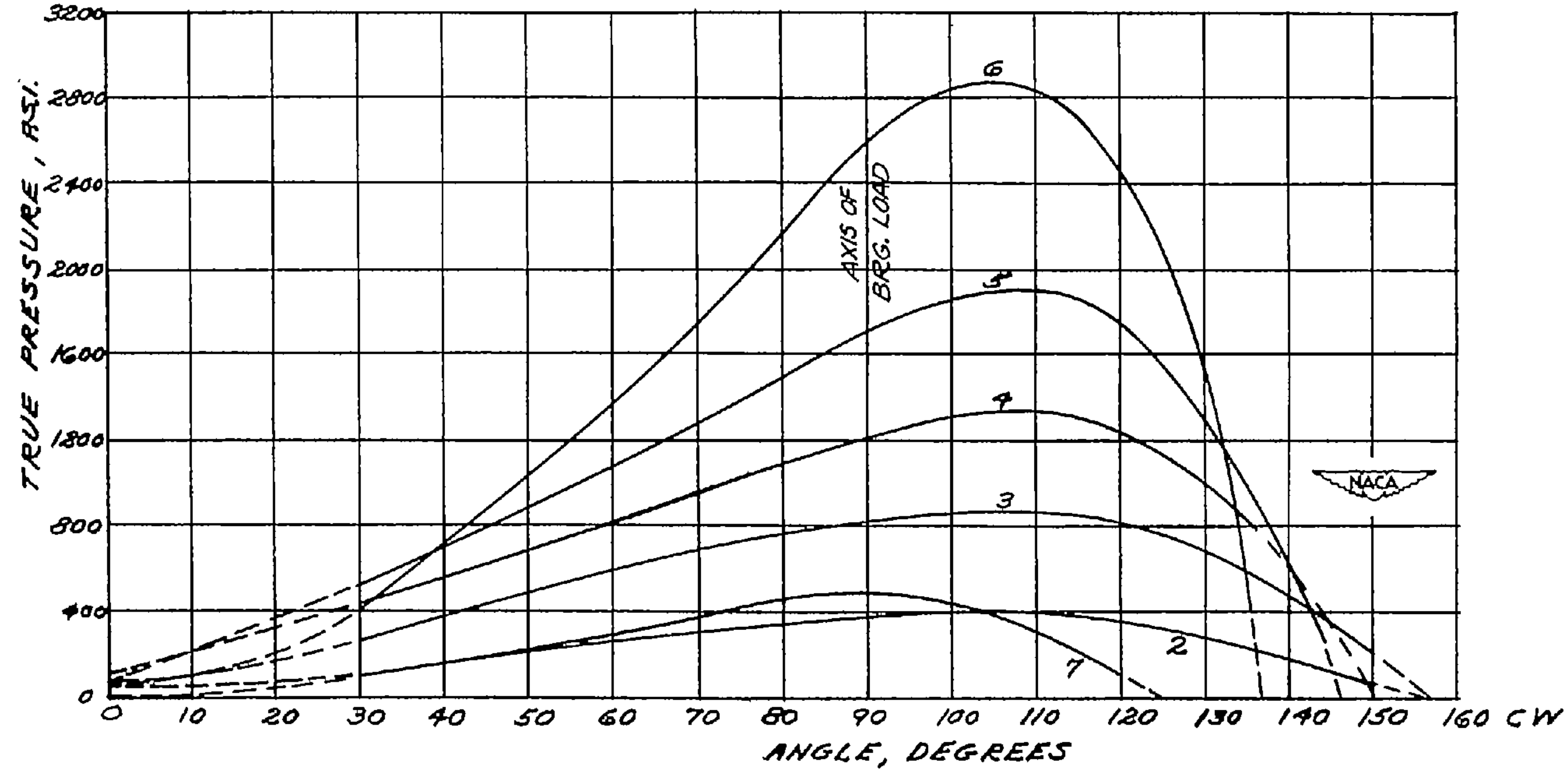

(g) Longitudinal sections of model 1.

Figure 15.- Continued.

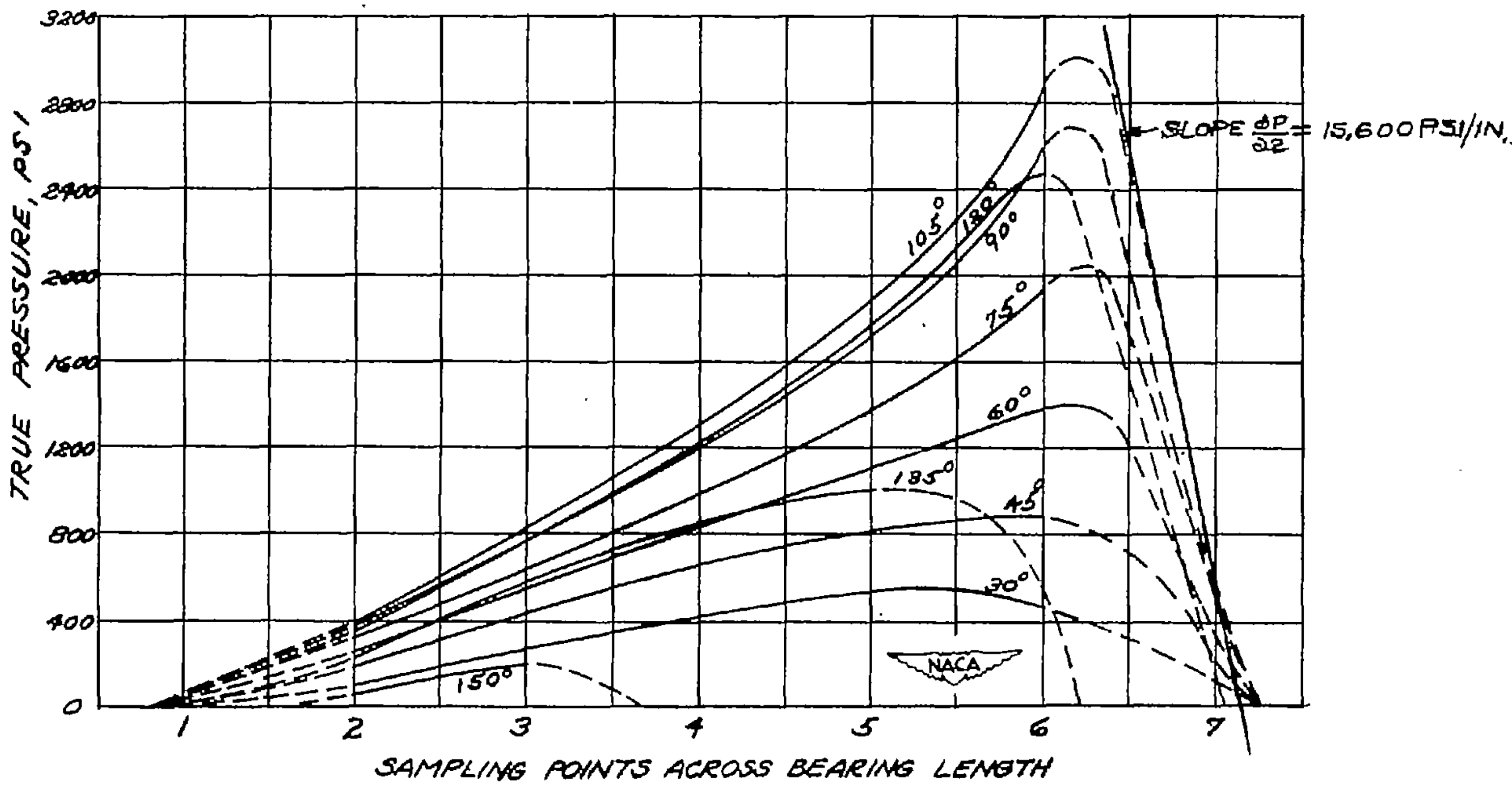

(h) Transverse sections of model 1.

Figure 15.- Concluded.

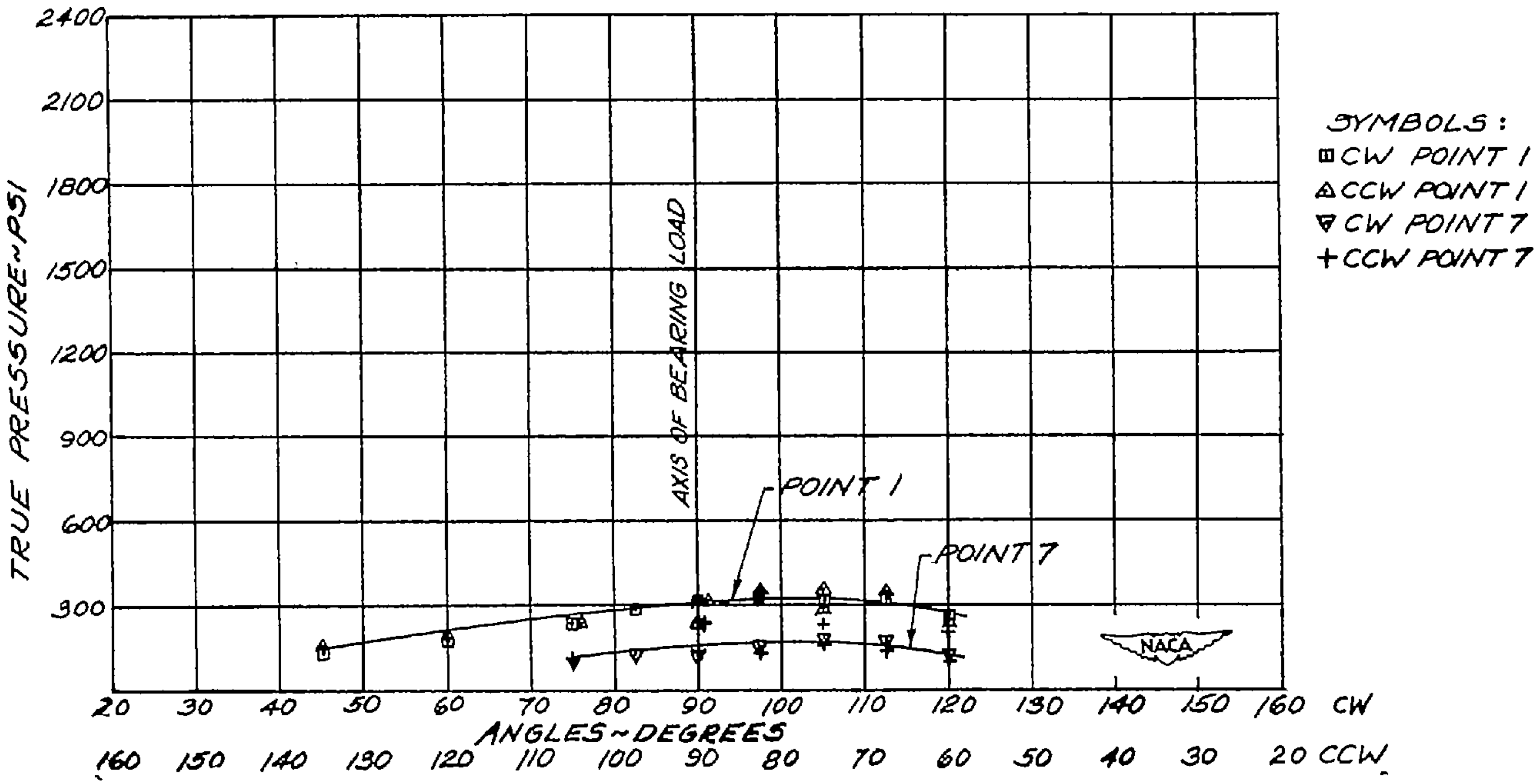

(a) Circumferential pressure distribution at points 1 and 7, average of clockwise and counterclockwise rotation.

Figure 16.- Oil film pressure distribution with central load and zero misalinement (data for model 2). Shaft speed, 5000 rpm; load on projected area, 850 pounds per square inch; bearing diameter, 1.62 inches; bearing length, 1.62 inches; bearing clearance, 0.002 inch per inch of diameter.

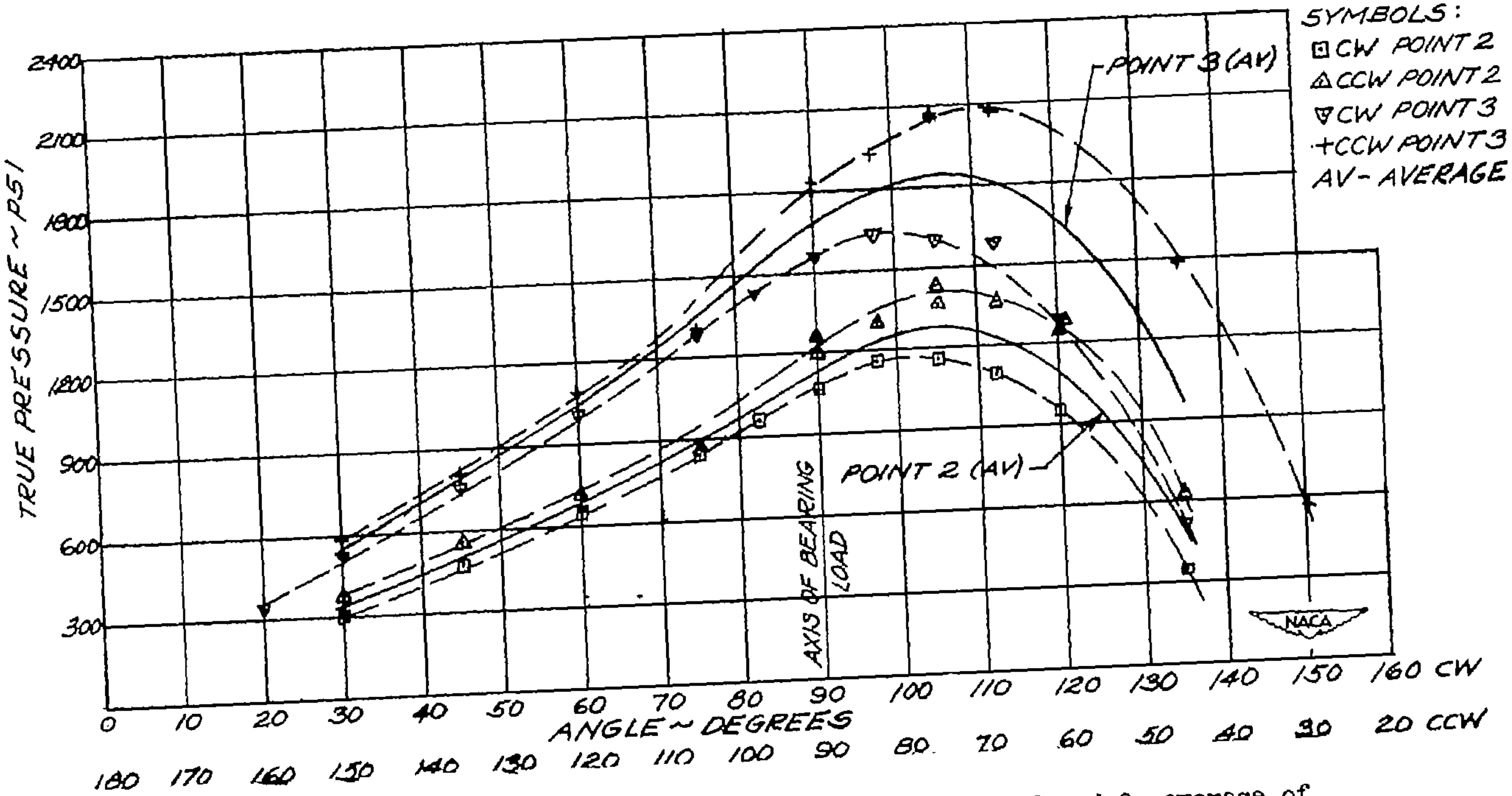

(b) Circumferential pressure distribution at points 2 and 3, average of clockwise and counterclockwise rotation.

Figure 16.- Continued.

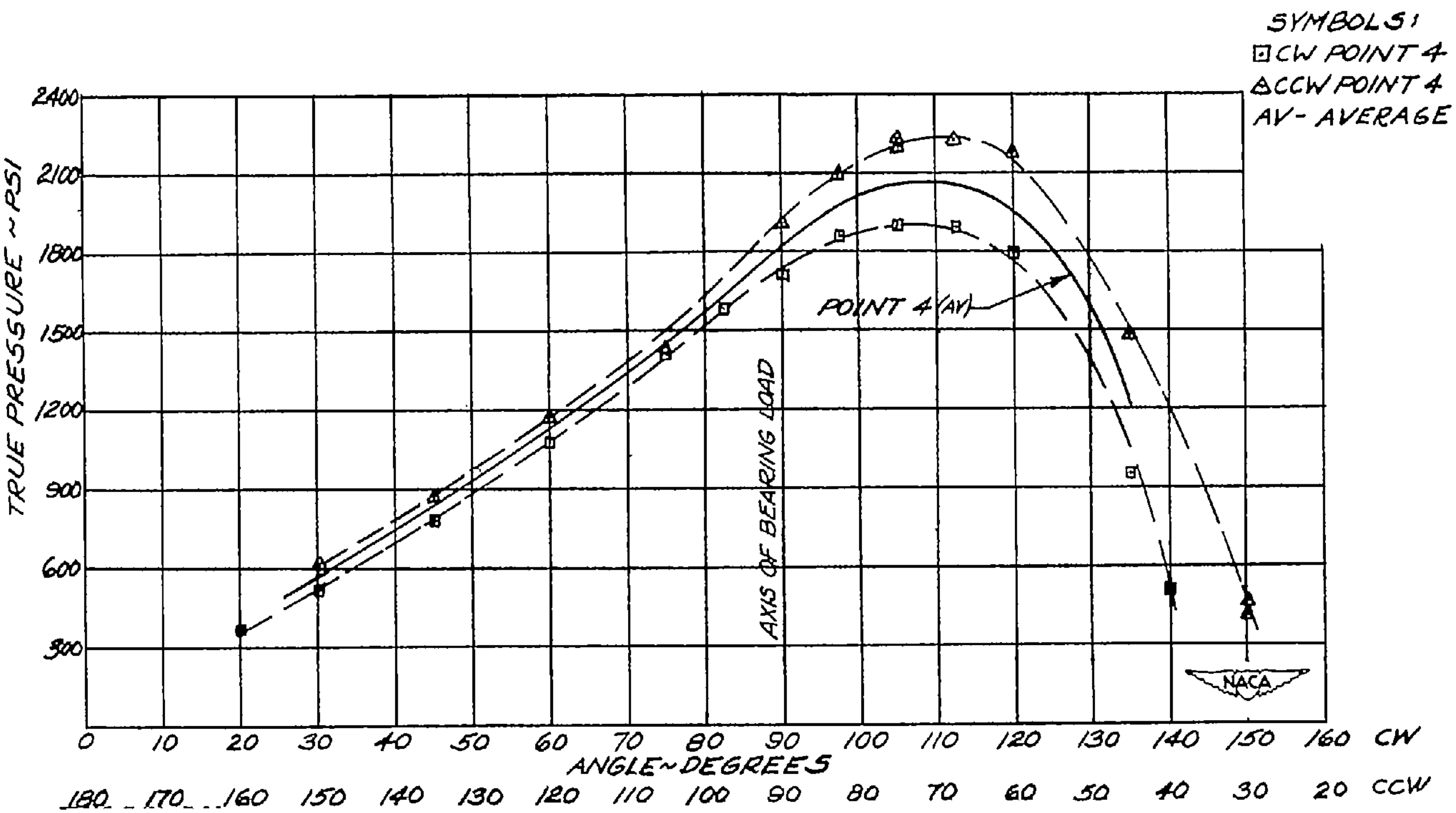

(c) Circumferential pressure distribution at midpoint of bearing (point 4), average of clockwise and counterclockwise rotation.

Figure 16.- Continued.

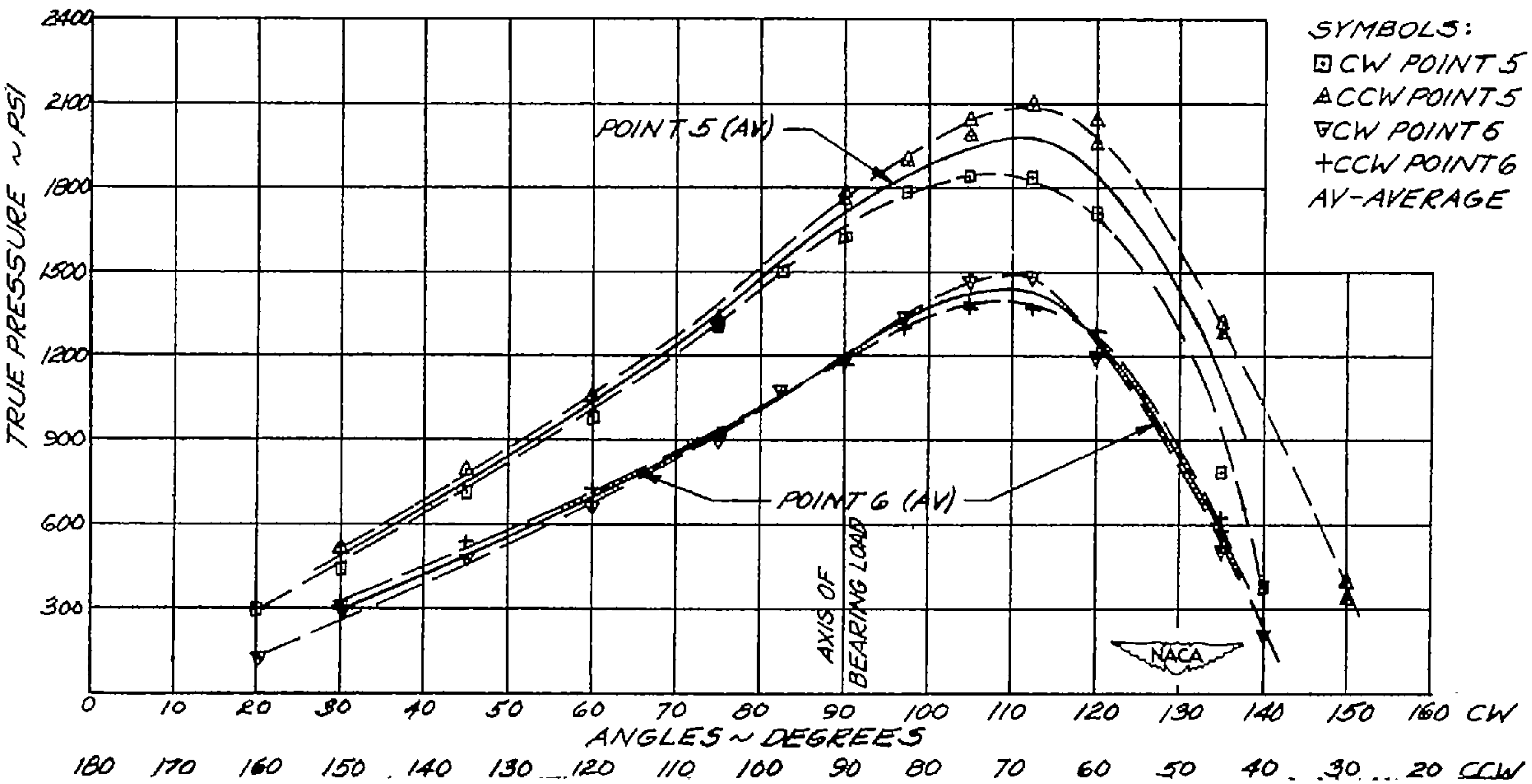

(d) Circumferential pressure distribution at points 5 and 6, average of clockwise and counterclockwise rotation.

Figure 16.- Continued.

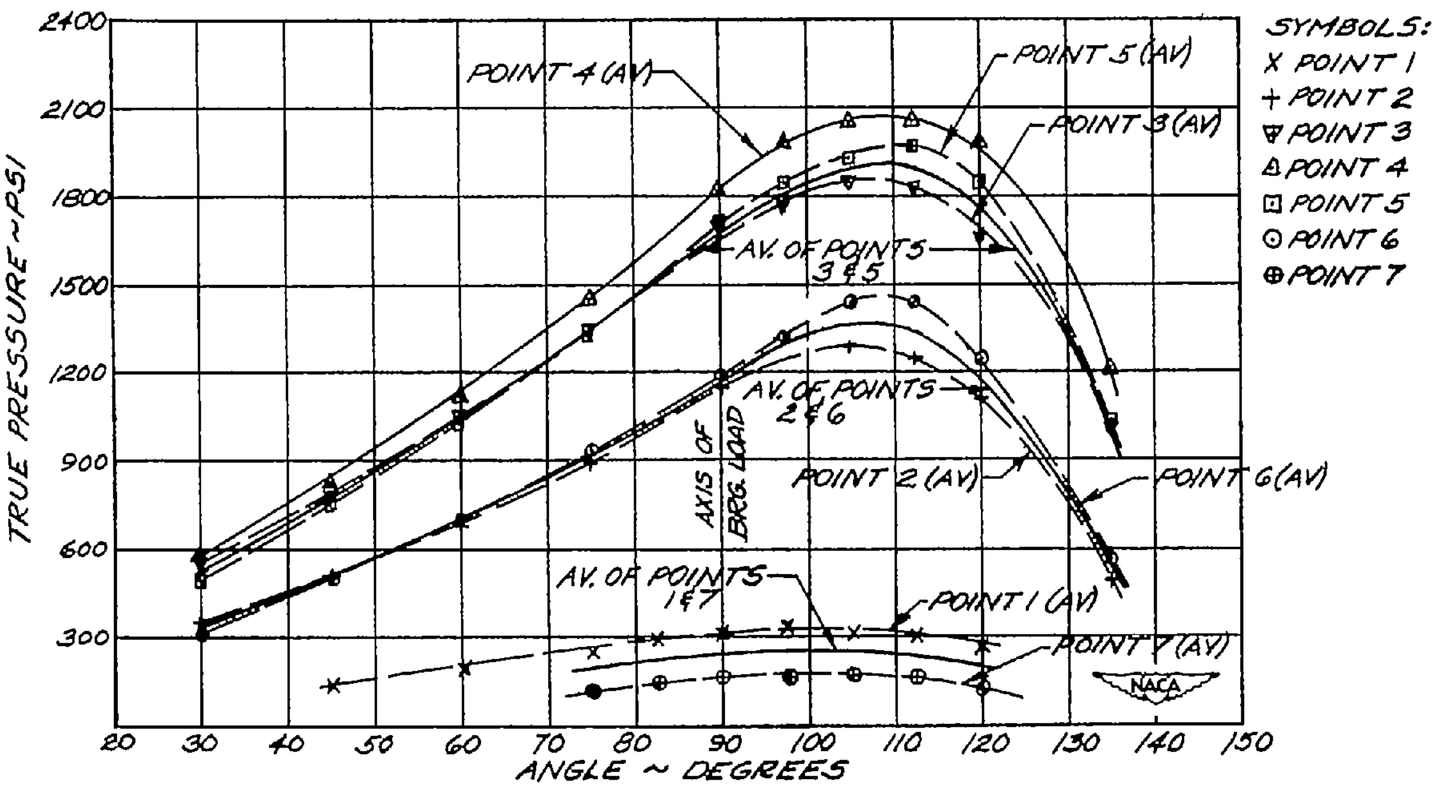

(e) Circumferential pressure distribution, averages of points 1 and 7, 2 and 6, 3 and 5, and 4.

Figure 16.- Continued.

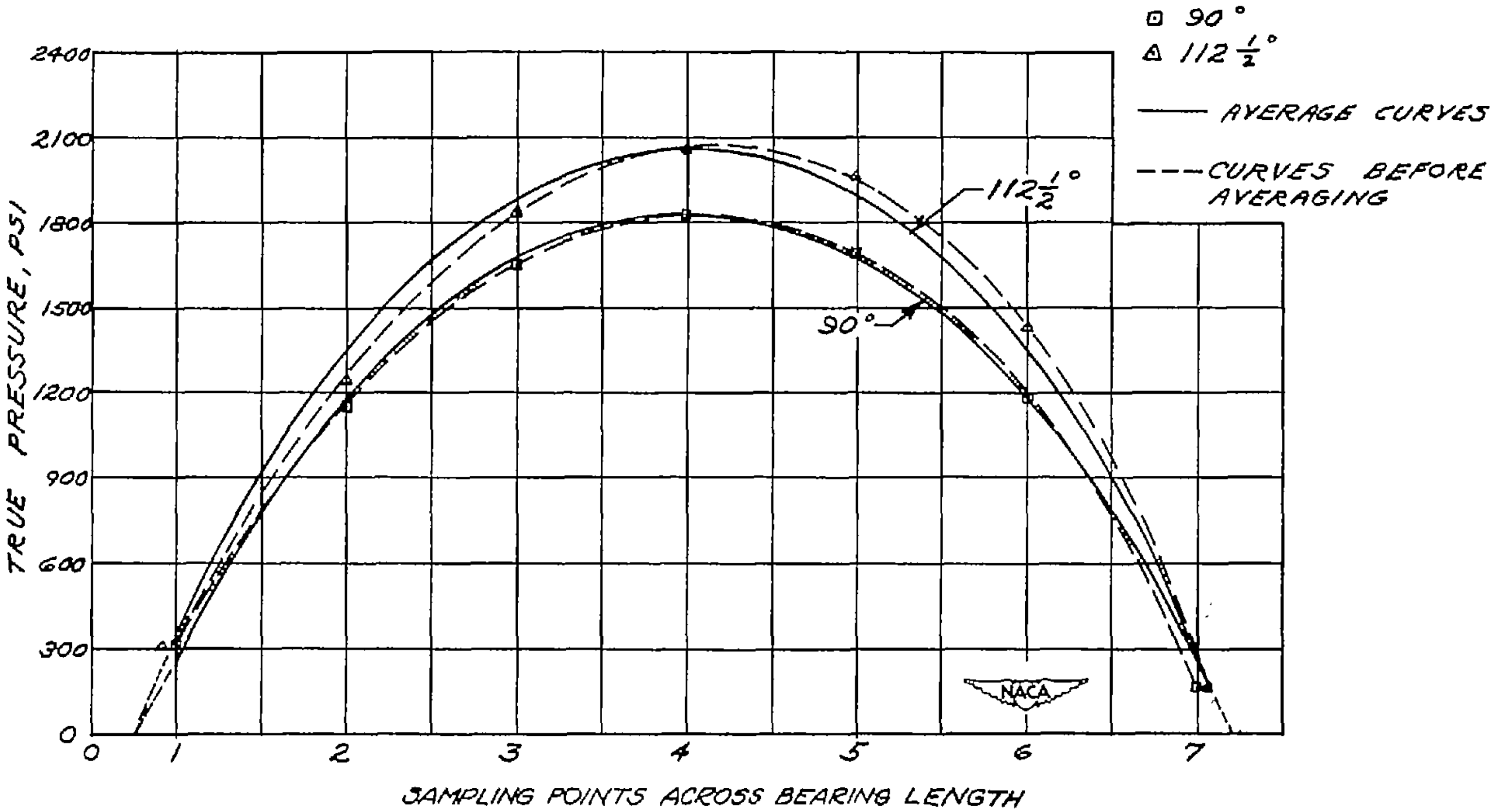

(f) Pressure distribution along length of bearing for given angular locations. Cross plot of pressures from figure 16(e). See figure 16(h) for complete transverse section.

Figure 16.- Continued.

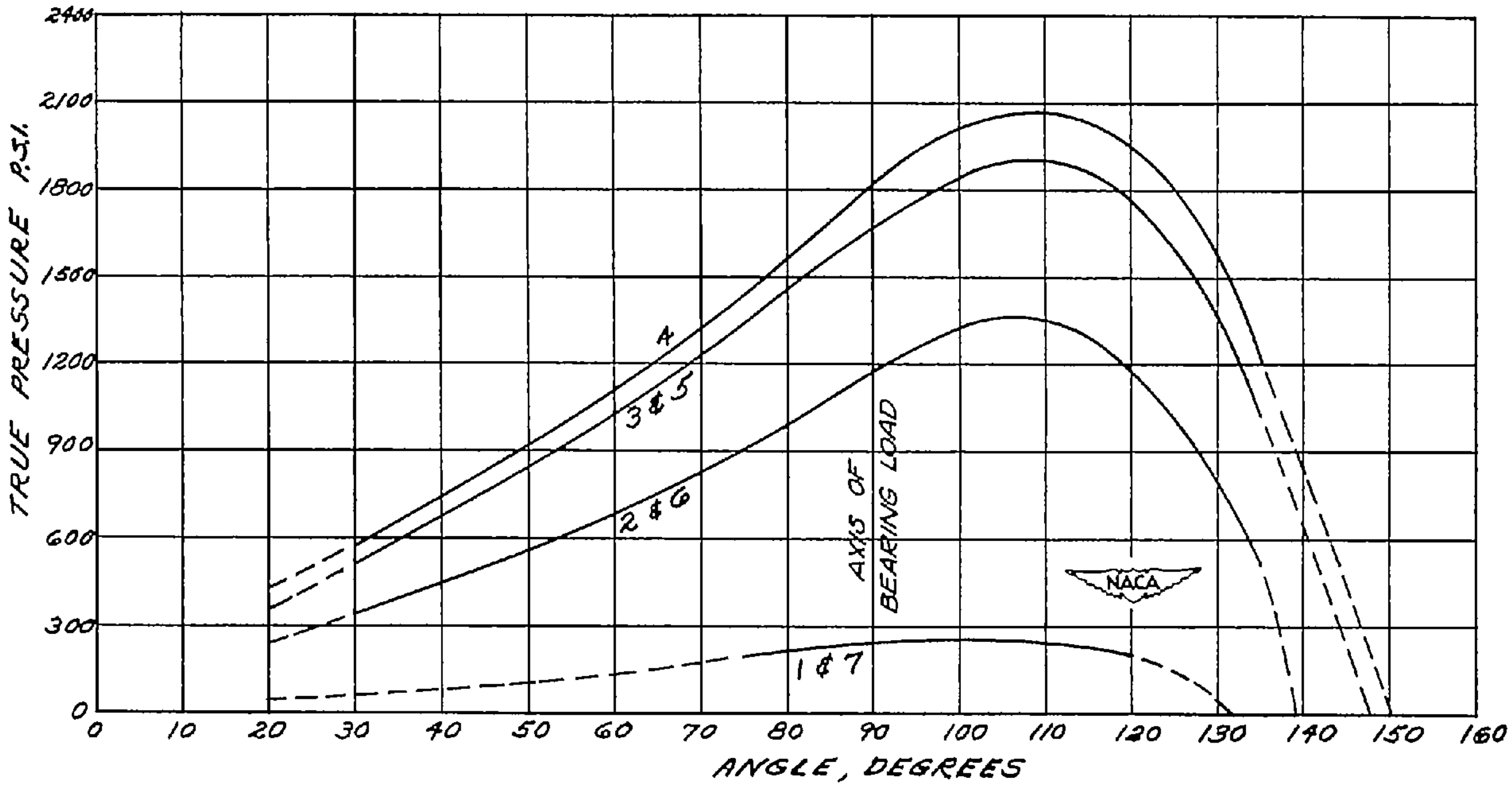

(g) Longitudinal sections of model 2.

Figure 16.- Continued.

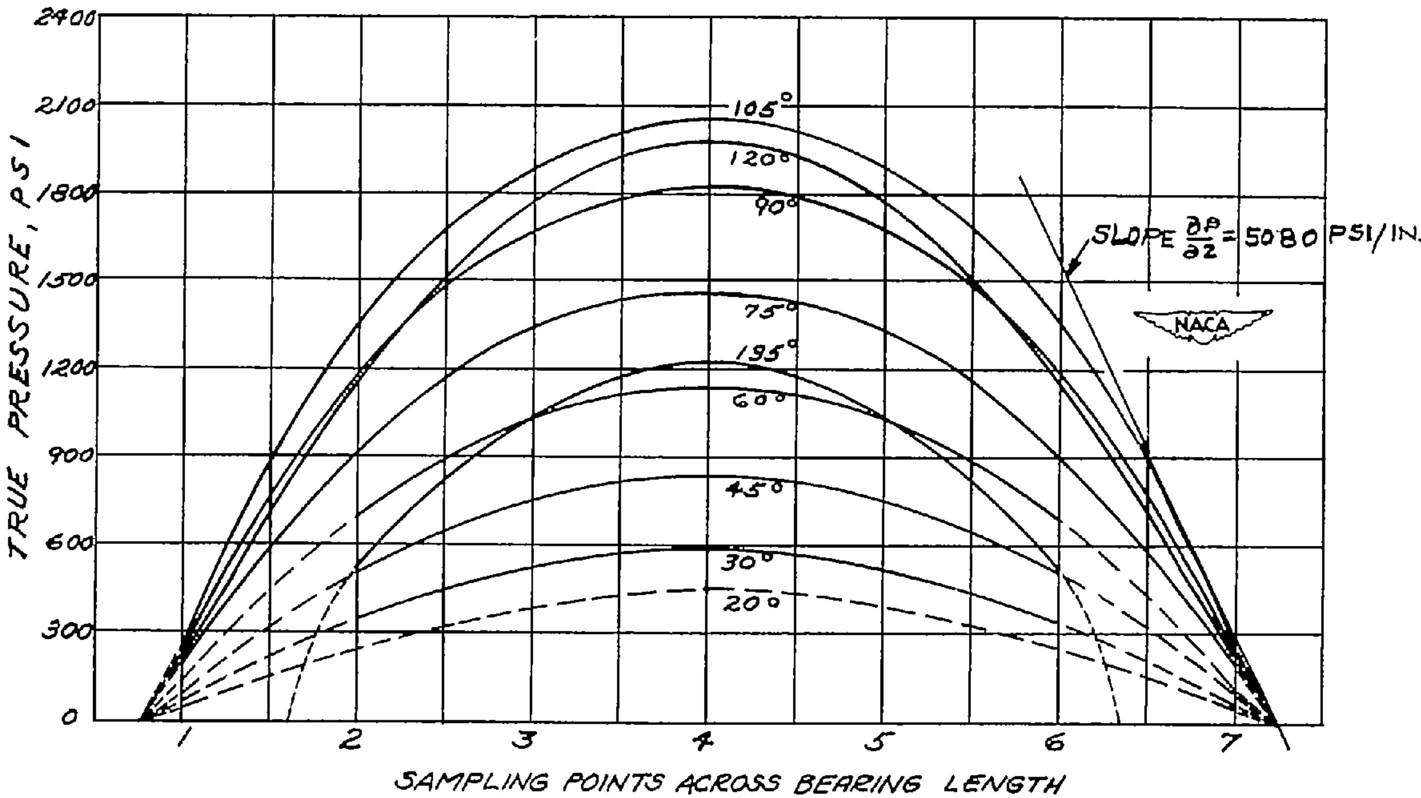

(h) Transverse sections of model 2.

Figure 16.- Concluded.

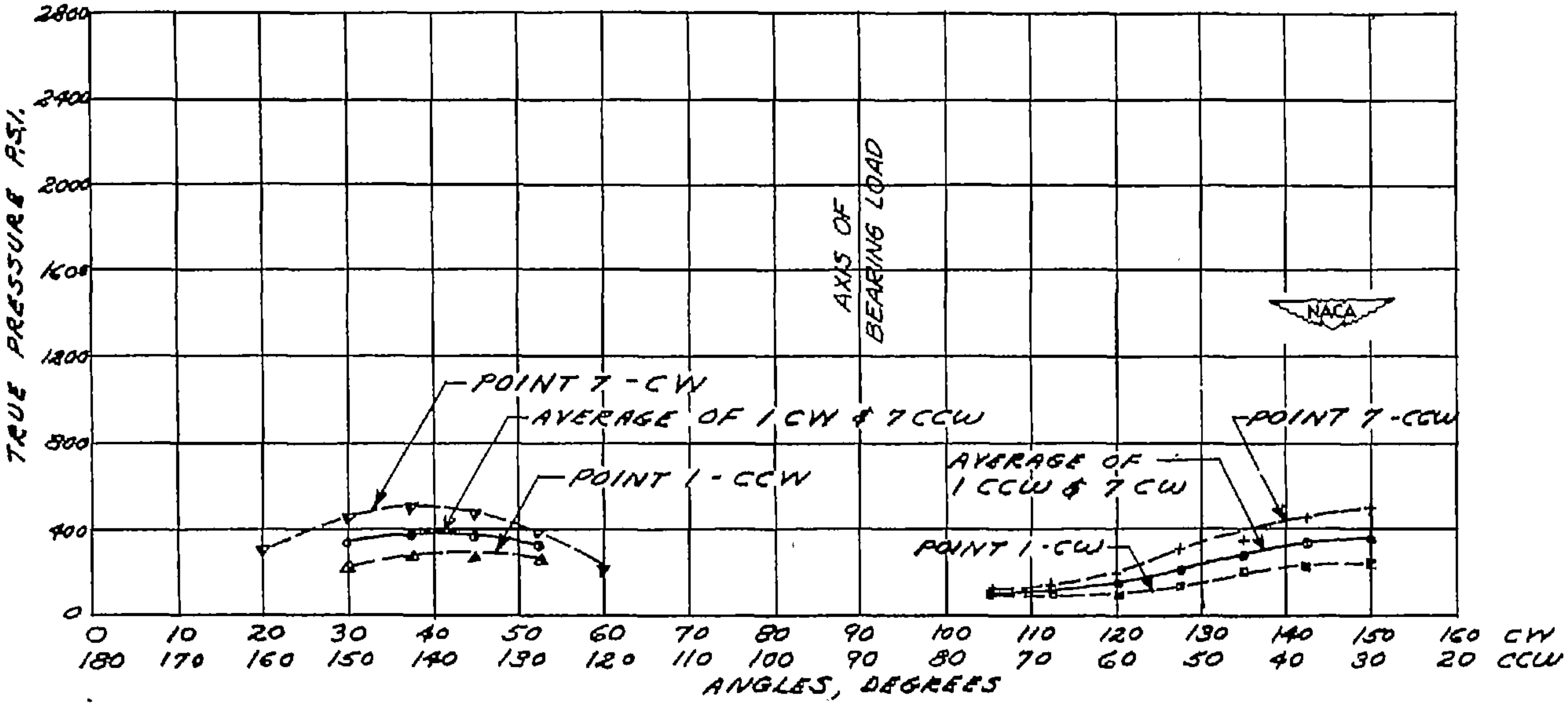

(a) Circumferential pressure distribution at points 1 and 7, average of clockwise and counterclockwise rotation.

Figure 17.- Oil film pressure distribution with central load and 17-percent twist (data for model 3). Shaft speed, 5000 rpm; load on projected area, 850 pounds per square inch; bearing diameter, 1.60 inches; bearing length, 1.62 inches; bearing clearance, 0.0026 inch per inch of diameter.

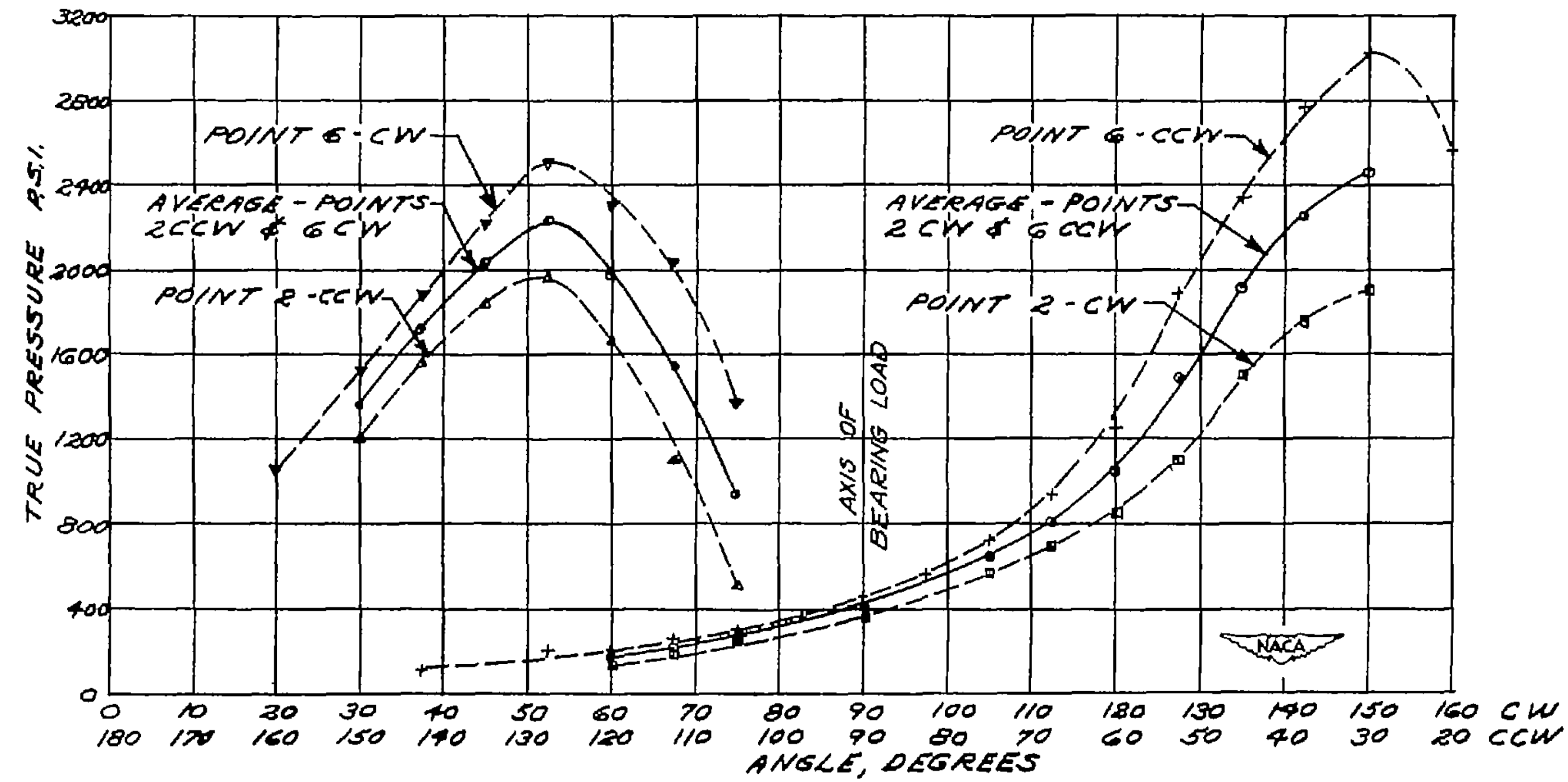

(b) Circumferential pressure distribution at points 2 and 6, average of clockwise and counterclockwise rotation.

Figure 17.- Continued.

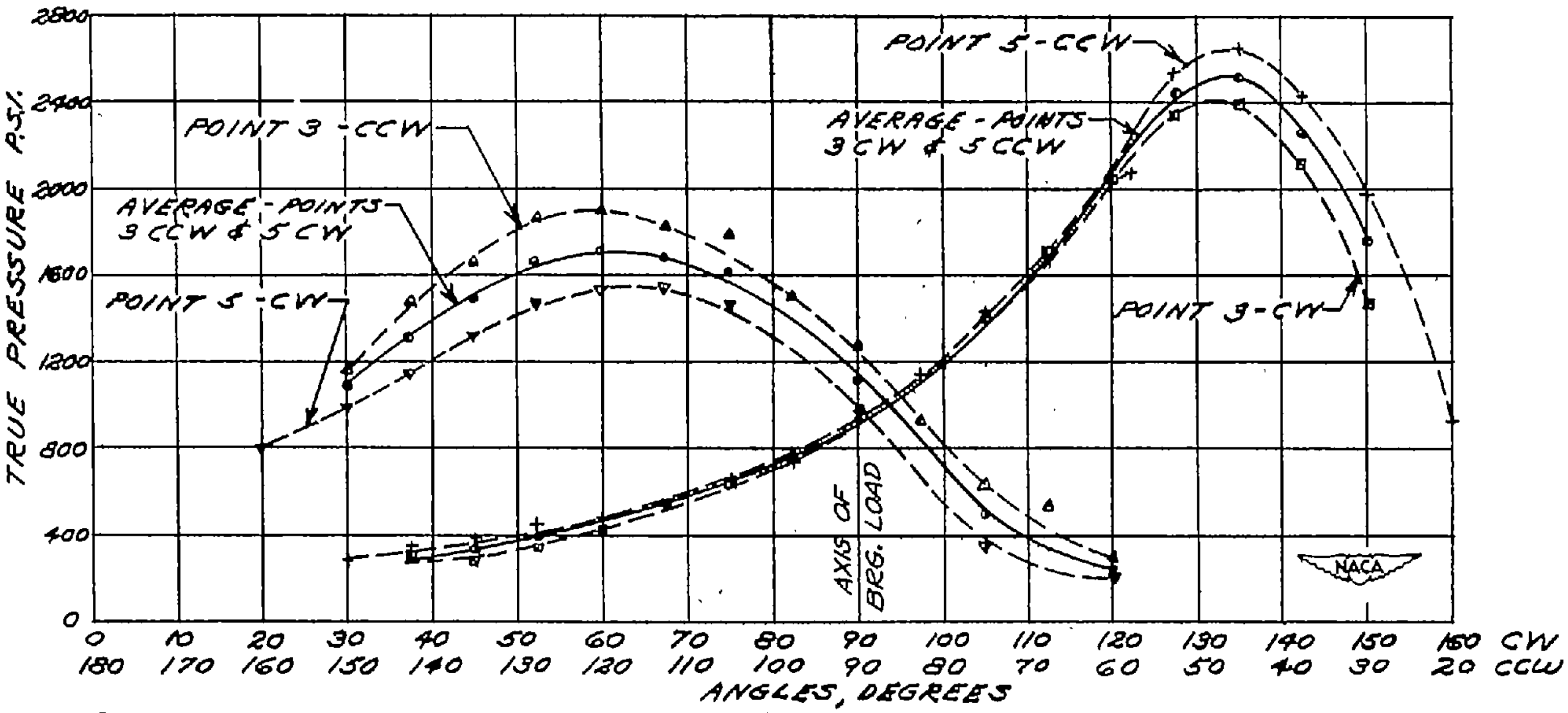

(c) Circumferential pressure distribution at points 3 and 5, average of clockwise and counterclockwise rotation.

Figure 17.- Continued.

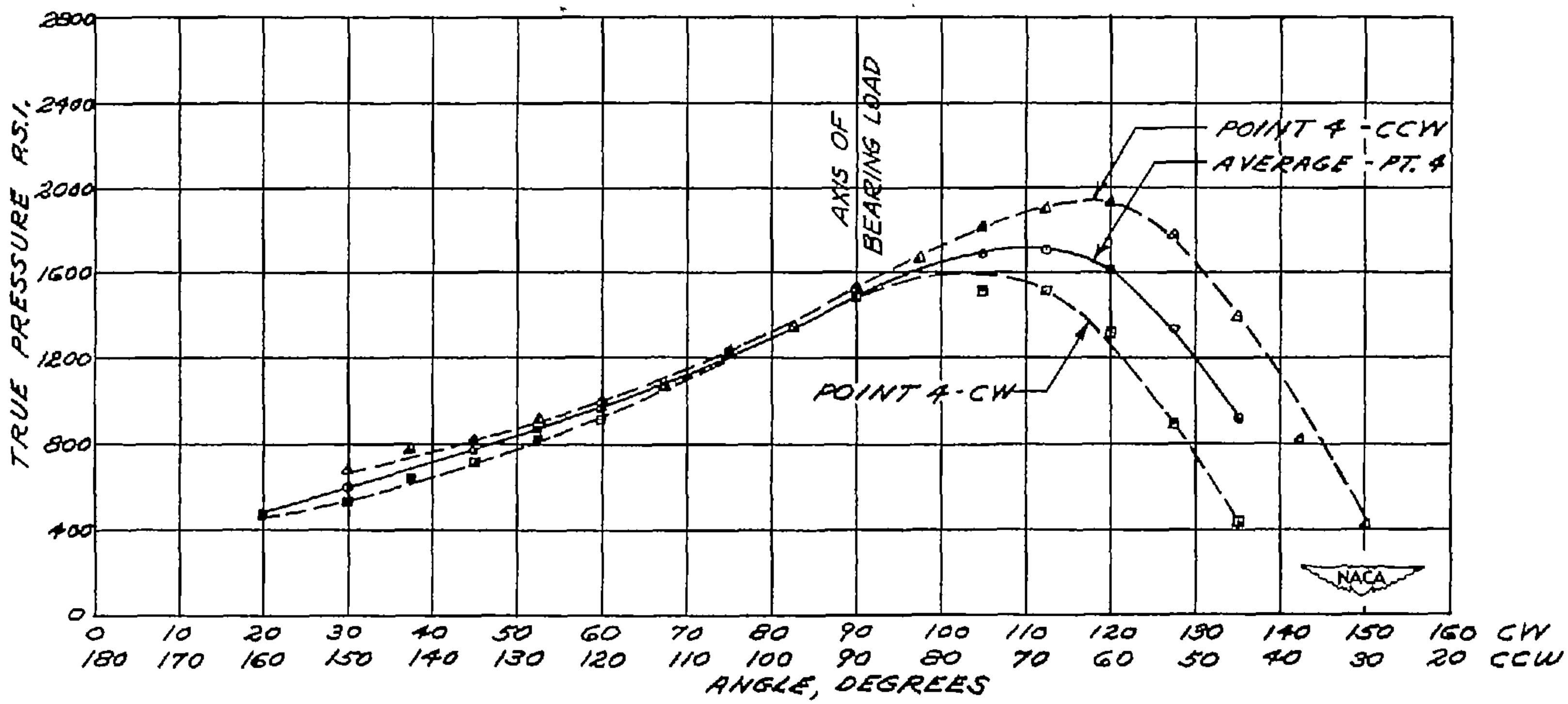

(d) Circumferential pressure distribution at midpoint of bearing (point 4), average of clockwise and counterclockwise rotation.

Figure 17.- Continued.

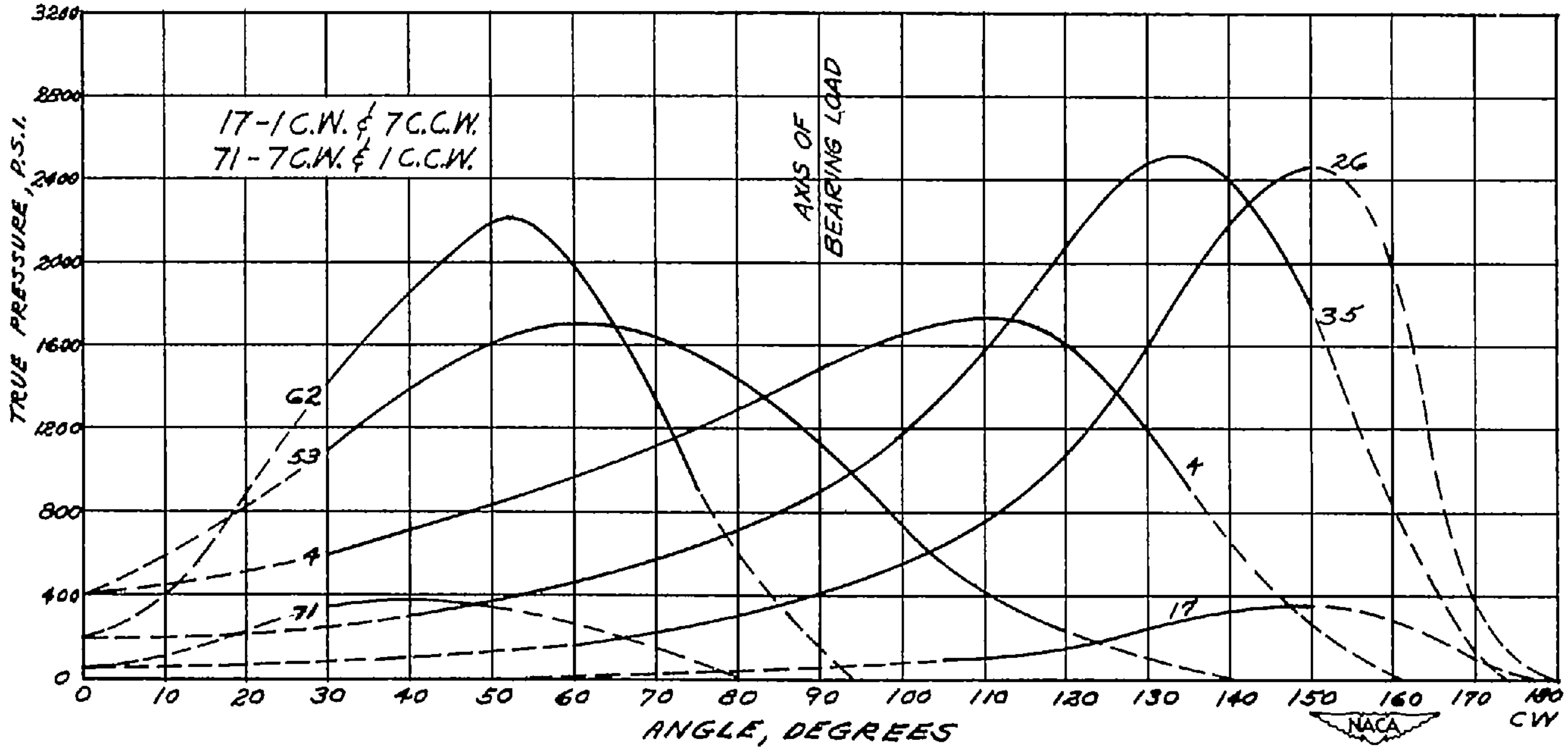

(e) Longitudinal sections of model 3.

Figure 17.- Continued.

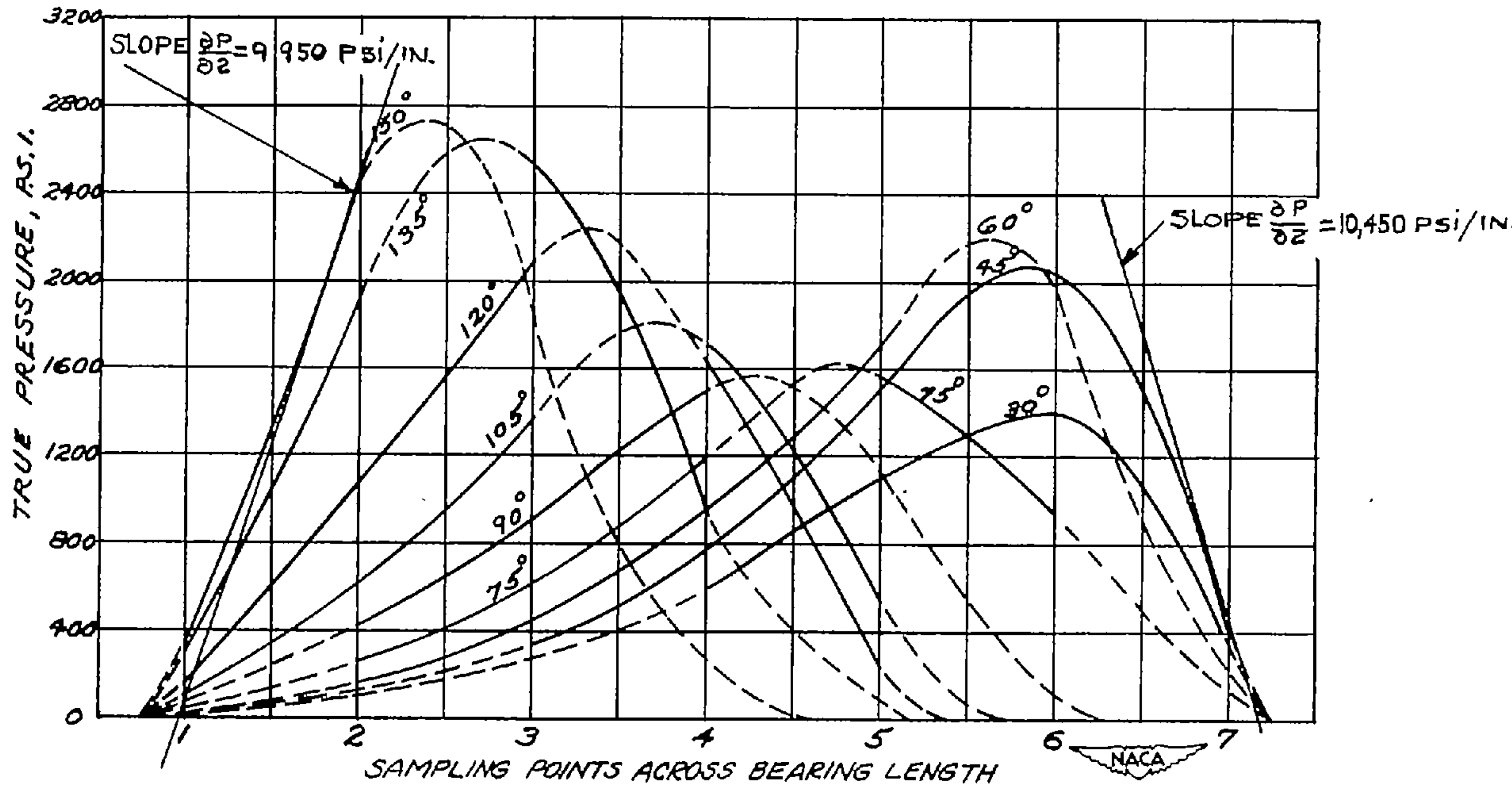

(f) Transverse sections of model 3.

Figure 17.- Concluded.

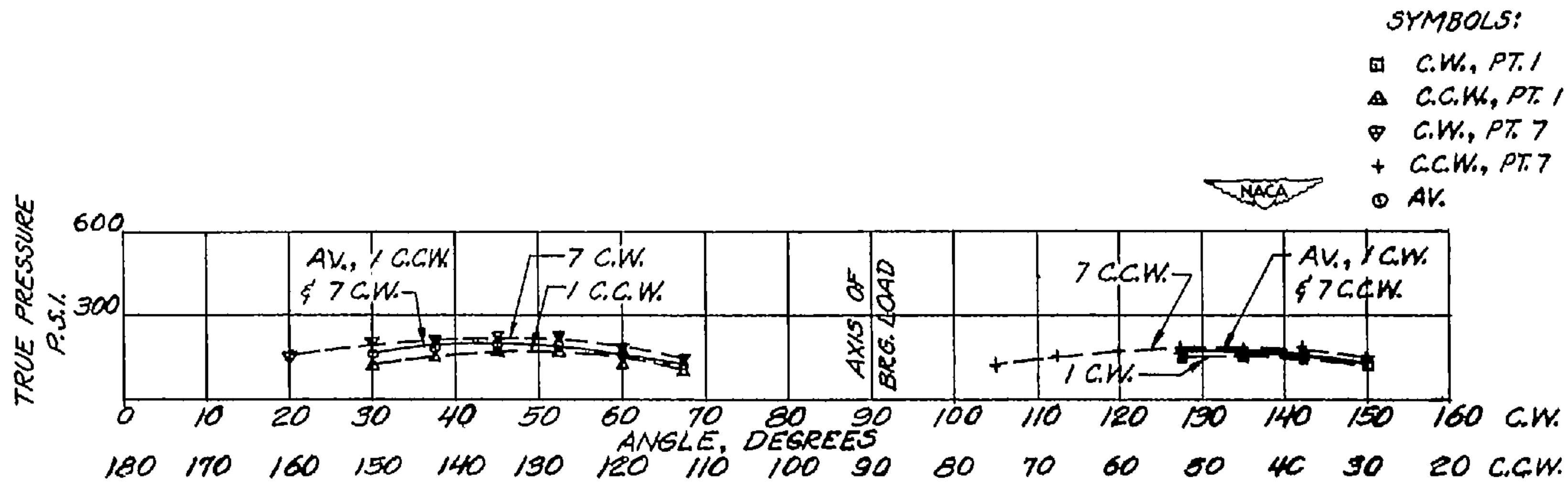

(a) Circumferential pressure distribution at points 1 and 7, average of clockwise and counterclockwise rotation.

Figure 18.- Oil film pressure distribution with central load and 8-percent twist (data for model 4). Shaft speed, 5000 rpm; load on projected area, 850 pounds per square inch; bearing diameter, 1.60 inches; bearing length, 1.62 inches; bearing clearance, 0.0026 inch per inch of diameter.

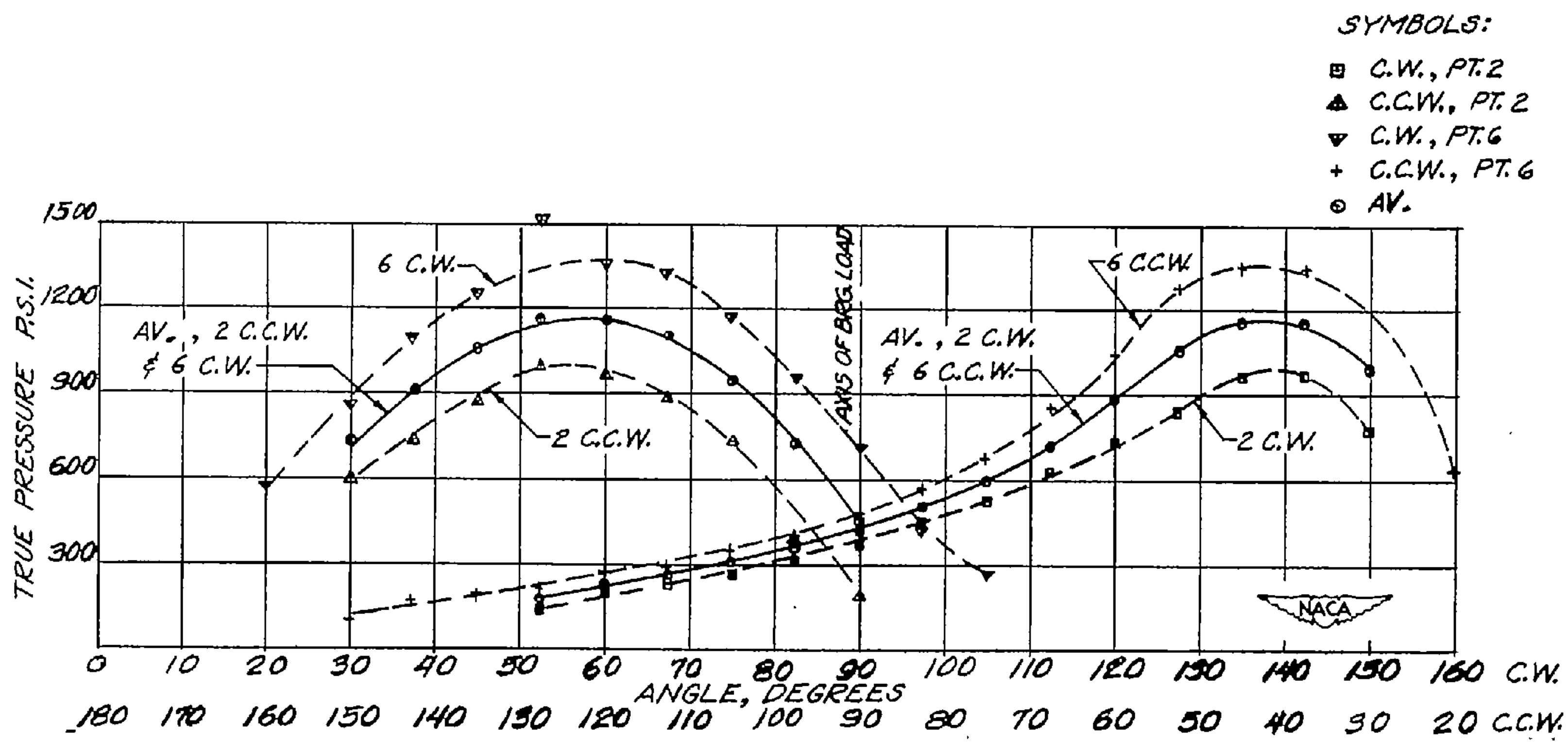

(b) Circumferential pressure distribution at points 2 and 6, average of clockwise and counterclockwise rotation.

Figure 18.- Continued.

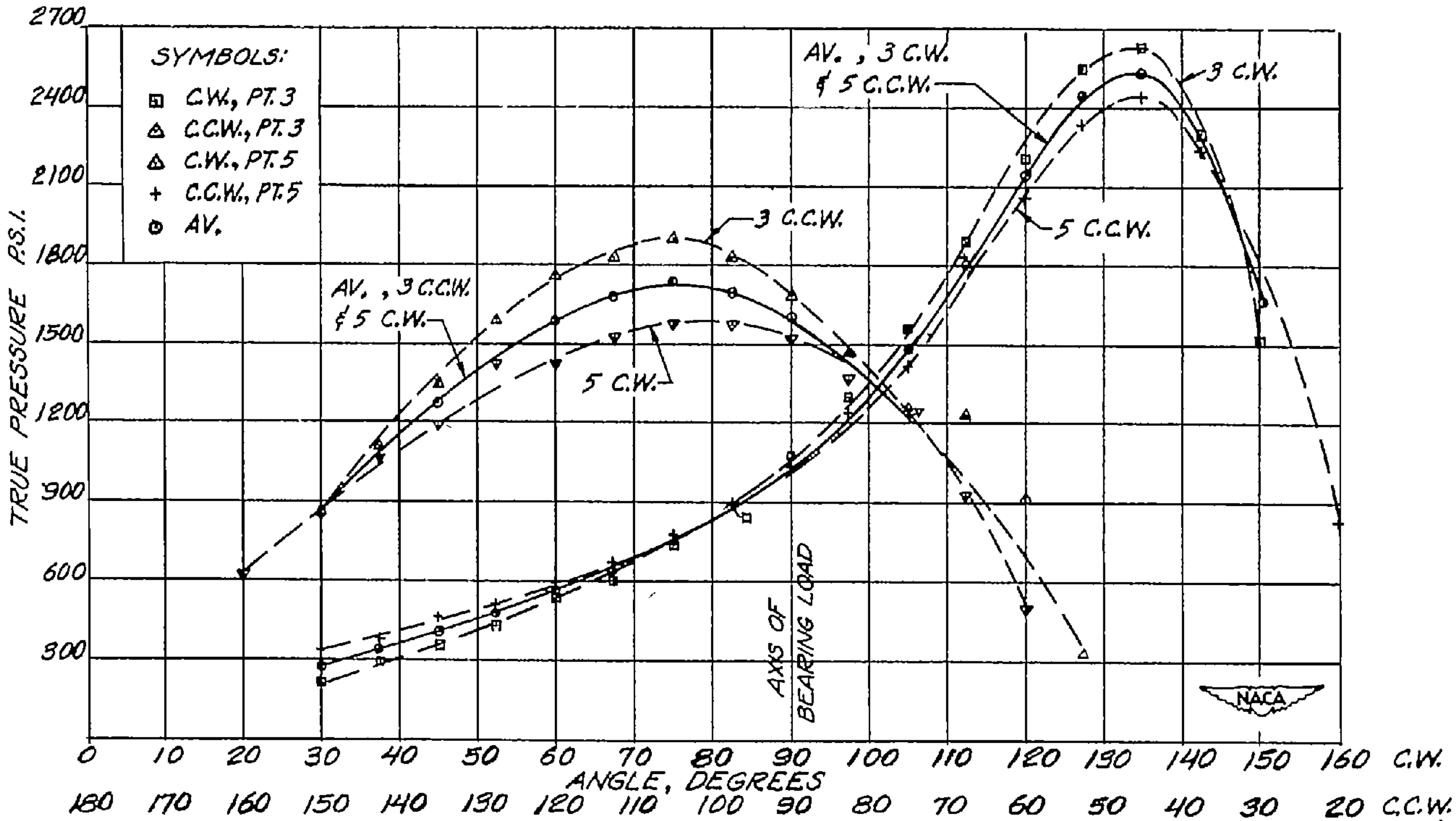

(c) Circumferential pressure distribution at points 3 and 5, average of clockwise and counterclockwise rotation.

Figure 18.- Continued.

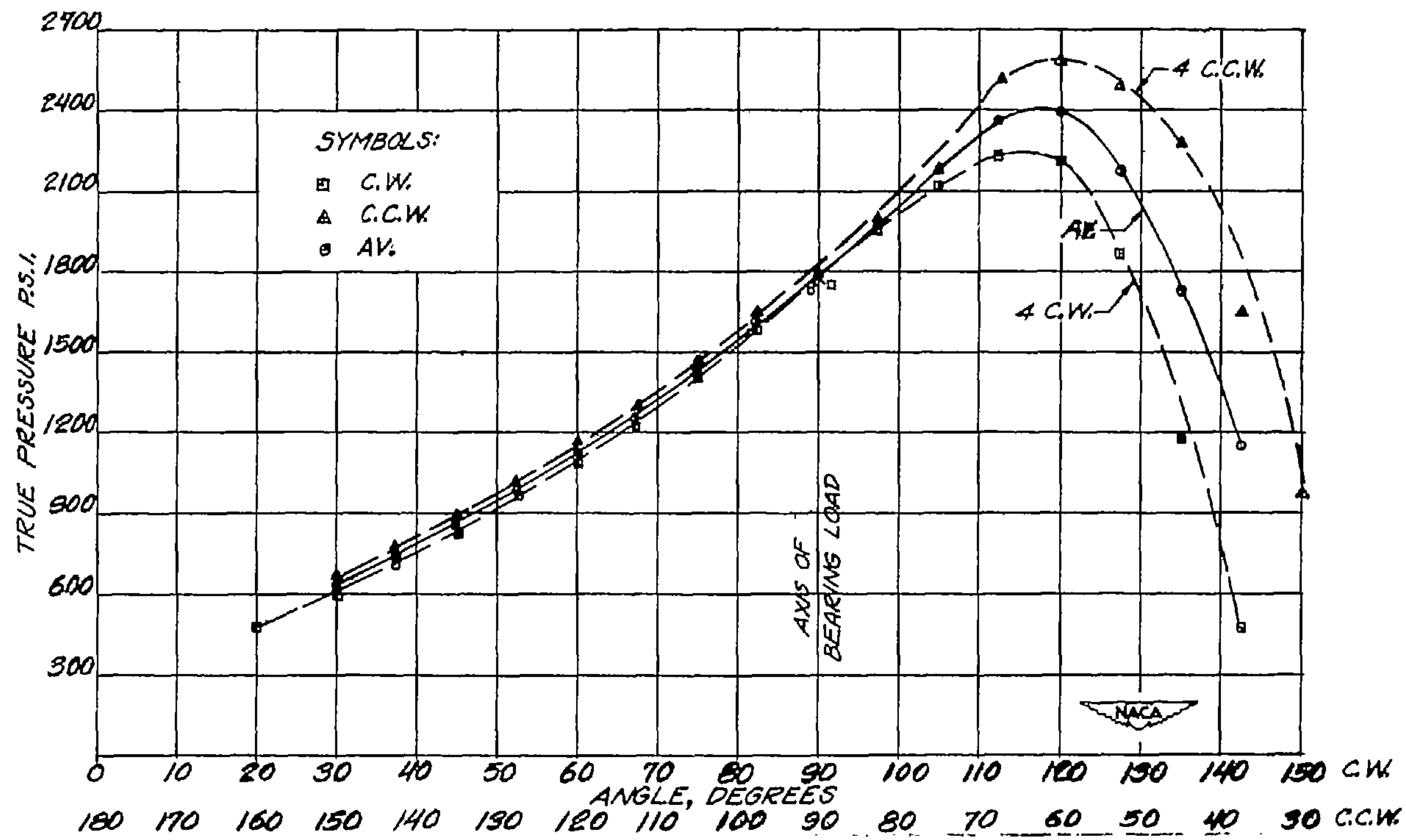

(d) Circumferential pressure distribution at midpoint of bearing (point 4), average of clockwise and counterclockwise rotation.

Figure 18.- Continued.

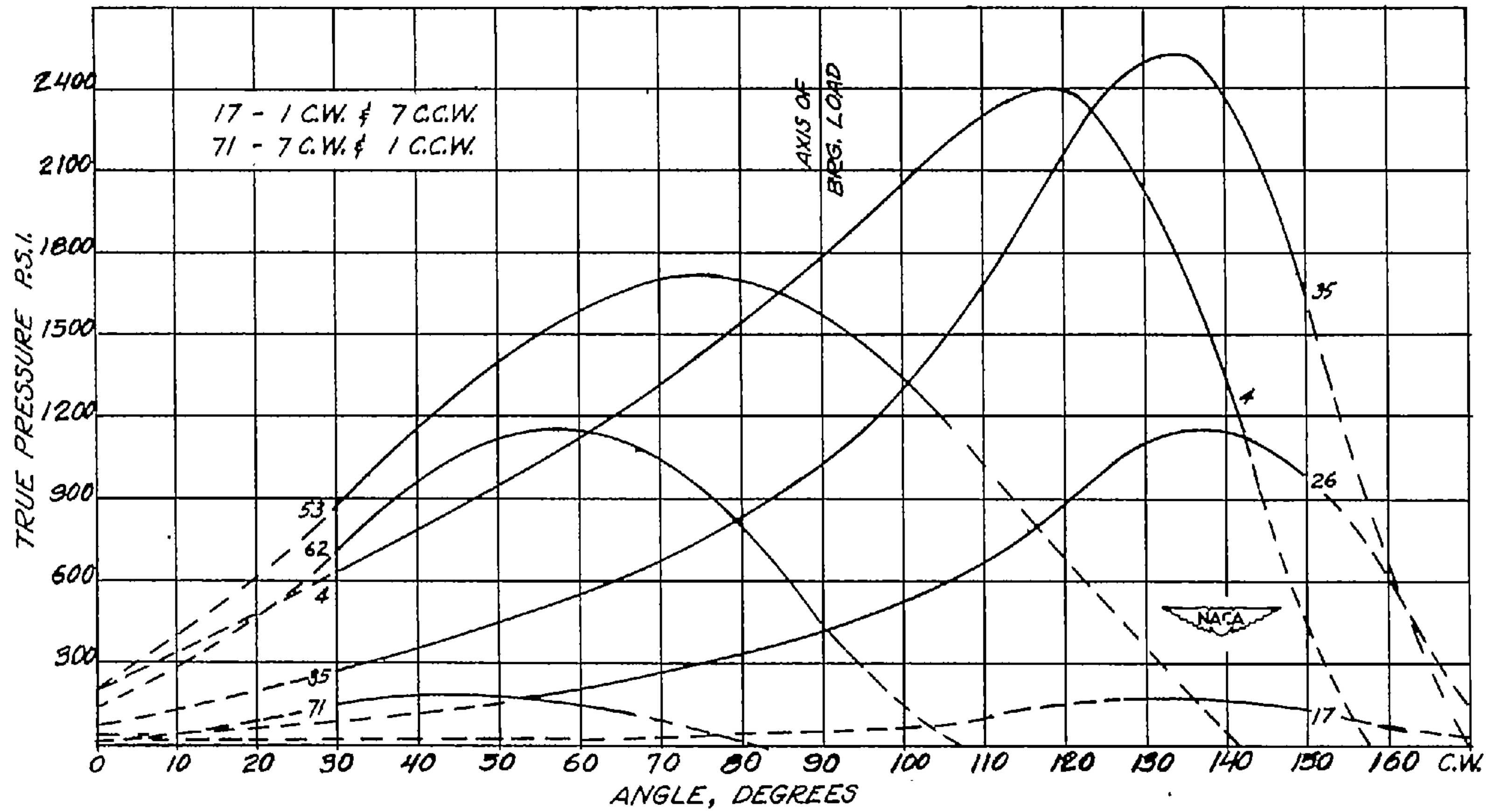

(e) Longitudinal sections of model 4.

Figure 18.- Continued.

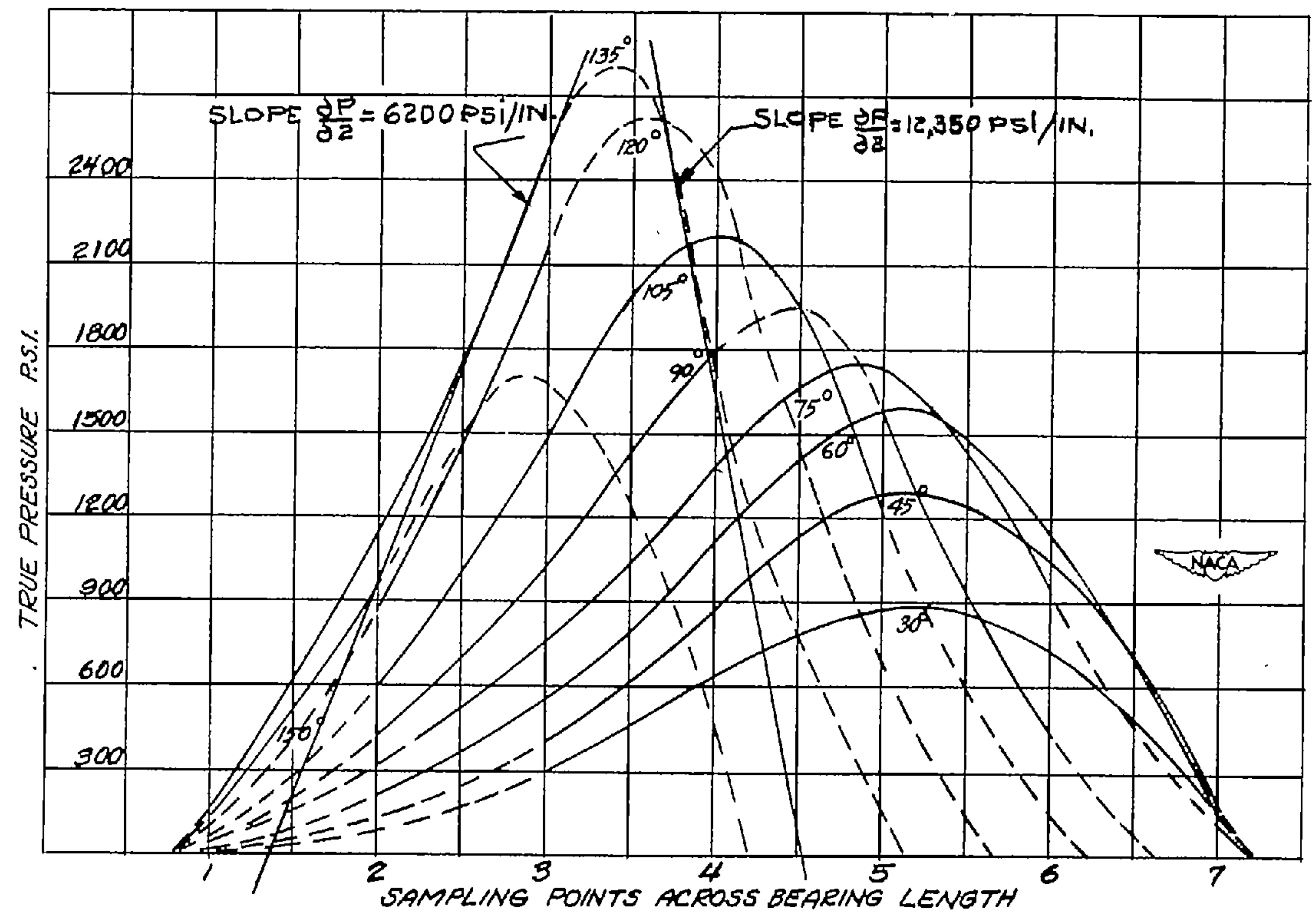

(f) Transverse sections of model 4.

Figure 18.- Concluded.

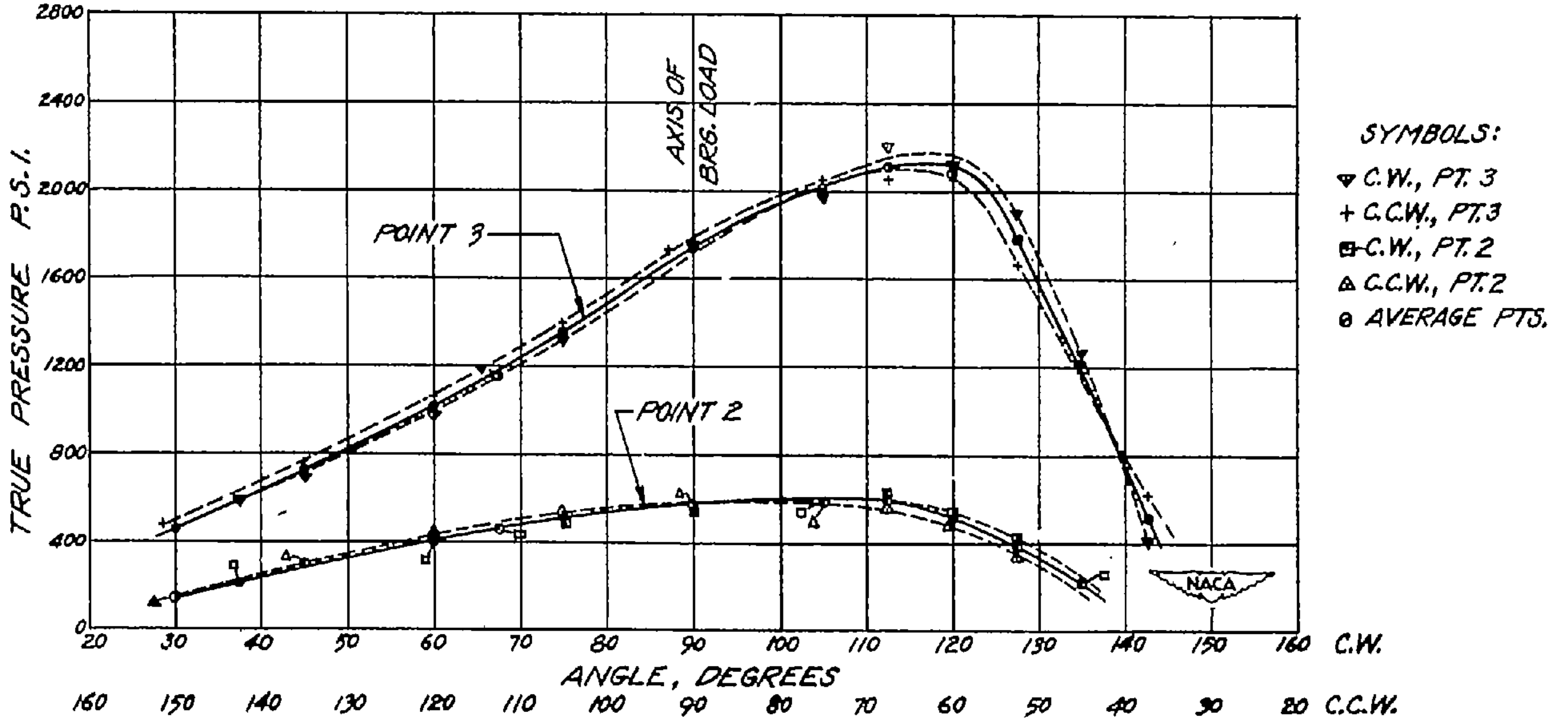

(a) Circumferential pressure distribution at points 2 and 3, average of clockwise and counterclockwise rotation.

Figure 19.- Oil film pressure distribution with central load and zero misalinement after bellmouthing by misalinement tests (data for model 5). Shaft speed, 5000 rpm; load on projected area, 850 pounds per square inch; bearing diameter, 1.60 inches; bearing length, 1.62 inches; bearing clearance, 0.0026 inch per inch of diameter.

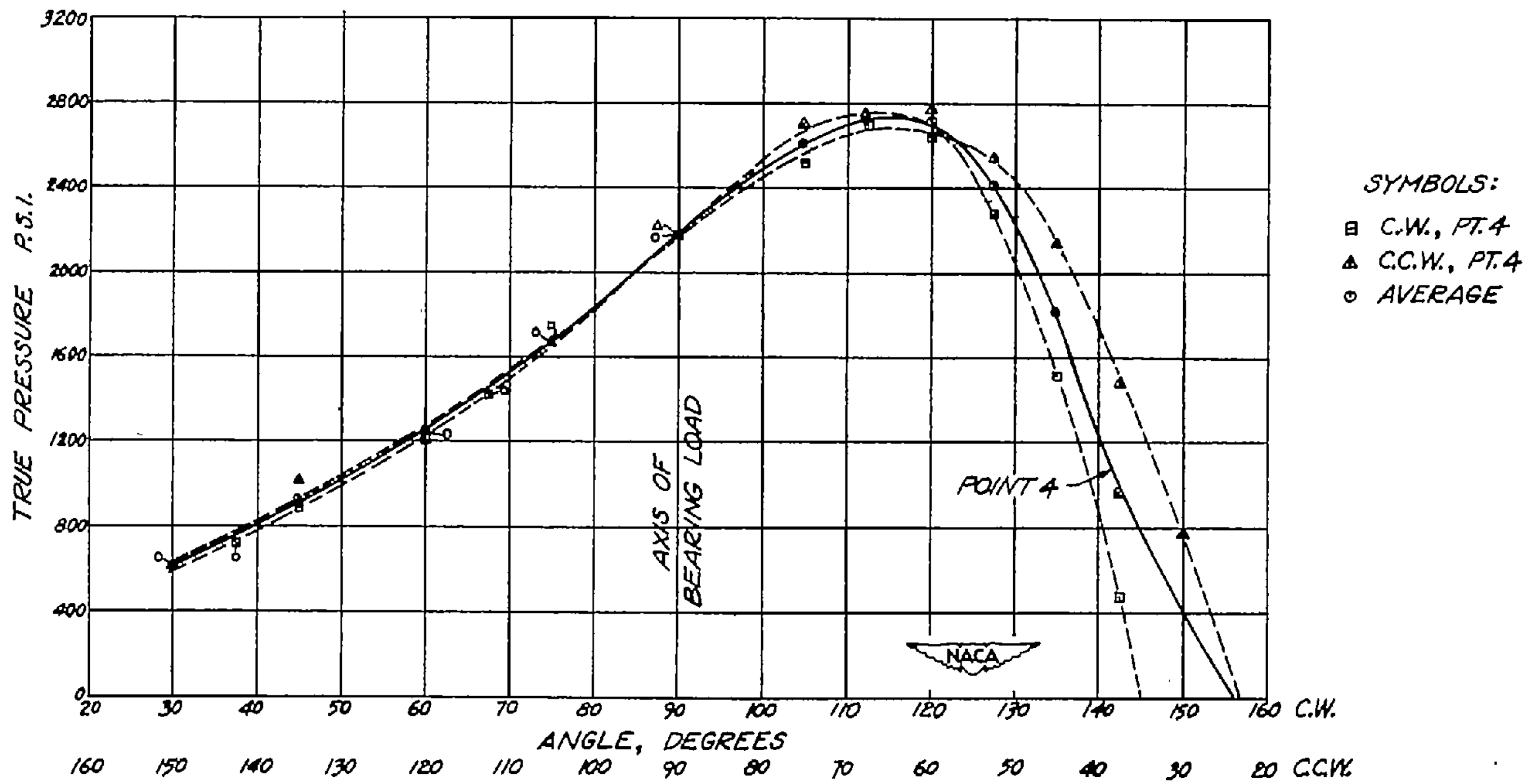

(b) Circumferential pressure distribution at midpoint of bearing (point 4), average of clockwise and counterclockwise rotation.

Figure 19.- Continued.

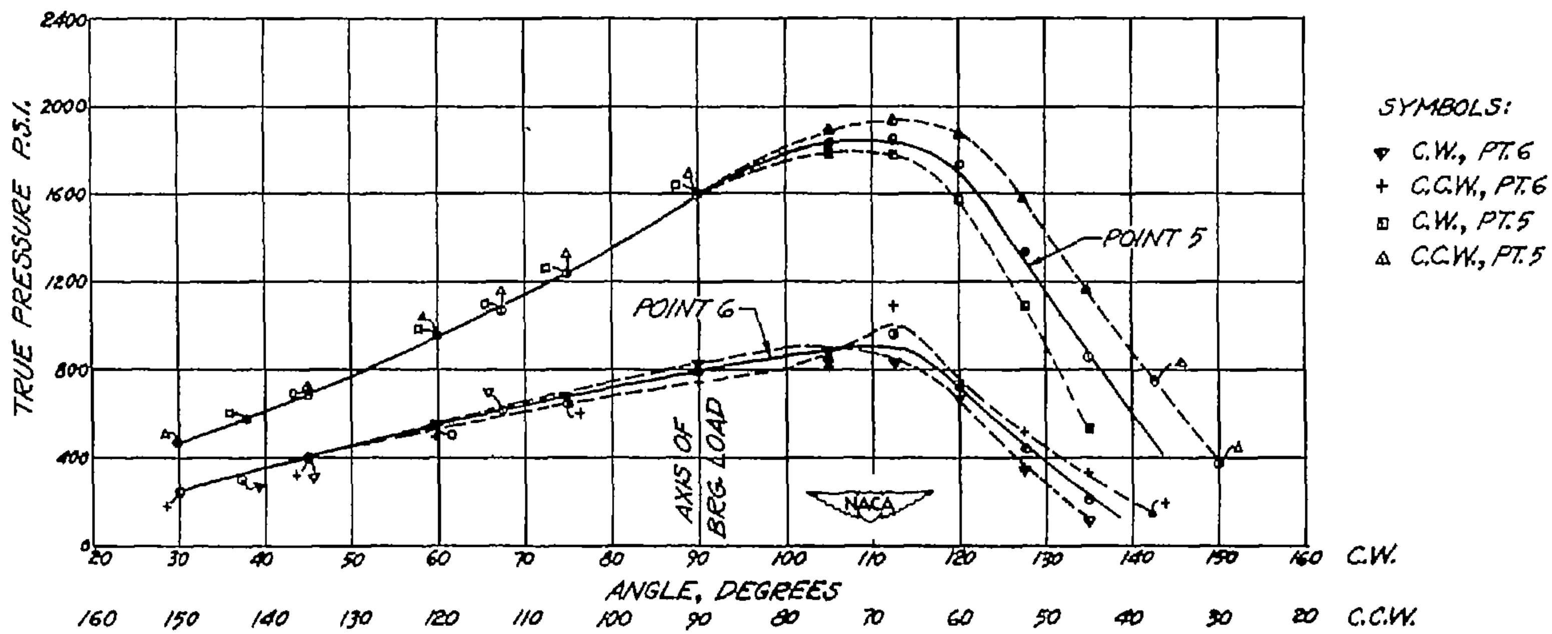

(c) Circumferential pressure distribution at points 5 and 6, average of clockwise and counterclockwise rotation.

Figure 19.- Continued.

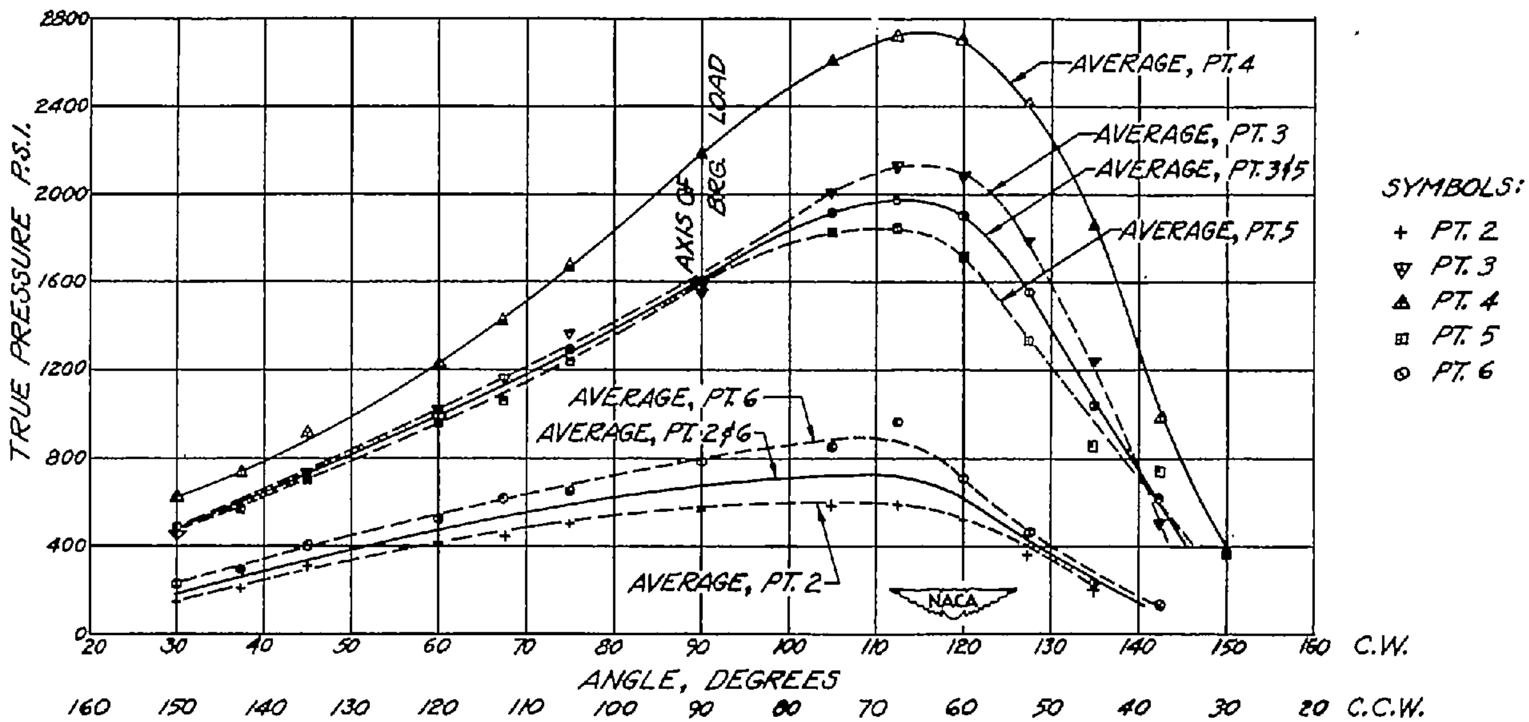

(d) Circumferential pressure distribution, averages of points 2 and 6, 3 and 5, and 4.

Figure 19.- Continued.

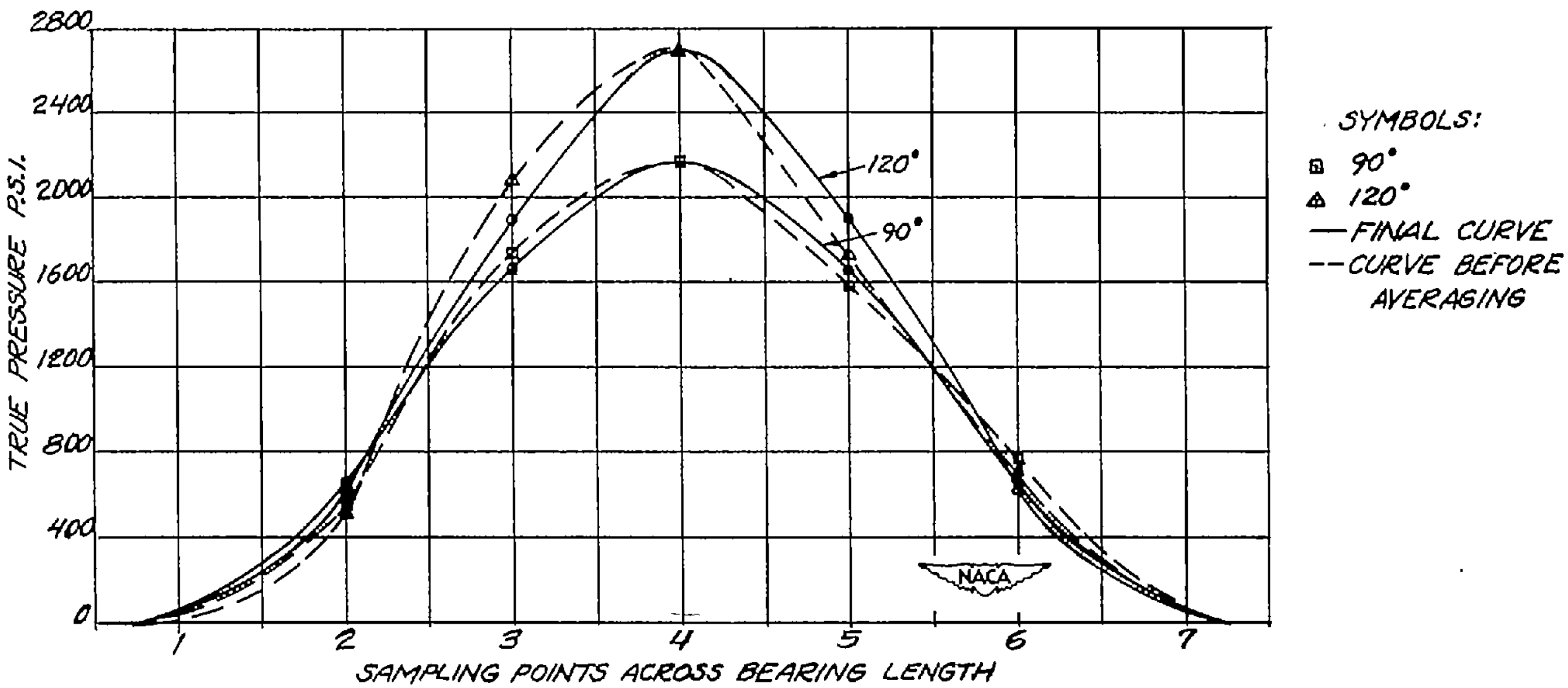

(e) Pressure distribution along length of bearing for given angular locations. Cross plot of pressures from figure 19(d). See figure 19(g) for complete transverse section.

Figure 19.- Continued.

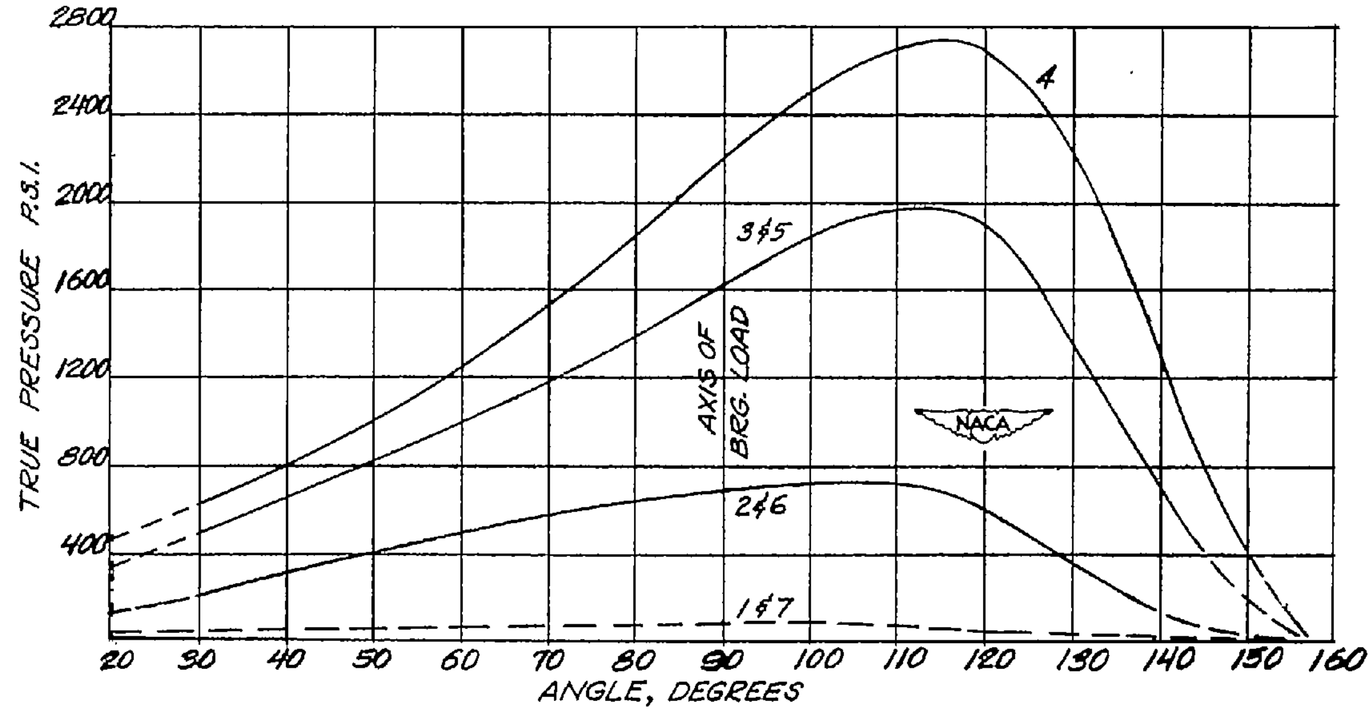

(f) Longitudinal sections of model 5.

Figure 19.- Continued.

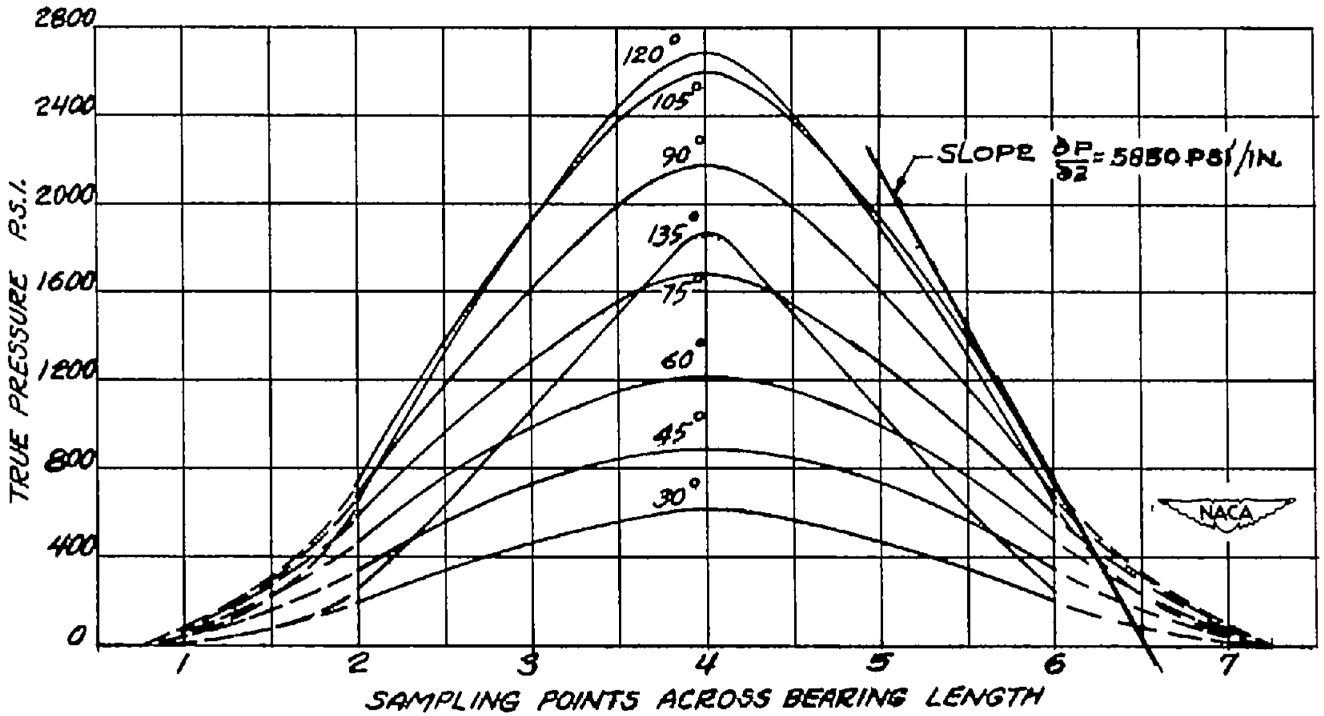

(g) Transverse sections of model 5.

Figure 19.- Concluded.

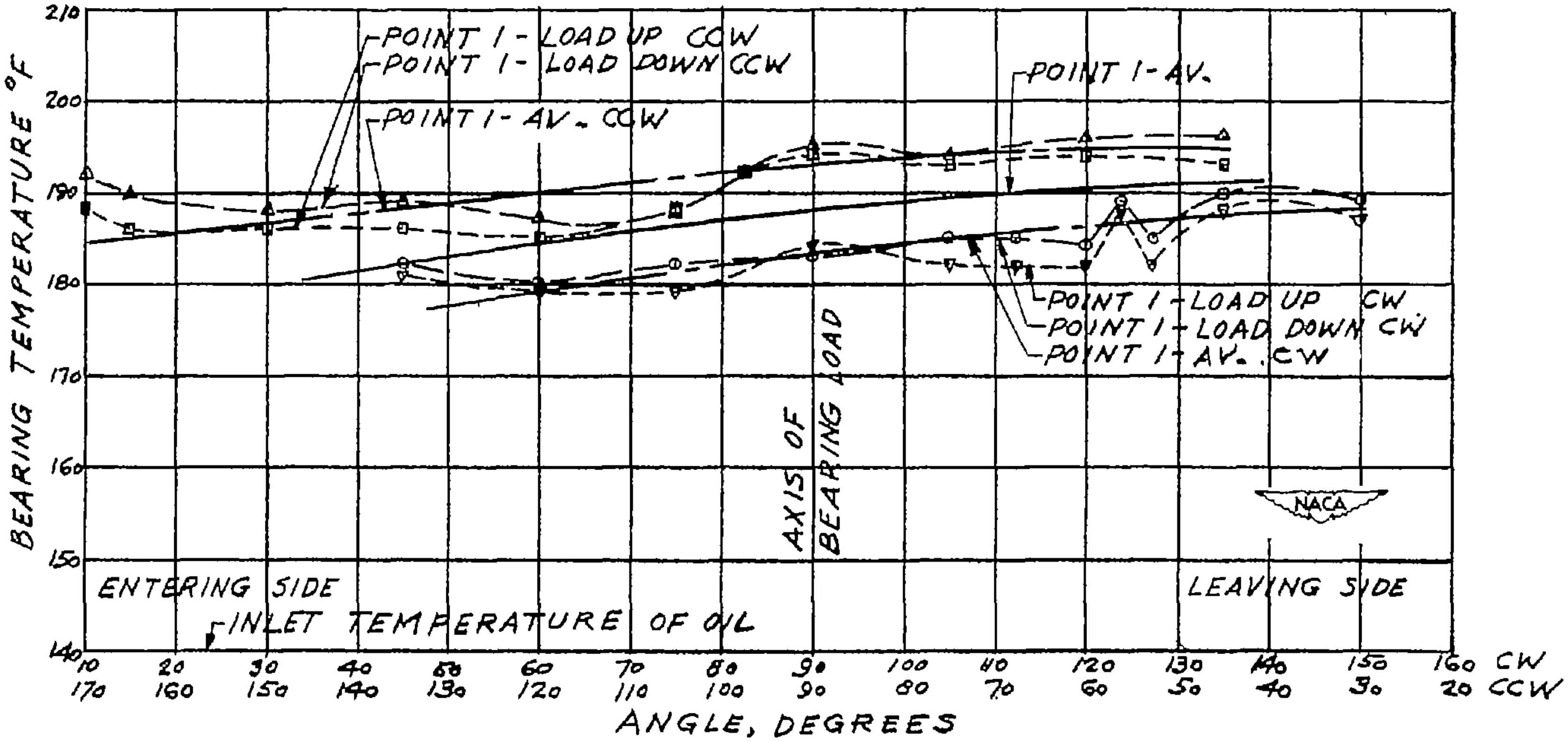

(a) Circumferential bearing temperature distribution of point 1, average of up and down axial misalinement, clockwise and counterclockwise rotation.

Figure 20.- Bearing temperature distribution with central load and 16-percent axial misalinement (data for model 1). Shaft speed, 5000 rpm; load on projected area, 850 pounds per square inch; bearing diameter, 1.62 inches; bearing length, 1.62 inches; bearing clearance, 0.002 inch per inch of diameter; inlet temperature of no. 1120 Aviation oil at 40 pounds per square inch, 140° F.

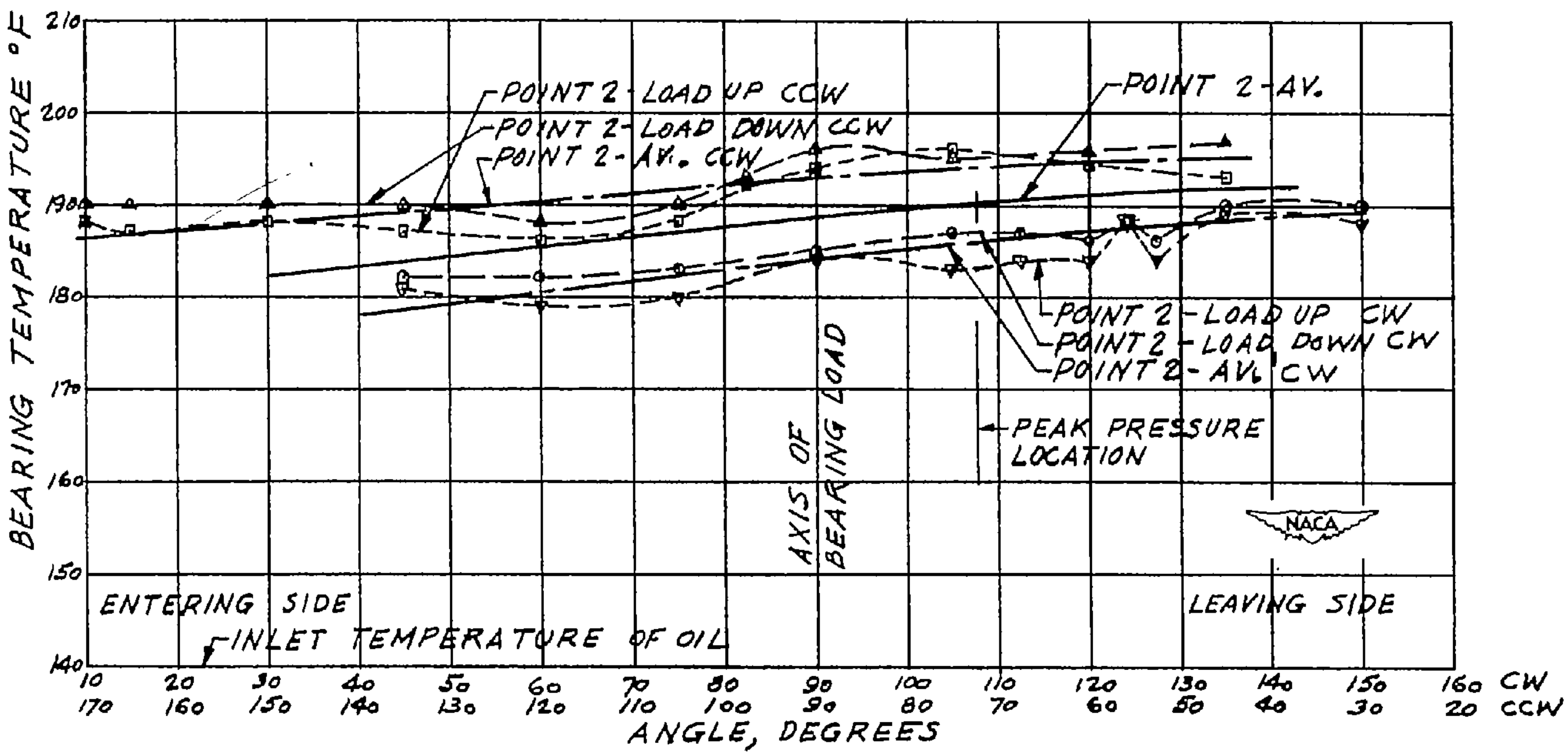

(b) Circumferential bearing temperature distribution of point 2, average of up and down axial misalinement, clockwise and counterclockwise rotation.

Figure 20.- Continued.

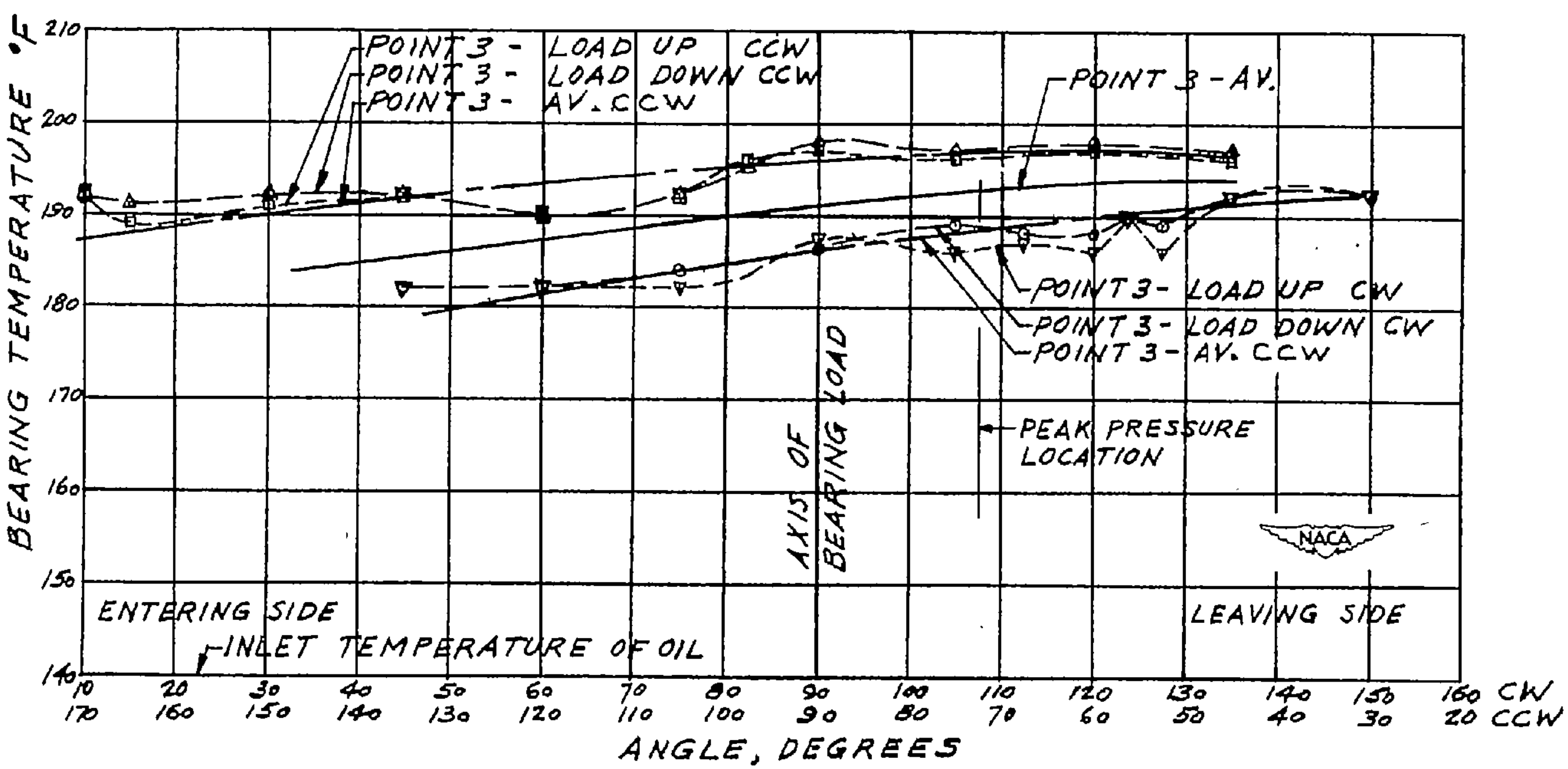

(c) Circumferential bearing temperature distribution of point 3, average of up and down axial misalinement, clockwise and counterclockwise rotation.

Figure 20.- Continued.

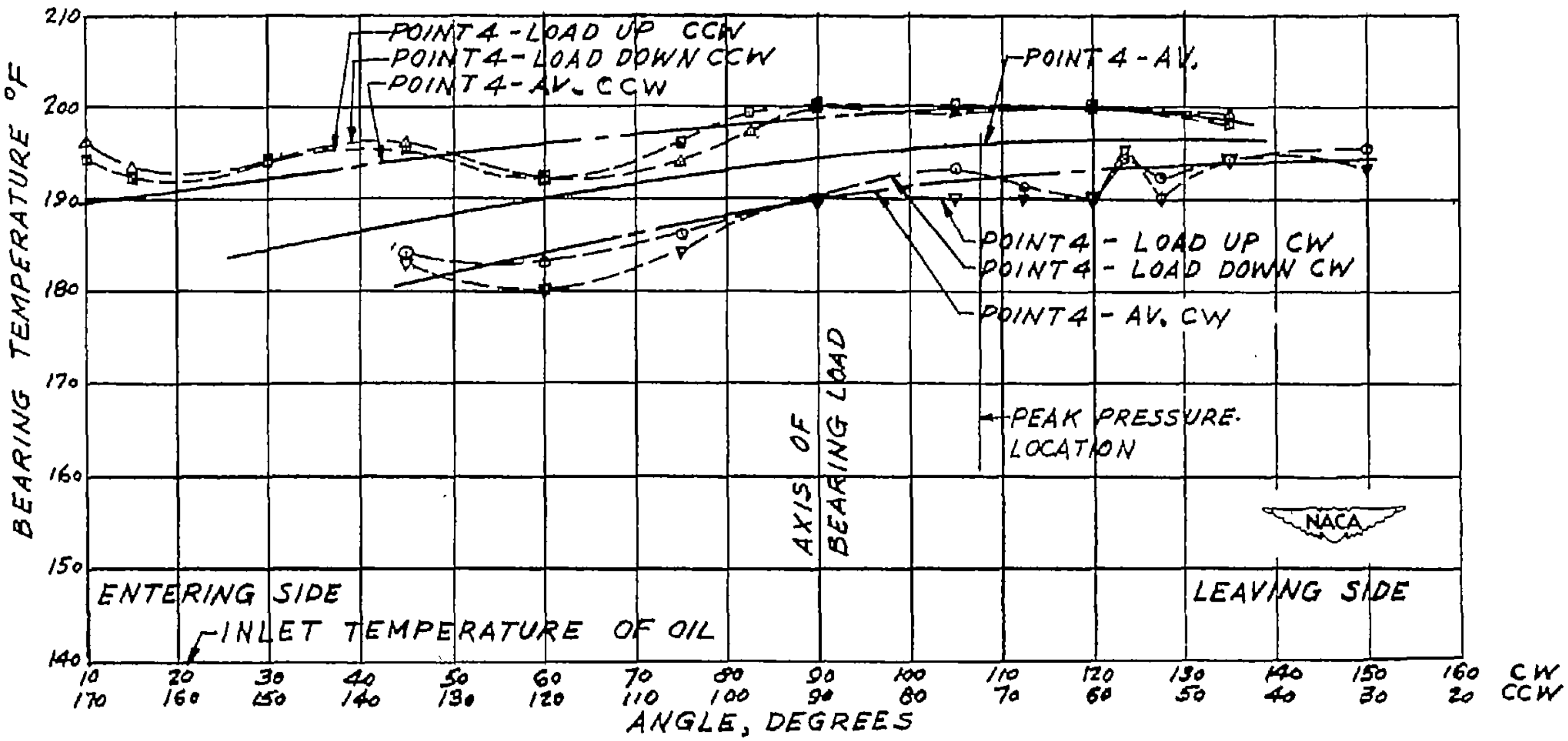

(d) Circumferential bearing temperature distribution of point 4, average of up and down axial misalinement, clockwise and counterclockwise rotation.

Figure 20.- Continued.

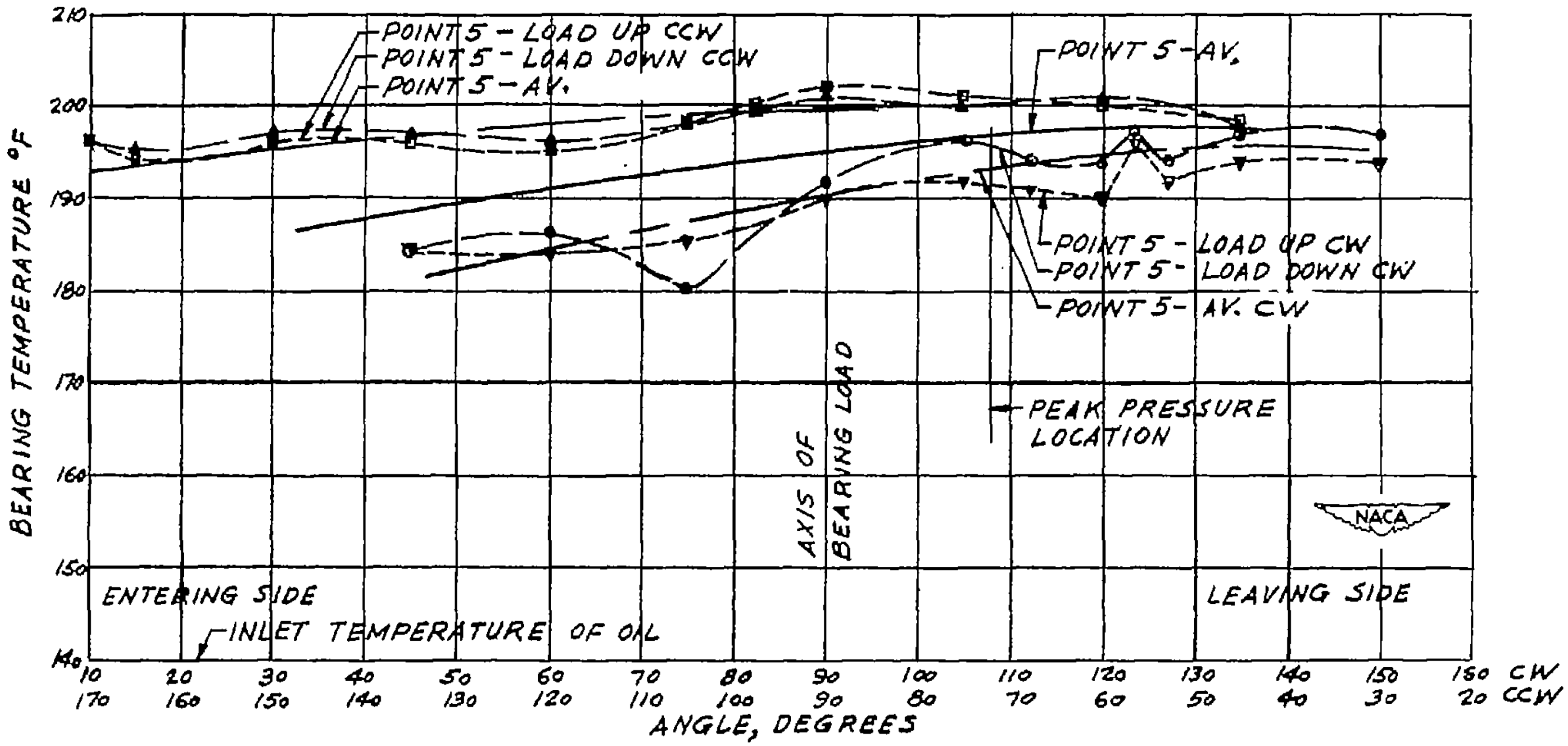

(e) Circumferential bearing temperature distribution of point 5, average of up and down axial misalinement, clockwise and counterclockwise rotation.

Figure 20.- Continued.

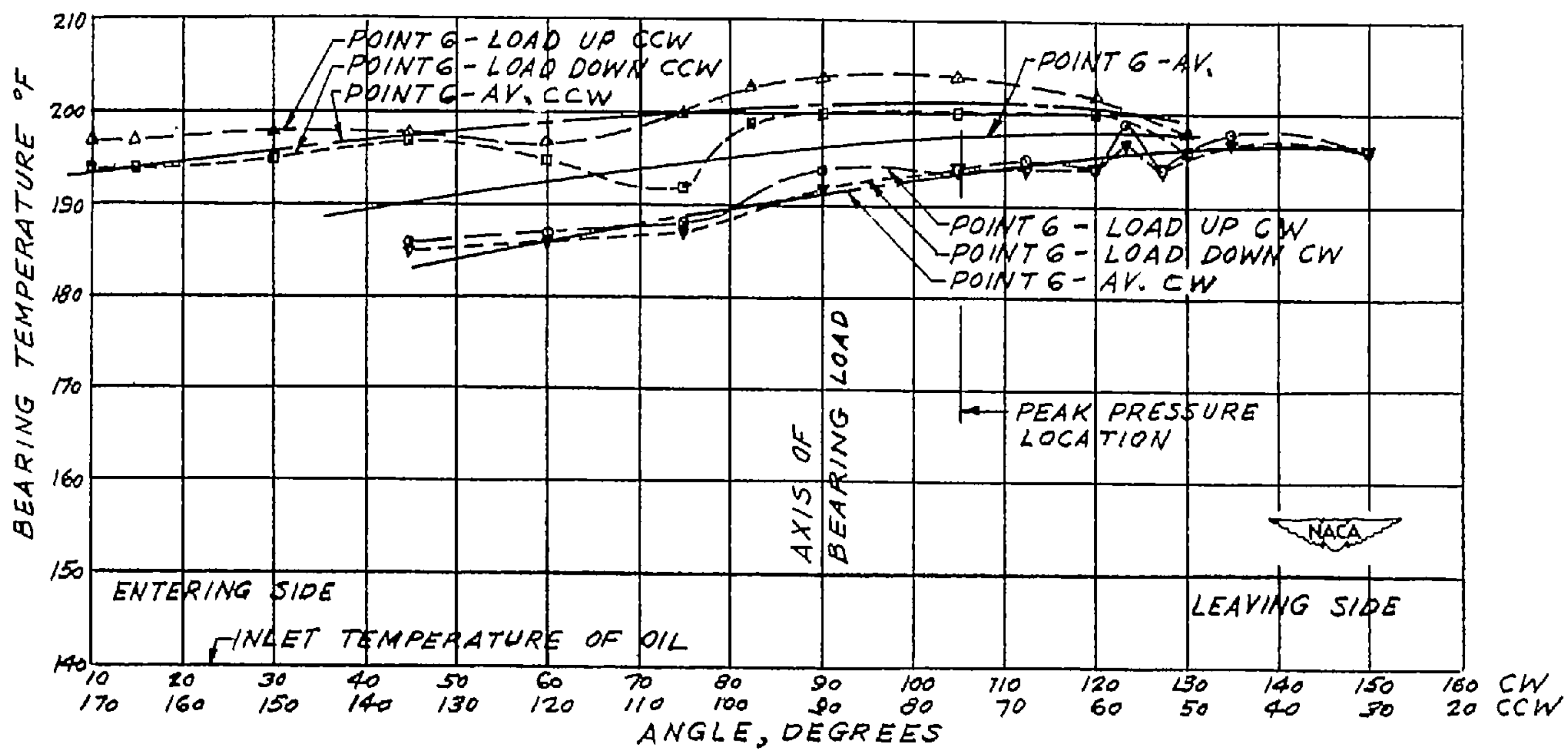

(f) Circumferential bearing temperature distribution of point 6, average of up and down axial misalinement, clockwise and counterclockwise rotation.

Figure 20.- Continued.

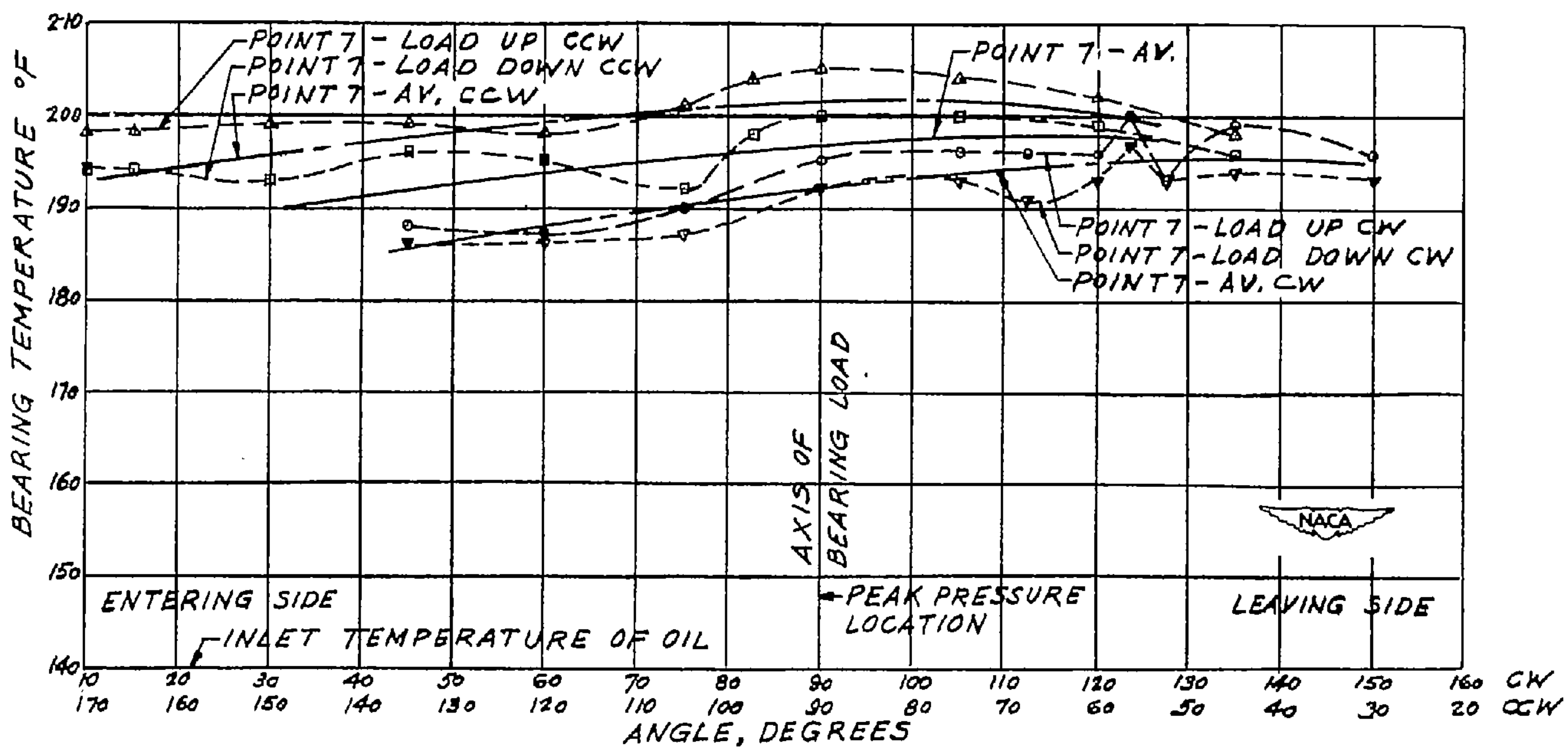

(g) Circumferential bearing temperature distribution of point 7, average of up and down axial misalinement, clockwise and counterclockwise rotation.

Figure 20.- Continued.

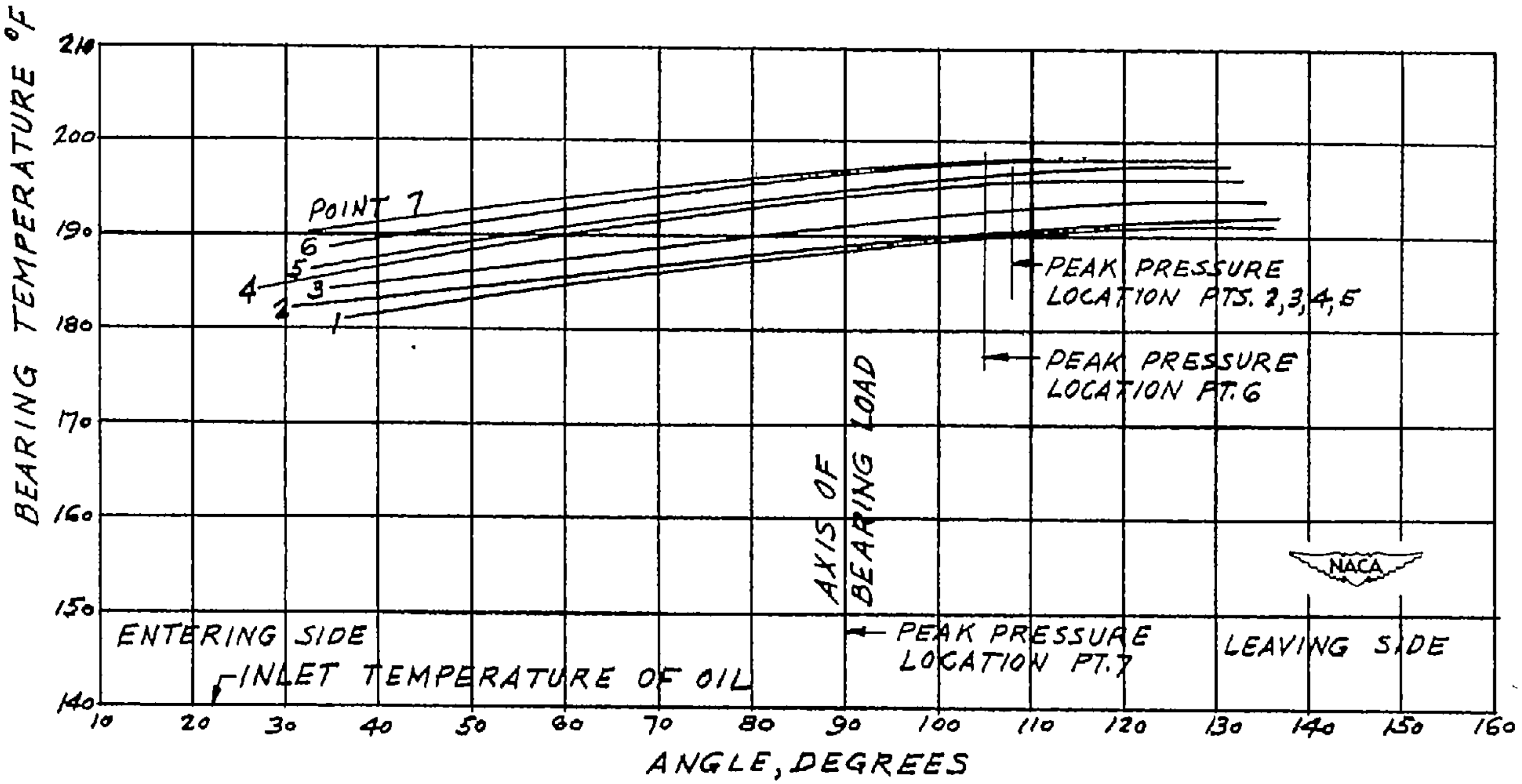

(h) Average circumferential bearing temperature distribution of points 1 through 7.

Figure 20.- Concluded.

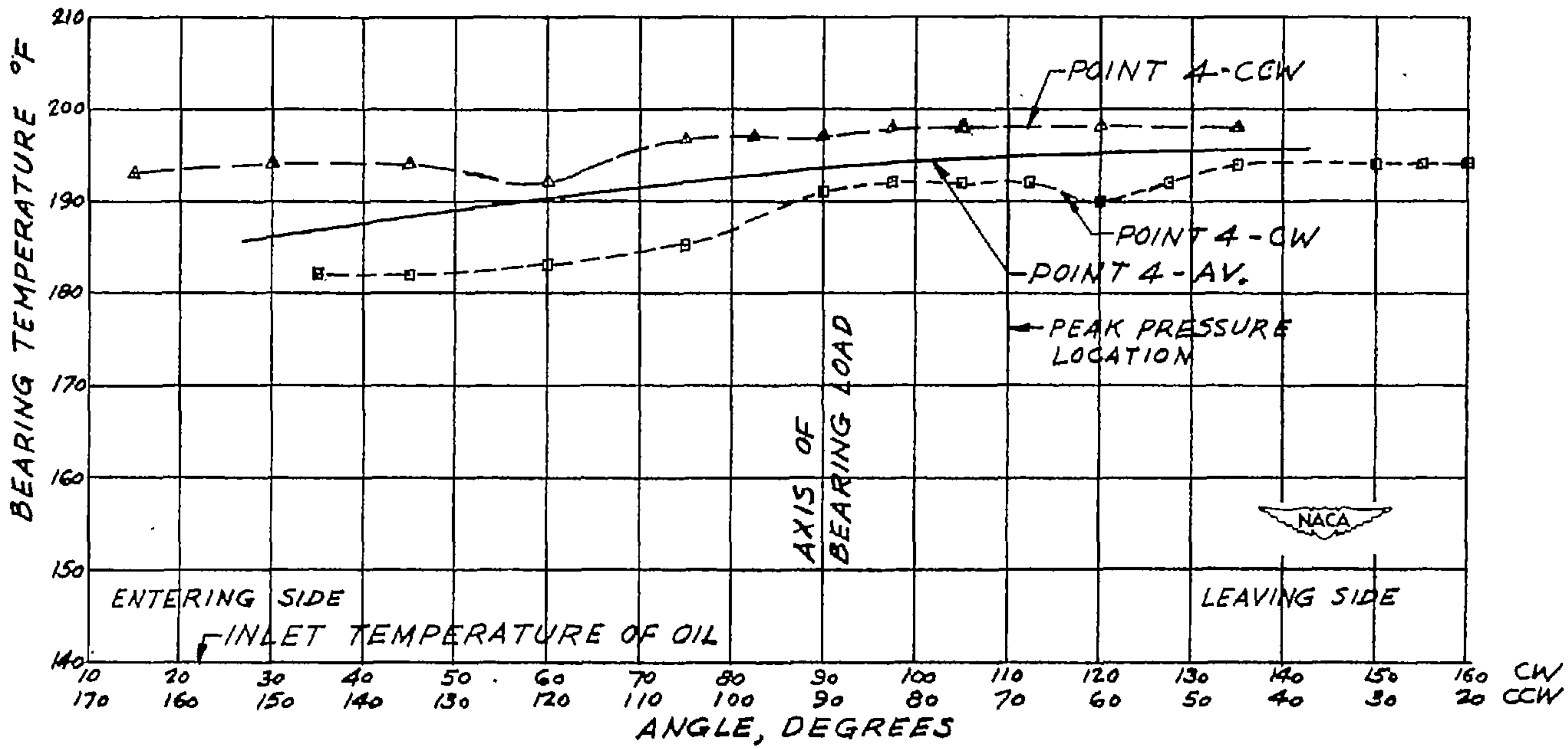

Figure 21.- Circumferential bearing temperature distribution with central load and zero misalinement (data for model 2) at midpoint of bearing (point 4), average of clockwise and counterclockwise rotation. Shaft speed, 5000 rpm; load on projected area, 850 pounds per square inch; bearing diameter, 1.62 inches; bearing length, 1.62 inches; bearing clearance, 0.002 inch per inch of diameter; inlet temperature of no. 1120 Aviation oil at 40 pounds per square inch, 140° F.

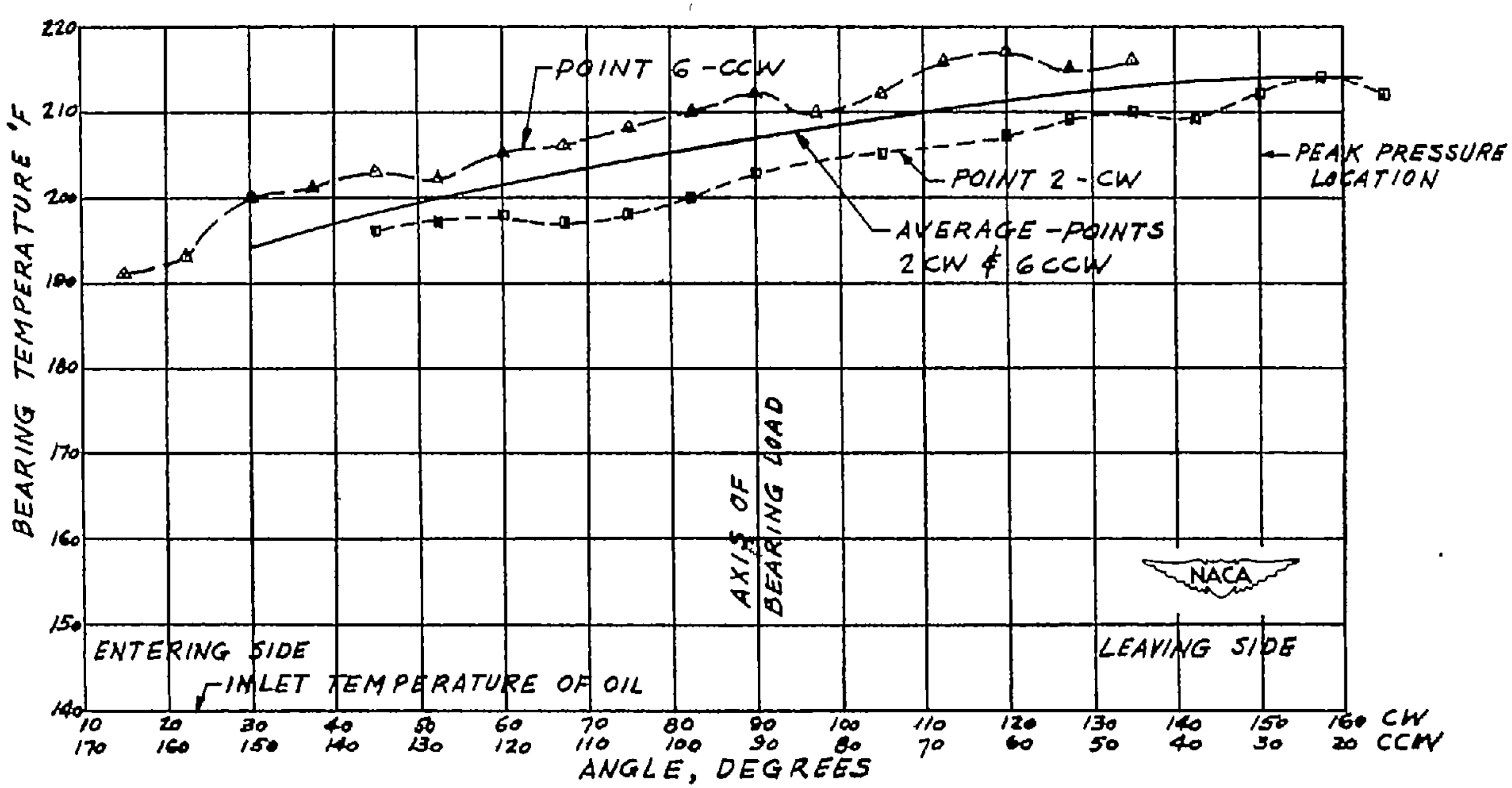

(a) Circumferential bearing temperature distribution at points 2 and 6, average of clockwise and counterclockwise rotation.

Figure 22.- Bearing temperature distribution with central load and 17-percent twist (data for model 3). Shaft speed, 5000 rpm; load on projected area, 850 pounds per square inch; bearing diameter, 1.60 inches; bearing length, 1.62 inches; bearing clearance, 0.0026 inch per inch of diameter; inlet temperature of no. 1120 Aviation oil at 40 pounds per square inch, 140° F.

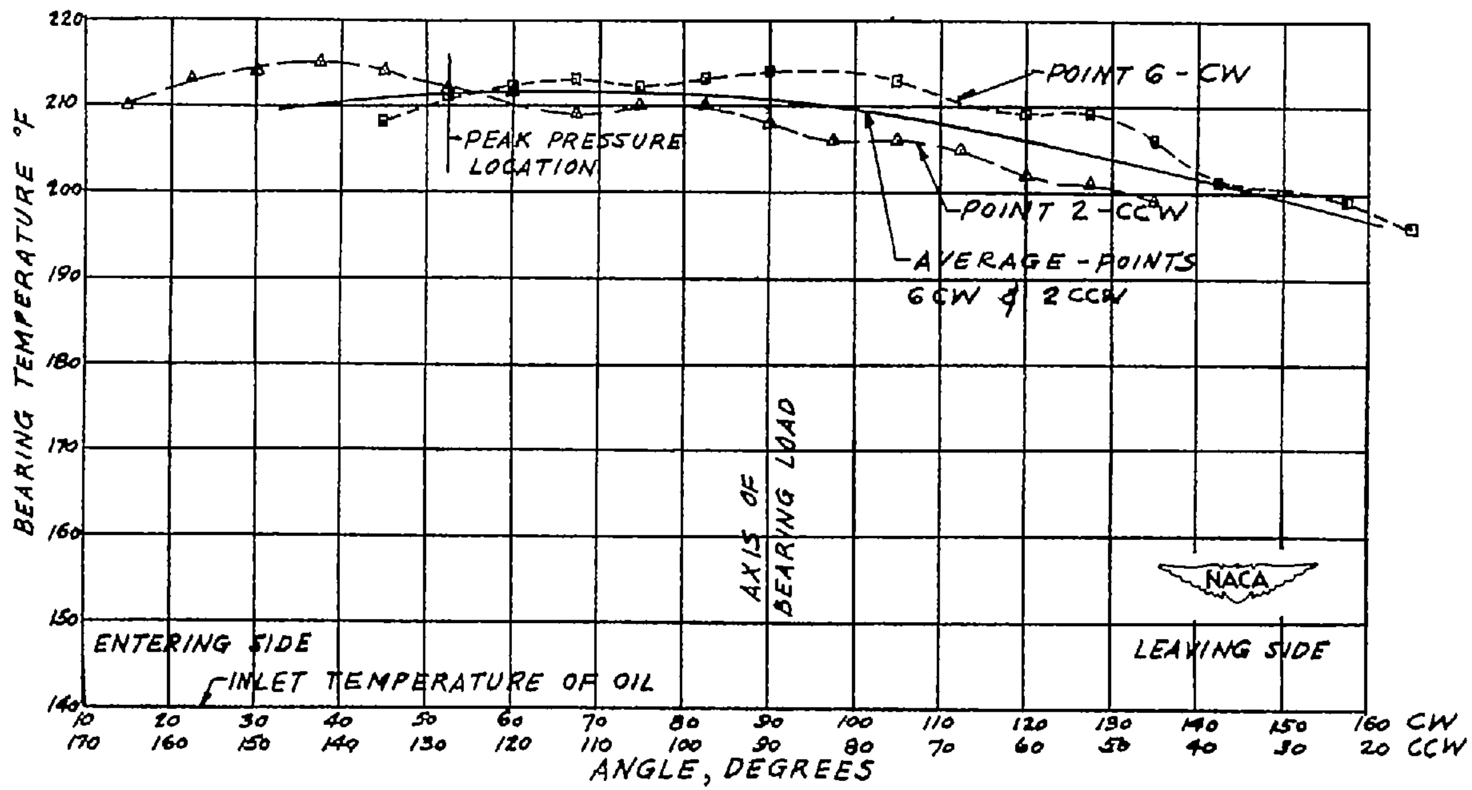

(b) Circumferential bearing temperature distribution at points 6 and 2 of bearing, average of clockwise and counterclockwise rotation.

Figure 22.- Continued.

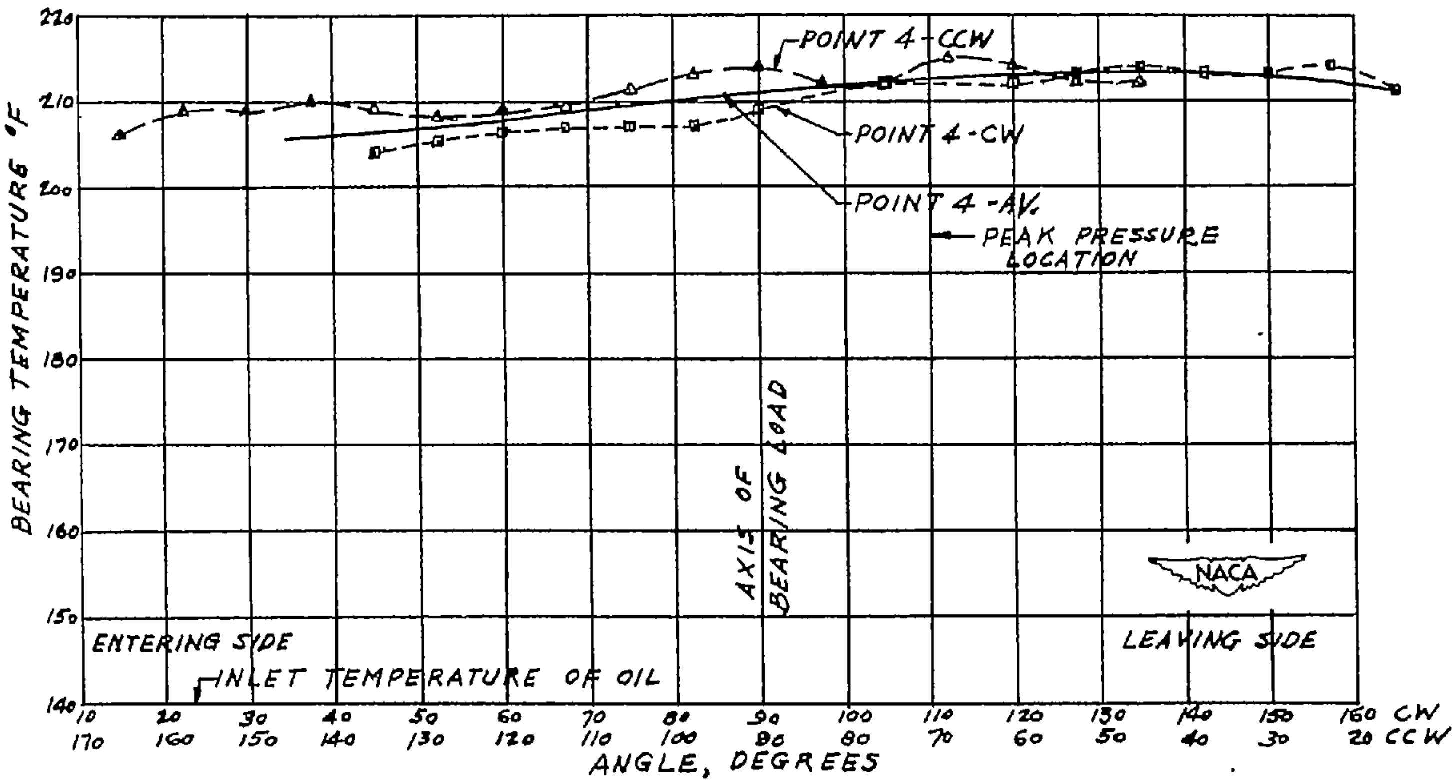

(c) Circumferential bearing temperature distribution at midpoint of bearing (point 4), average of clockwise and counterclockwise rotation.

Figure 22.- Continued.

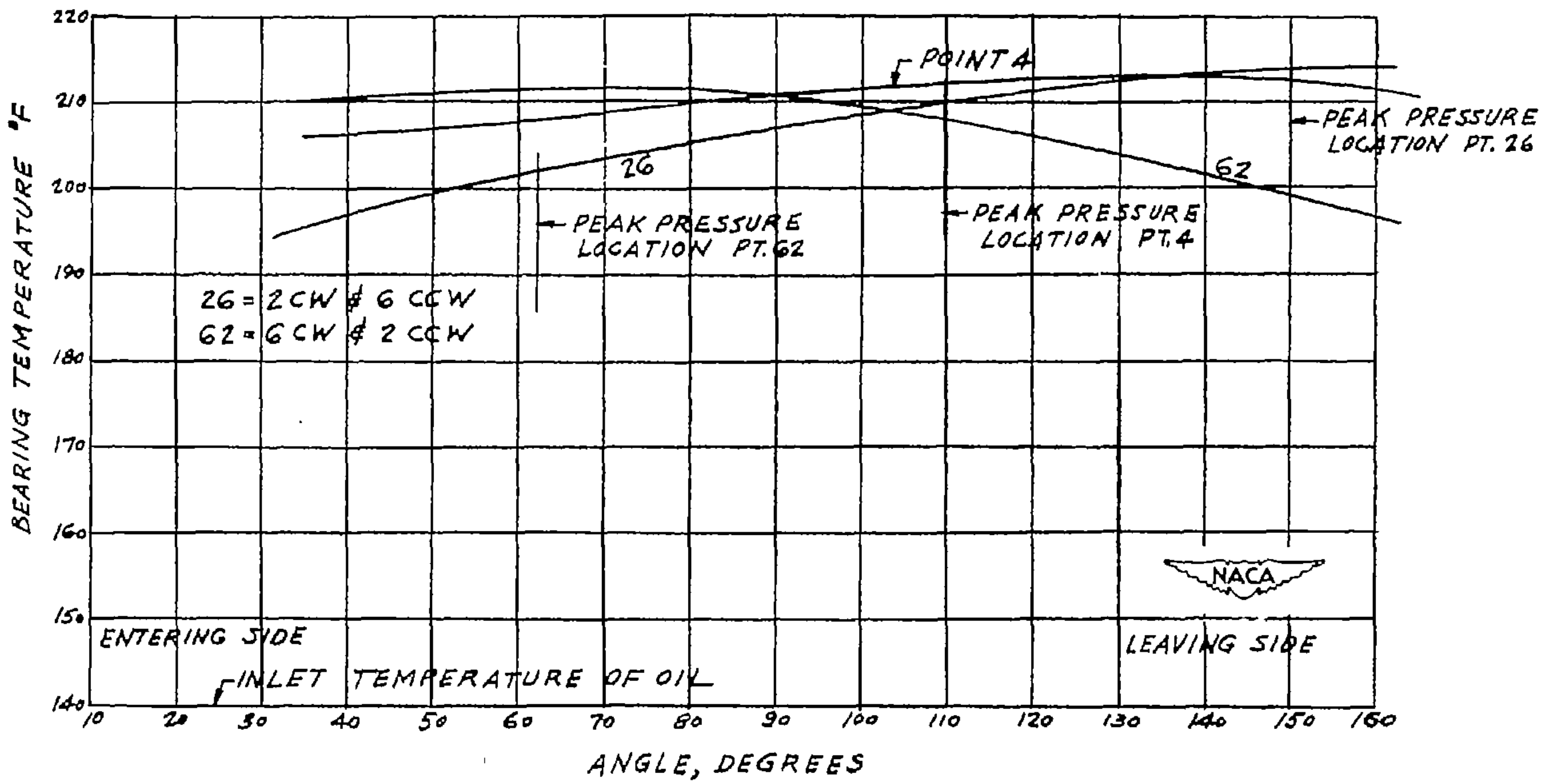

(d) Average circumferential bearing temperature distribution of points 2, 4, and 6.

Figure 22.- Concluded.

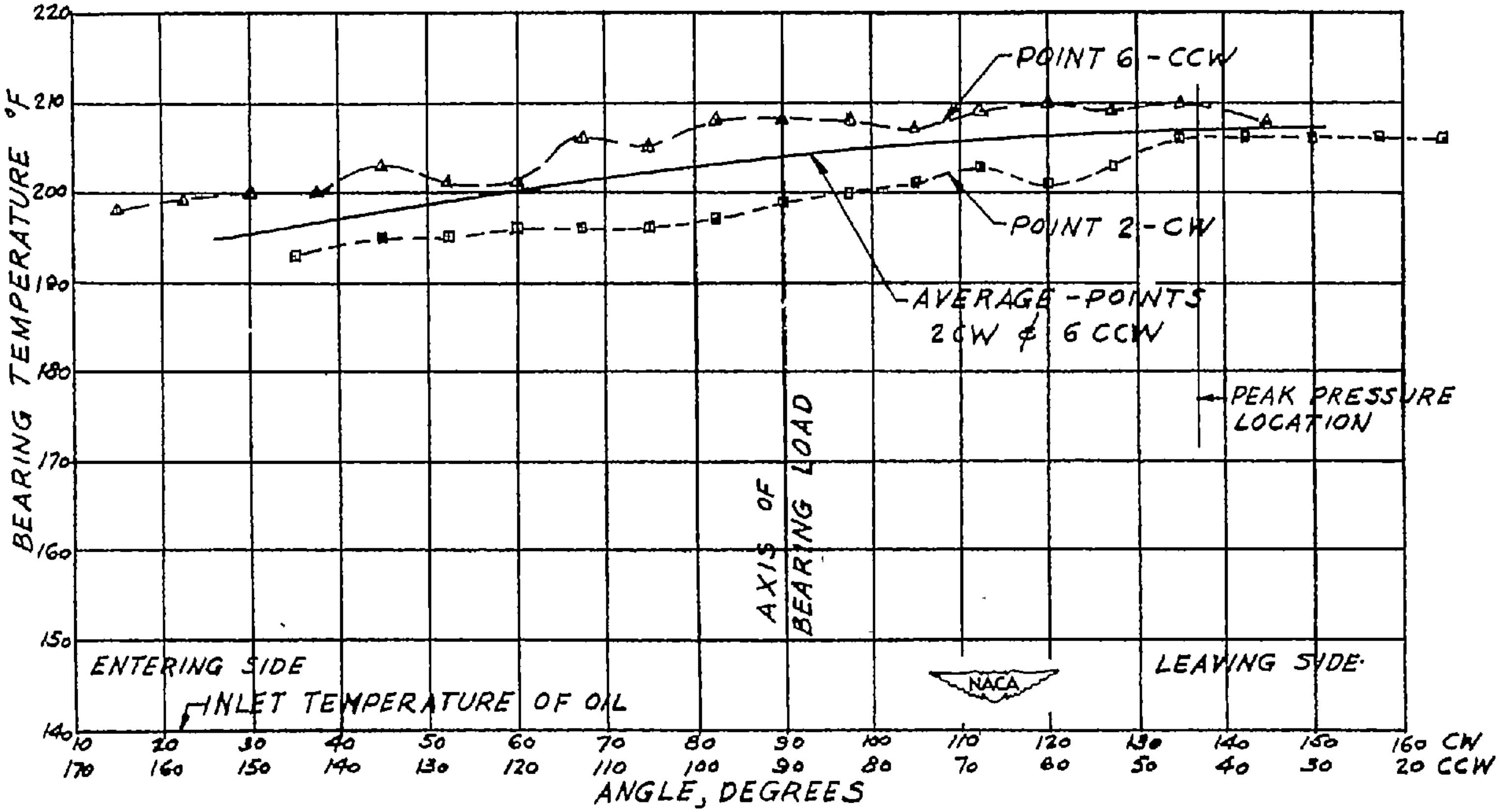

(a) Circumferential bearing temperature distribution of points 2 and 6, average of clockwise and counterclockwise rotation.

Figure 23.- Bearing temperature distribution with central load and 8-percent twist (data for model 4). Shaft speed, 5000 rpm; load on projected area, 850 pounds per square inch; bearing diameter, 1.60 inches; bearing length, 1.62 inches; bearing clearance, 0.0026 inch per inch of diameter; inlet temperature of no. 1120 Aviation oil at 40 pounds per square inch, 140° F.

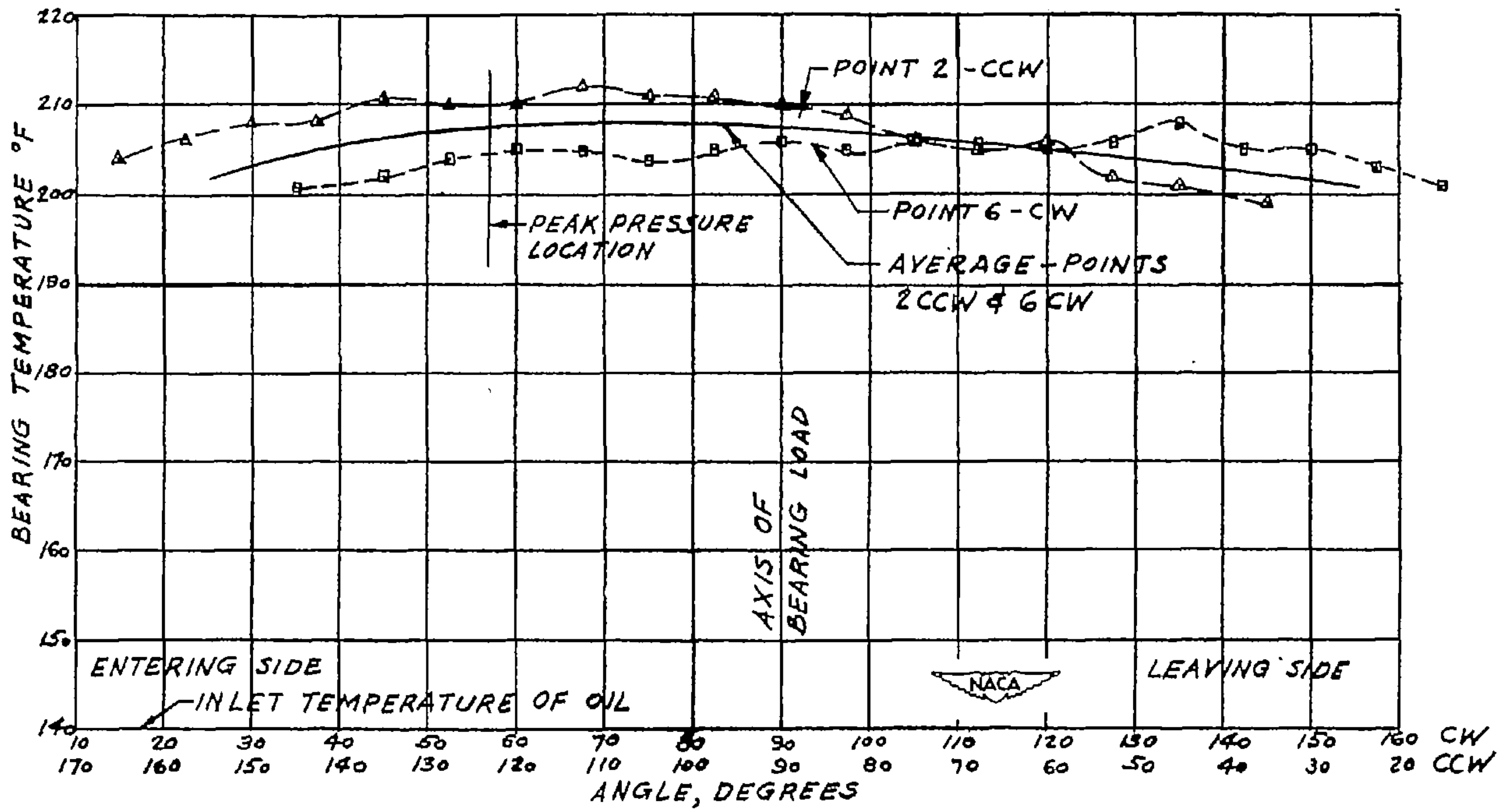

(b) Circumferential bearing temperature distribution of points 6 and 2 of bearing, average of clockwise and counterclockwise rotation.

Figure 23.- Continued.

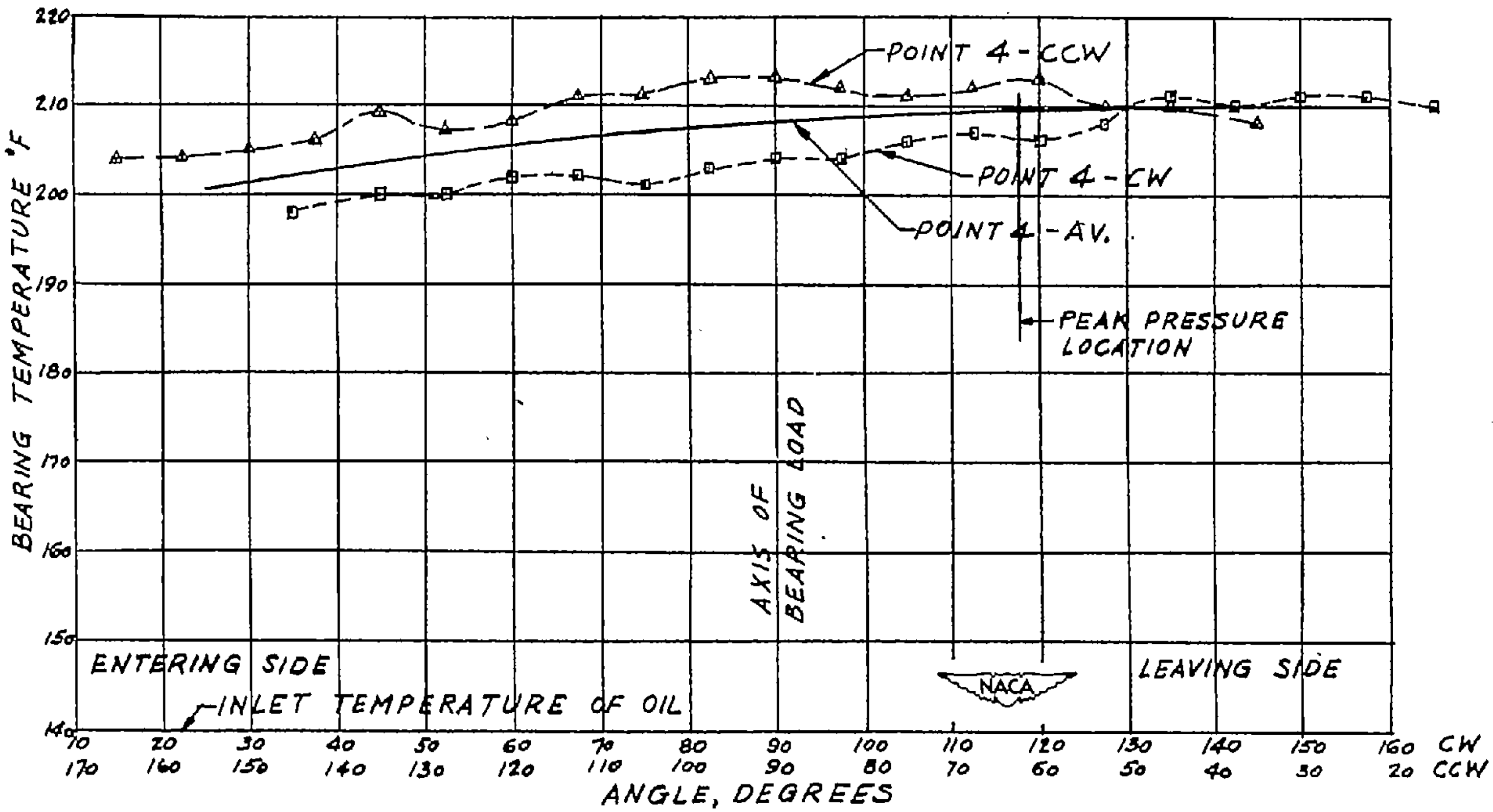

(c) Circumferential bearing temperature distribution at midpoint of bearing (point 4), average of clockwise and counterclockwise rotation.

Figure 23.- Continued.

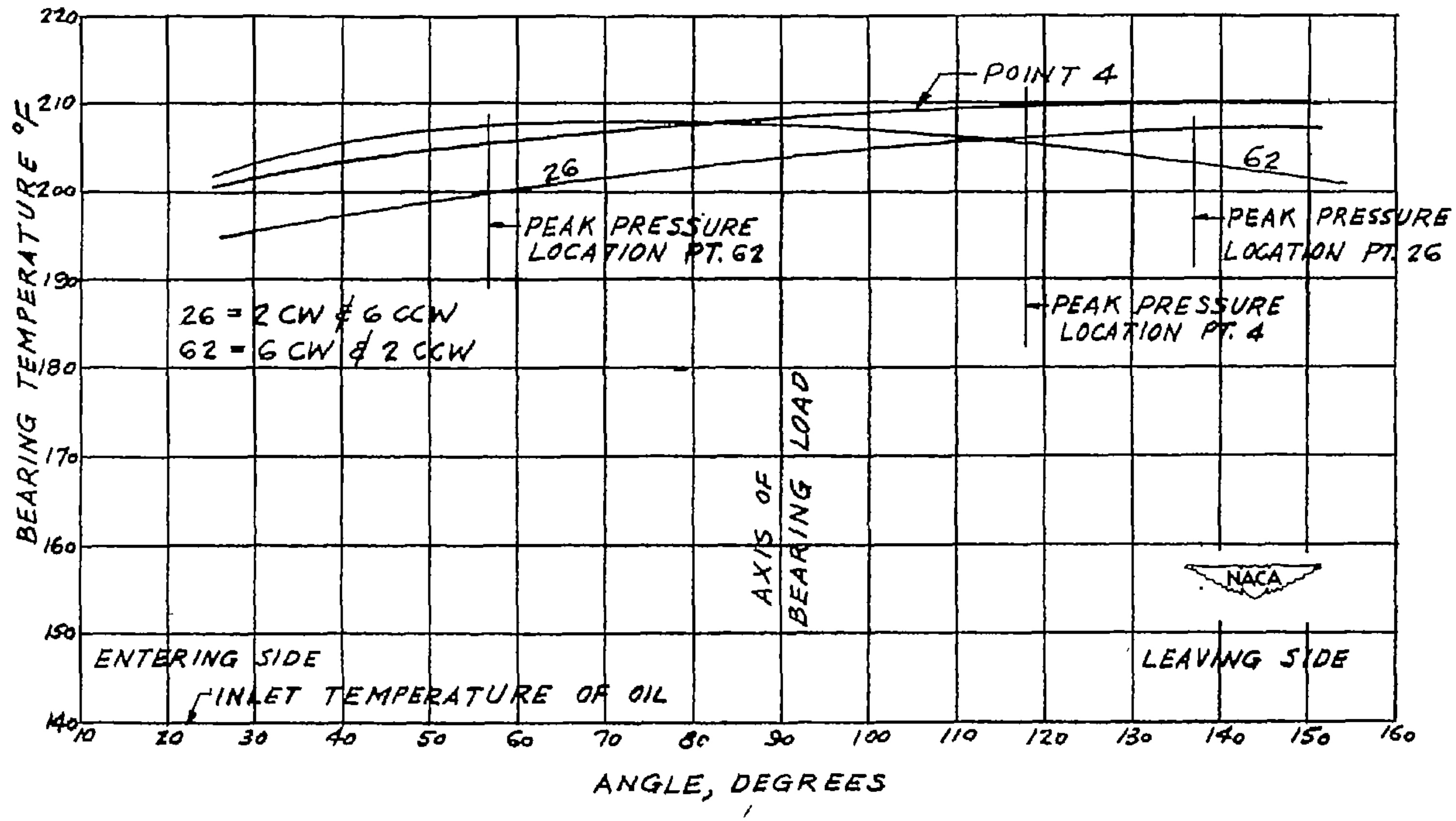

(d) Average circumferential bearing temperature distribution of points 2, 4, and 6.

Figure 23.- Concluded.

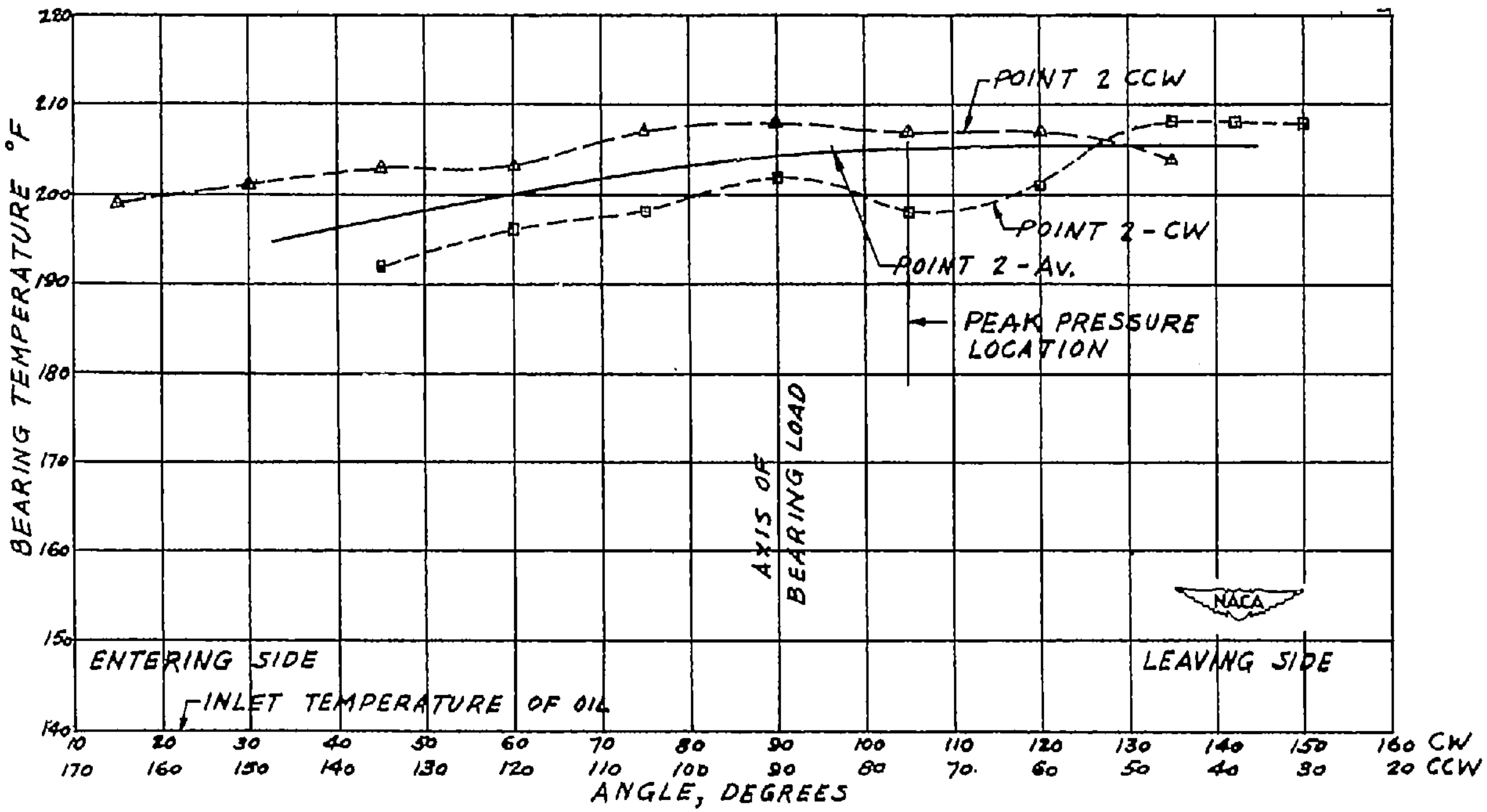

(a) Circumferential bearing temperature distribution at point 2, average of clockwise and counterclockwise rotation.

Figure 24.- Bearing temperature distribution with central load and zero misalinement after bellmouthing by misalinement tests (data for model 5). Shaft speed, 5000 rpm; load on projected area, 850 pounds per square inch; bearing diameter, 1.60 inches; bearing length, 1.62 inches; bearing clearance, 0.0026 inch per inch of diameter; inlet temperature of no. 1120 Aviation oil at 40 pounds per square inch, 140° F.

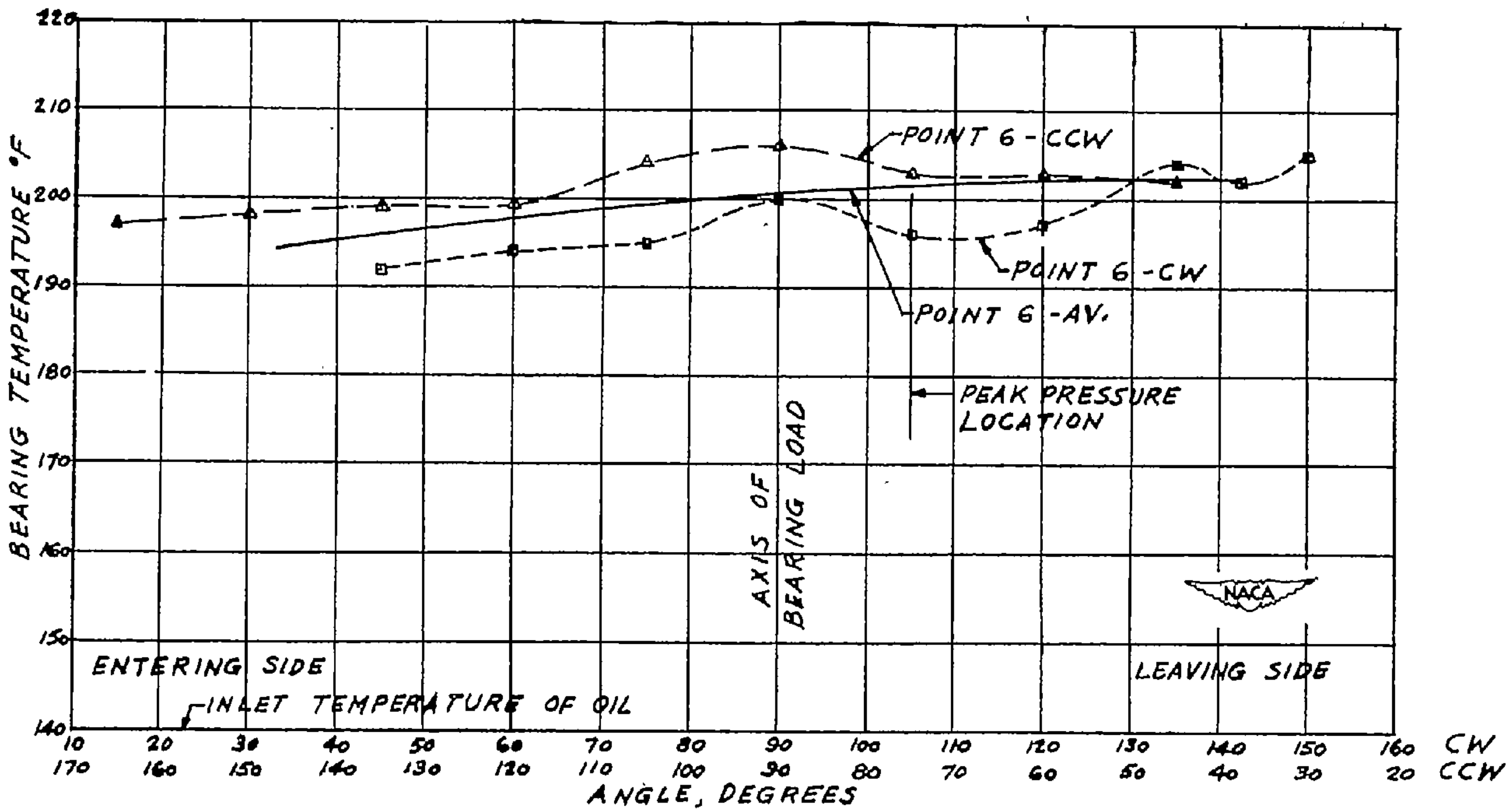

(b) Circumferential bearing temperature distribution of point 6 of bearing, average of clockwise and counterclockwise rotation.

Figure 24.- Continued.

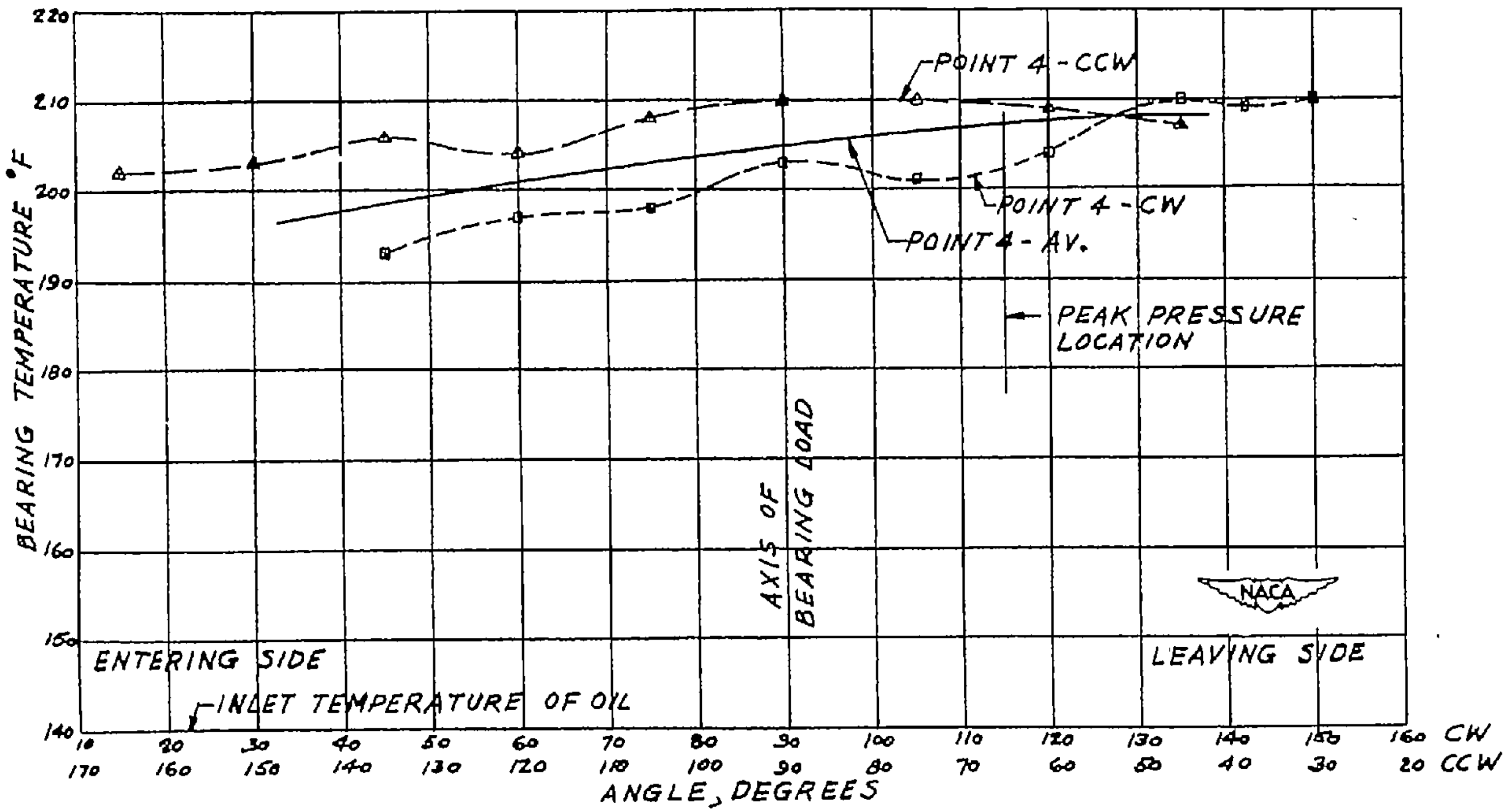

(c) Circumferential bearing temperature distribution at midpoint of bearing (point 4), average of clockwise and counterclockwise rotation.

Figure 24.- Continued.

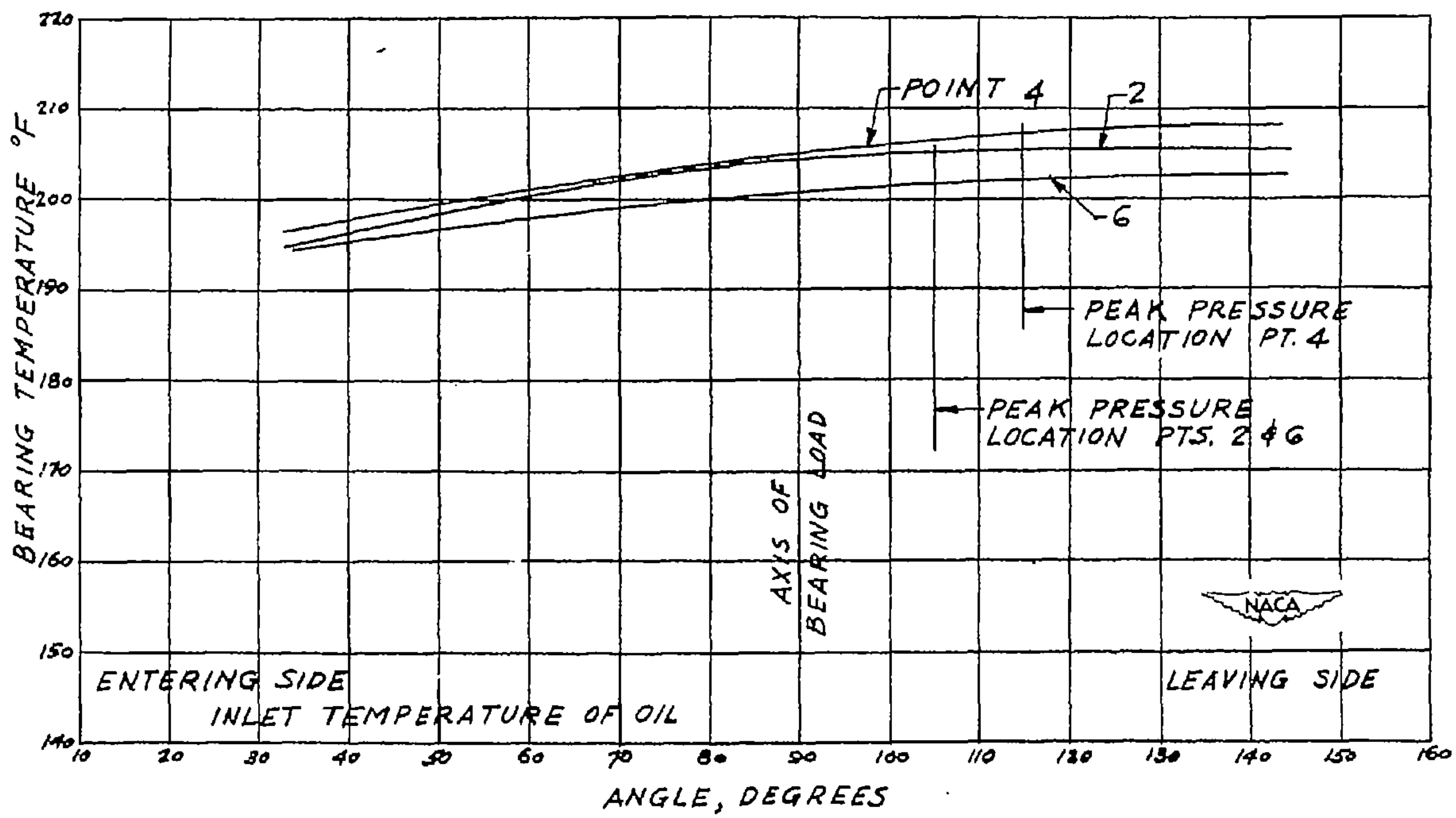

(d) Average circumferential bearing temperature distribution of points 2, 4, and 6.

Figure 24.- Concluded.

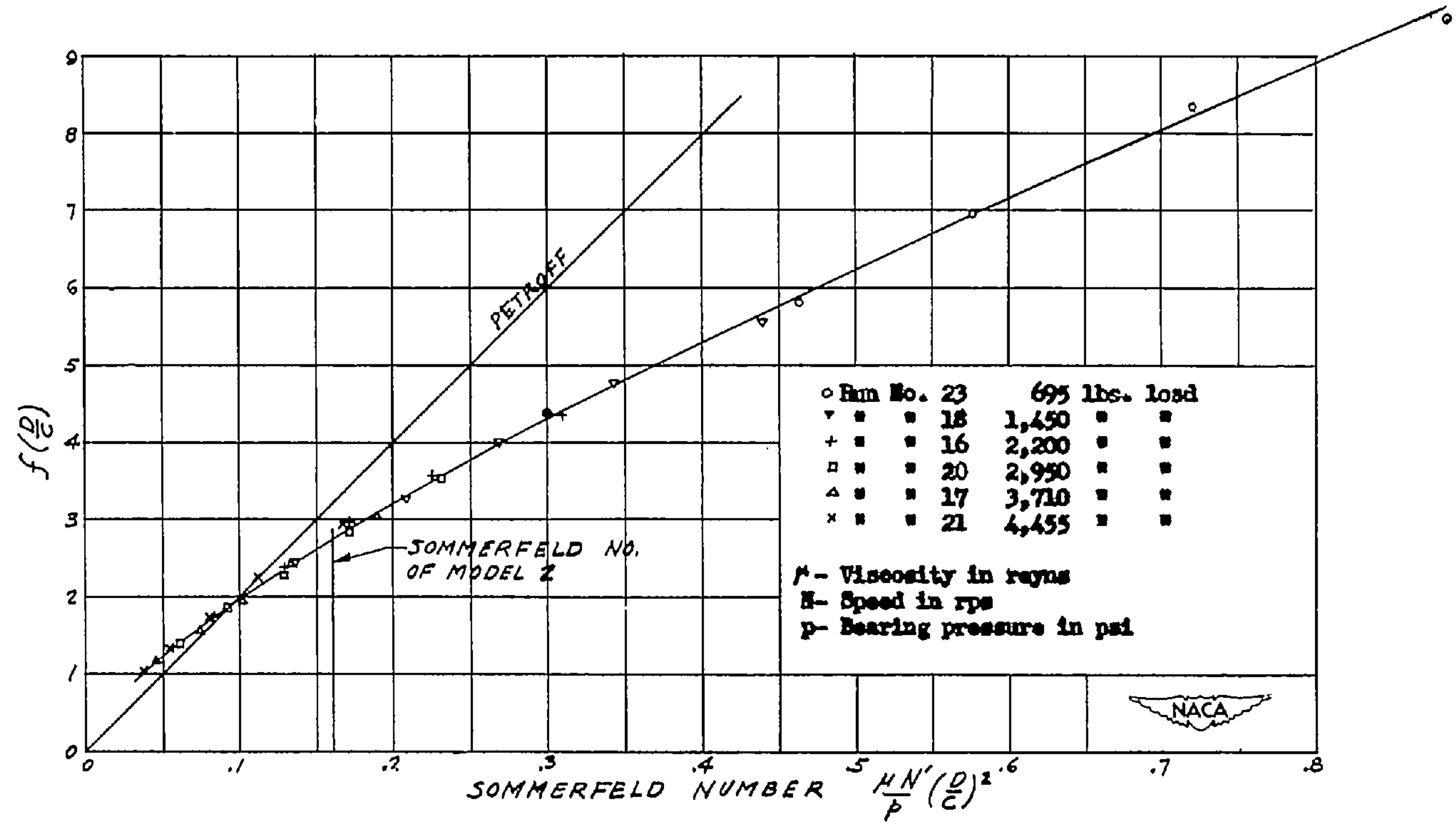

Figure 25.- Friction characteristics plotted against Sommerfeld number for bearing 2 under conditions of central load and zero misalinement as in model 2. Bearing diameter, 1.62 inches; bearing length, 1.62 inches; bearing clearance, 0.002 inch per inch of diameter; inlet temperature of no. 1120 Aviation oil at 40 pounds per square inch, 140° F.

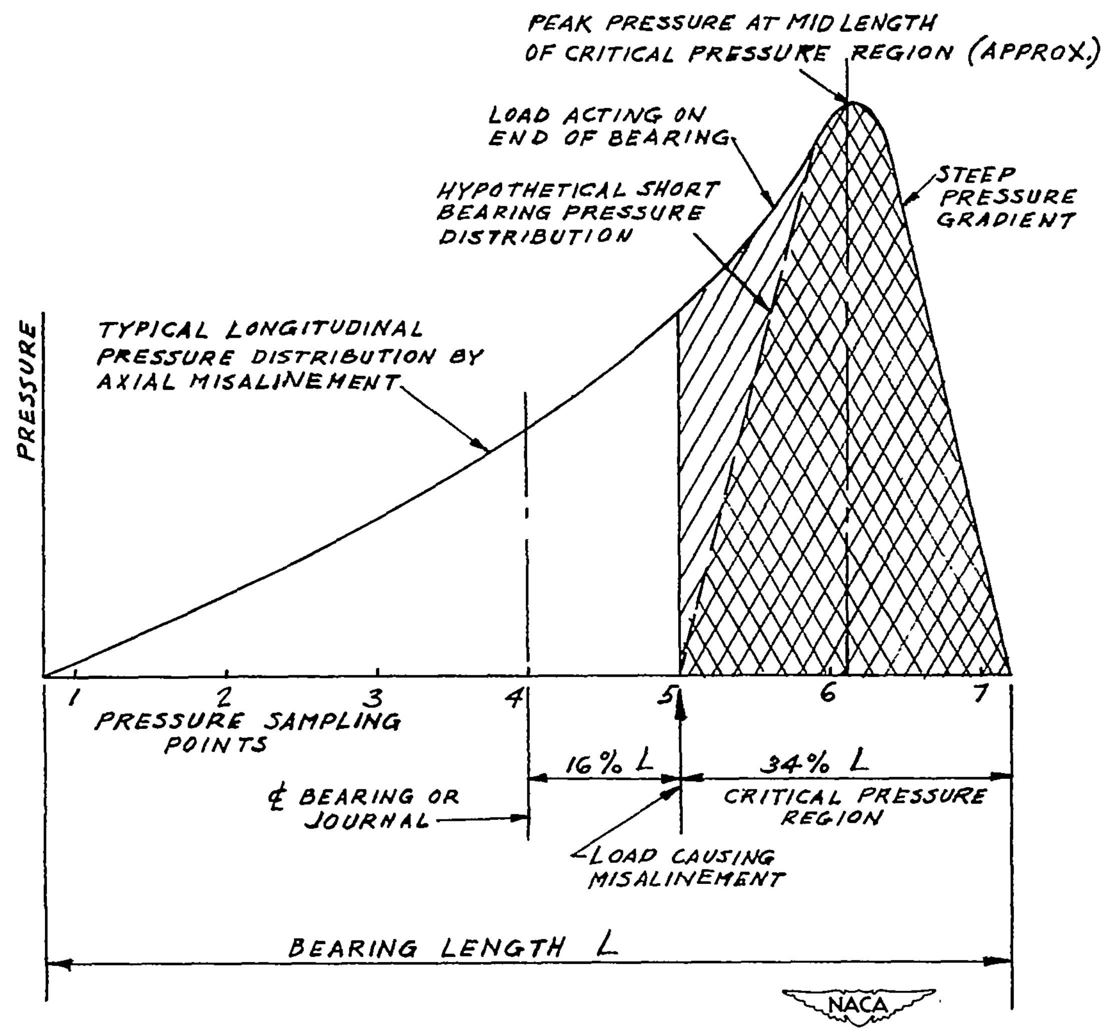

Figure 26.- Critical pressure region of bearing with 16-percent axial misalinement (model 1). Bearing diameter, 1.62 inches; bearing length, 1.62 inches; pressure on projected area, 850 pounds per square inch. Shaded areas compare the critical pressure region caused by axial misalinement with a heavily loaded hypothetical short bearing.

NACA-Langley - 4-22-55 - 75